# Southeastern Geology: Volume 47, No. 1
# February 2010

Editor in Chief: S. Duncan Heron, Jr.

**Abstract**

Academic journal published quarterly by the Department of Geology, Duke University.

# SOUTHEASTERN GEOLOGY


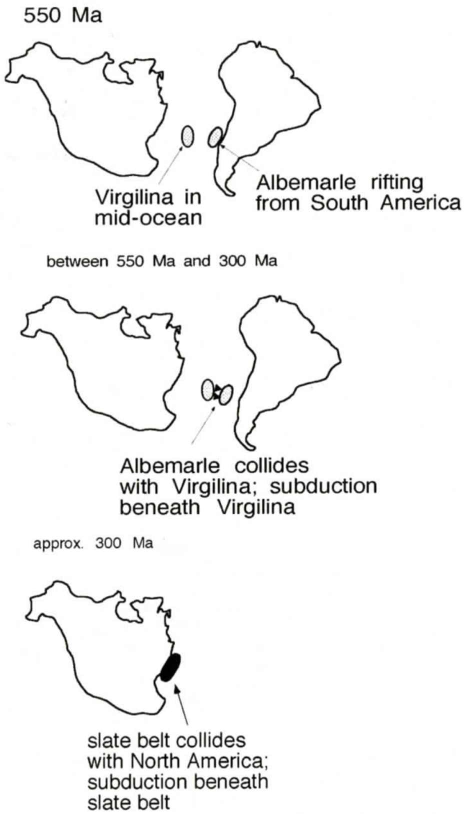



**Vol. 47, No. 1** **February 2010**

// SOUTHEASTERN GEOLOGY

PUBLISHED

at

DUKE UNIVERSITY

Duncan Heron

Editor-in-Chief

David M. Bush

Editor

This journal publishes the results of original research on all phases of geology, geophysics, geochemistry and environmental geology as related to the Southeast. Send manuscripts to **David Bush, Department of Geosciences, University of West Georgia, Carrollton, Georgia 30118, for Fed-X, etc. 1601 Maple St.,** Phone: 678-839-4057, Fax: 678-839-4071, Email: dbush@westga.edu. Please observe the following:

1) Type the manuscript with double space lines and submit in duplicate, or submit as an Acrobat file attached to an email.
2) Cite references and prepare bibliographic lists in accordance with the method found within the pages of this journal. Data citations examples can be found at http://www.geoinfo.org/TFGeosciData.htm
3) Submit line drawings and complex tables reduced to final publication size (no bigger than 8 x 5 3/8 inches).
4) Make certain that all photographs are sharp, clear, and of good contrast.
5) Stratigraphic terminology should abide by the North American Stratigraphic Code (American Association Petroleum Geologists Bulletin, v. 67, p. 841-875).
6) Email Acrobat (pdf) submissions are encouraged.

Subscriptions to *Southeastern Geology* for volume 47 are: individuals - $26.00 (paid by personal check); corporations and libraries - $40.00; foreign $55. Inquiries should be sent to: **SOUTHEASTERN GEOLOGY, DUKE UNIVERSITY, DIVISION OF EARTH & OCEAN SCIENCES, BOX 90233, DURHAM, NORTH CAROLINA 27708-0233**. Make checks payable to: *Southeastern Geology.*

Information about **SOUTHEASTERN GEOLOGY** is on the World Wide Web including a searchable author-title index 1958-2010 (Acrobat format). The URL for the Web site is: http://www.southeasterngeology.org

**SOUTHEASTERN GEOLOGY** is a peer review journal.

ISSN 0038-3678

## SOUTHEASTERN GEOLOGY

## Table of Contents

Volume 47, No. 1 February 2010

SOUTHEASTERN GEOLOGY
V. 47, No.1, February 2010, p. 1-13

# EVOLUTION OF THE SLATE BELT IN NORTH CAROLINA

JOHN J.W. ROGERS AND DREW S. COLEMAN

*Department of Geological Sciences*
*University of North Carolina at Chapel Hill*
*Chapel Hill, NC 27599*

## ABSTRACT

**The slate belt in North Carolina contains two bimodal volcanic and volcaniclastic rock sequences. The Virgilina sequence comprises most of the slate belt, and its development was complete by about 600 Ma. The Albemarle sequence is in the Uwharrie Mountains, and its evolution spanned the Precambrian–Cambrian boundary. Compositions of both sequences show that they were formed above subduction zones. $T_{DM}$ values about 100 m.y. older than eruption ages suggest that Virgilina rocks formed in a primitive intra-oceanic island arc. Conversely, $T_{DM}$ ages several hundred m.y. older than eruption ages are consistent with formation of the Albemarle rocks above a subduction zone on a newly formed continental margin. We propose: the Albemarle sequence formed along the continental margin of South America after it rifted from Rodinia; the Albemarle sequence then rifted away from South America; the Albemarle and Virgilina sequences joined to form the slate belt in the ocean between South America and North America; the slate belt then accreted to North America by subduction of the intervening ocean beneath the slate belt.**

## INTRODUCTION

The Carolina slate belt is variously defined by different investigators, and some recent publications abandon the term "slate belt" in favor of different terminologies (review by Hibbard et al., 2002, 2007a, 2007b, 2009). We retain the term because of its historical significance and define the slate belt in North Carolina as a suite of low-grade supracrustal rocks that extend from Triassic–Jurassic rift basins and coastal plain overlap on the southeast to a tectonic contact with higher grade rocks of the Charlotte belt on the northwest (Figure 1).

The slate belt has been grouped with other belts to form the Carolina terrane (Hibbard et al., 2002) or Carolinia (Hibbard et al., 2007a, 2007b). This terrane is part of a group of terranes commonly referred to as "Avalonian" after the type terrane Avalonia in Newfoundland, and Hibbard et al. (2002, 2007) refer to them as part of an Appalachian peri-Gondwana realm (APGR). Among the APGR terranes, Hibbard et al. (2007a, 2007b) particularly correlate Carolinia with the Ganderia terrane of Newfoundland. Although different in detailed history, all of the Avalonian terranes contain volcano-sedimentary suites of late-Neoproterozoic to early-Paleozoic age and were deformed later in the Paleozoic.

Most investigators regard Avalonian terranes as fragments that were rifted from Gondwana in the late Neoproterozoic or early Paleozoic and accreted to eastern North America in the middle to later Paleozoic (Secor et al., 1983; Vick et al., 1987; Mueller et al., 1996; Ingle et al., 2003). Pollock (2007) supported an origin of the slate belt from Gondwana by finding zircons with ages from about 500 to 1800 Ma in the Aaron formation and zircons with ages in the general range of 500 to 1000 Ma in Albemarle rocks. These ages suggest that some of the sediments in the slate belt contain debris from western South America. Landing et al. (2003), however, proposed that Avalonia originated as a separate block that was never attached to Gondwana. The Avalonian terranes appear to have a similar origin to the Cadomian terranes of Europe (D'Lemos et al., 1990), and Mallard and Rogers (1997) proposed that Avalonian terranes were derived from western South America and Cadomian terranes from northern Africa.

Many investigators have demonstrated that late Neoproterozoic rocks of the slate belt were

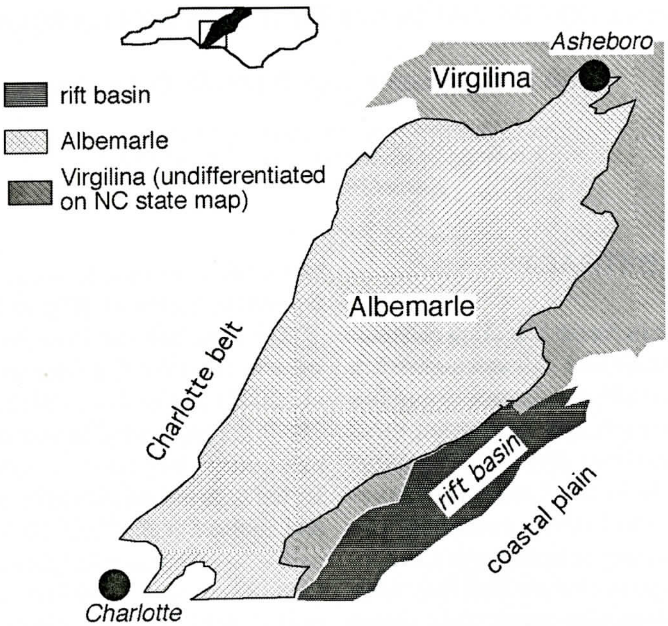


**Figure 1. Map of part of slate belt in North Carolina. Generalized from North Carolina Geological Survey (1991) and Hibbard et al. (2002). Inset shows the location of the slate belt and the area covered by this investigation.**

juvenile at their time of formation (Whitney et al., 1978; Scott Samson et al., 1995a; Dennis and Shervais, 1996). Some isotopic evidence, however, shows inheritance of old isotopic systems in rocks of the slate belt (Ingle et al., 2003). These differences in interpretation demonstrate the occurrence of at least two very different sequences of rocks in the slate belt, and Hibbard et al. (2002) separated the slate belt into the Virgilina and Albemarle sequences. The Albemarle sequence occurs primarily in the Uwharrie Mountains, and the Virgilina sequence comprises the rest of the slate belt (Figure 1).

This paper summarizes bulk compositional and isotopic Sm–Nd data for both the Virgilina and Albemarle sequences. We present new isotopic and compositional data for basalts in both sequences; data for individual samples can be obtained from the North Carolina Geological Survey: Contact Phil Bradley, Piedmont Geologist, by email at pbradley@ncdenr.gov. Data for the felsic rocks are from a recently published geological–archaeological survey (Steponaitis et al., 2006). That survey contains petrographic, bulk compositional, and Sm–Nd isotopic information for 65 samples of felsic rocks from Native American quarry sites in the slate belt, including both the Virgilina and Albemarle sequences.

## GEOLOGIC AND AGE RELATIONSHIPS OF THE VIRGILINA SEQUENCE

Stratigraphic relationships have been established in only one area of the Virgilina sequence (Bradley et al., 2006). Along the eastern edge of the slate belt, Glover and Sinha (1973), Harris (1984), and Harris and Glover (1988) proposed a sequence from the Hyco Formation at the base, upward through the Aaron Formation, to the Virgilina Formation at the top. It has not been possible, however, to correlate these formations throughout the Virgilina sequence (Hibbard et al., 2002), and we use the term "Virgilina" for all supracrustal rocks in the sequence.

Rocks of the Virgilina sequence apparently extend eastward from the conventional eastern

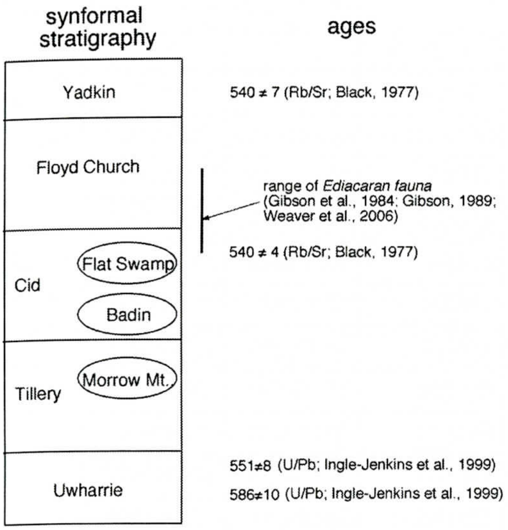


**Figure 2. Stratigraphy of Albemarle sequence. Based largely on Milton (1984).**

margin of the slate belt. Similar rocks exposed east of the Durham Triassic–Jurassic basin have been described by Parnell et al. (2006). Rocks buried beneath the coastal plain in South Carolina and Georgia also appear to be similar to Virgilina rocks (Dennis et al., 2004).

Because of the lack of definable stratigraphy and the complete absence of fossils, all ages of the Virgilina sequence are based on radiometric dates. Wortman et al. (2000) and Ingle et al. (2003) used U-Pb ages to show that volcanism in the Virgilina occurred between 633 Ma and 578 Ma. The limited information shows no geographic pattern but demonstrates that all of the Virgilina supracrustal rocks are older than the Albemarle sequence. The eruptive ages are consistent with ages slightly younger than 600 Ma in the oldest plutons intrusive into the supracrustal sequence (LeHuray, 1989; Wortman et al., 2000; Tadlock and Loewy, 2006).

## GEOLOGIC AND AGE RELATIONSHIPS OF THE ALBEMARLE SEQUENCE

Stratigraphic relationships for rocks of the Albemarle sequence are based on the assumption that all of the rocks occupy a broad synform (Conley and Bain, 1965). Figure 2 shows the stratigraphy proposed by Milton (1984) without indicating thicknesses because the base of the sequence is unexposed, an unknown amount of rock has been eroded from the top, and deformation obscures relationships within the exposed section.

The lowermost unit in the Albemarle suite is the Uwharrie Formation, a sequence of silicic flow and volcaniclastic rocks. The Uwharrie Formation is overlain by the Tillery Formation, which contains minor basalt but consists mostly of planar-laminated silicic siltstones and mudstones; they may represent the distal parts of turbidites that episodically filled the Albemarle basin. Morrow Mountain rocks are ignimbrites whose stratigraphic position is unclear.

The Cid Formation, above the Tillery, appears to have been deposited in comparatively shallow water. It consists largely of silicic debris in beds 10 to 40 cm thick, with cross stratification in the lower part and thin laminations toward the top. The Badin member of the Cid Formation is mostly a series of basaltic epiclastic rocks, and the Flat Swamp member is distinguishable by its assemblage of silicic flows and ignimbrites. The Floyd Church Formation, above the Cid, consists almost wholly of mudstones. The uppermost unit is the Yadkin Formation, which consists of poorly sorted epiclastic basaltic rocks

Most available information shows that all of the rocks in the Albemarle sequence developed in the latest Neoproterozoic between about 600 Ma and 540 Ma. This age is based on radiometric dates (Figure 2) and the presence of Ediacaran fossils in the central part of the Albemarle suite (Gibson et al., 1984; Gibson, 1989; Hibbard et al., 2006; Weaver et al., 2006). This age range suggests that the exposed part of the Albemarle sequence in North Carolina is slightly older than the lithologically similar Asbill Pond suite in South Carolina, which contains Cambrian trilobites (LeHuray, 1987; Sara Samson et al., 1990; McMenamin and Weaver, 2004). This higher age in North Carolina probably results from deeper erosion of the slate belt on top of an uplift that raises North Carolina about 200 m above corresponding regions of Virginia and South Carolina (Rogers, 1999).

**Locations of all of the felsic rocks**

| Sample number | Latitude | Longitude |
|---|---|---|
| **Tillery** | | |
| FBL001 | 35.400389 | -80.036940 |
| FBL002 | 35.402057 | -80.038131 |
| FBL003 | 35.404874 | -80.044276 |
| FBL004 | 35.402679 | -80.042672 |
| FBL005 | 35.366999 | -80.089006 |
| FBL006 | 35.364465 | -80.078214 |
| FBL007 | 35.372720 | -80.081291 |
| **Cid** | | |
| FBL008 | 35.392697 | -80.077188 |
| FBL009 | 35.402423 | -80.072166 |
| FBL010 | 35.401265 | -80.071640 |
| FBL011 | 35.408503 | -80.071381 |
| FBL012 | 35.408503 | -80.071381 |
| FBL013 | 35.399381 | -80.080008 |
| FBL014 | 35.480338 | -80.045026 |
| FBL021 | 35.754385 | -79.927650 |
| FBL022 | 35.757774 | -79.942824 |
| **Morrow Mt.,** | **Tater Top** | |
| FBL015 | 35.349756 | -80.092127 |
| FBL016 | 35.355983 | -80.071564 |
| FBL017 | 35.350154 | -80.093553 |
| FBL018 | 35.351670 | -80.092469 |
| FBL019 | 35.352915 | -80.091409 |
| **Uwharrie** | | |
| FBL020 | 35.675252 | -79.856069 |
| FBL023 | 35.724463 | -79.829185 |
| FBL024 | 35.675824 | -79.851763 |
| FBL025 | 35.316688 | -80.050485 |
| FBL026 | 35.316688 | -80.050485 |
| FBL051 | 35.364695 | -80.025960 |
| FBL052 | 35.364695 | -80.025960 |
| FBL053 | 35.364695 | -80.025960 |
| FBL054 | 35.364695 | -80.025960 |
| FBL055 | 35.676711 | -79.809474 |

| **Virgilina** | | |
|---|---|---|
| FBL031 | 35.812044 | -79.362232 |
| FBL032 | 35.812044 | -79.362232 |
| FBL033 | 35.812044 | -79.362232 |
| FBL034 | 35.812044 | -79.362232 |
| FBL035 | 35.728649 | -79.421146 |
| FBL036 | 35.730079 | -79.422931 |
| FBL037 | 35.731358 | -79.424907 |
| FBL038 | 35.730247 | -79.431674 |
| FBL043 | 36.266542 | -78.896403 |
| FBL044 | 36.266542 | -78.896403 |
| FBL045 | 36.266542 | -78.896403 |
| FBL046 | 36.266542 | -78.896403 |
| FBL047 | 36.119729 | -78.947456 |
| FBL048 | 36.119729 | -78.947456 |
| FBL049 | 36.119729 | -78.947456 |
| FBL050 | 36.119729 | -78.947456 |
| FBL060 | 35.974029 | -79.112614 |
| FBL061 | 35.973640 | -79.113044 |
| FBL062 | 35.974947 | -79.113645 |
| FBL063 | 35.959622 | -79.105062 |
| FBL064 | 35.960211 | -79.105802 |
| FBL065 | 35.959996 | -79.105863 |
| FBL066 | 36.117253 | -78.948143 |
| FBL067 | 36.120187 | -78.945789 |
| FBL068 | 36.263320 | -78.894653 |
| FBL069 | 36.269470 | -78.897860 |

## ROCKS ERODED FROM THE SLATE BELT

Paleozoic intrusive rocks in the slate belt show that a considerable thickness of supracrustal rock has been eroded from the slate belt above the present level of exposure. The plutons range from about 600 Ma to 300 Ma (Scott Samson et al., 1995a; Tadlock and Loewy, 2006), and they are exposed only because several kilometers of overlying rock was eroded after intrusion. We show later that the preserved

Virgilina and Albemarle rocks are both the oldest units of subduction-zone suites that may once have been overlain by other rocks now lost by erosion.

The intrusive rocks also demonstrate that collision of the slate belt with eastern North America occurred when the intervening ocean basin was consumed by subduction under the slate belt. This direction of subduction is consistent with the observation that subduction beneath accreting terranes occurred on all sides of North America in the Paleozoic (Rogers and Bernosky, 2008).

## VIRGILINA ROCKS ANALYZED

The Virgilina sequence is compositionally bimodal, with very few andesites and a ratio of mafic/felsic rocks that may be slightly higher than in the Albemarle sequence. All of the analyzed felsic rocks are lithified tuffs. Some are aphyric, but most contain small phenocrysts of plagioclase and sparse quartz. The rocks are generally less siliceous than rocks of the Albemarle sequence and can be regarded as dacites. None of the analyzed rocks contain xenoliths or debris from other sources, and we consider the chemical analyses to be representative of the composition of the eruptive units. Locations of the felsic samples are shown in Table 1.

The analyzed basalts of the Virgilina suite all appear to be flow rocks, with one sample both pillowed and amygdaloidal (Wilson and Allen, 1968). All samples show the effects of metamorphism to upper greenschist facies, with most samples containing fine-grained epidote, opaque minerals, sparse actinolitic amphibole, and ubiquitous sericitic alteration of the plagioclase. The three samples of basalt analyzed were all obtained near Hillsborough, North Carolina, and their locations can be obtained from the North Carolina Geological Survey: Contact Phil Bradley, Piedmont Geologist, by email at pbradley@ncdenr.gov.

## ALBEMARLE ROCKS ANALYZED

The Albemarle sequence is compositionally bimodal. It consists mostly of felsic rocks, with minor basalt and only small amounts of andesite (Seiders, 1978; Feiss, 1982). All of the felsic rocks that we analyzed are broadly identified as rhyodacites. Many of the rocks are aphyric, but some contain limited numbers of phenocrysts that consist entirely of quartz and sodic plagioclase. Some of the rocks are flows, but most were probably erupted pyroclastically and then lithified. They include a few breccias, but most are tuffaceous. The distinctive rocks of Morrow Mountain are fine-grained distal ignimbrites that were so hot that they apparently revitrified immediately after eruption. None of our analyzed rocks contain xenocrysts or fragments of other rocks, and we regard all of our analyses as representative of uncontaminated eruptive units. Locations of all of the felsic rocks are shown in Table 1.

Mafic rocks of the Albemarle sequence analyzed in this study include one sample of the Yadkin Formation and one of the Flat Swamp member of the Cid formation. Their locations can be obtained from the North Carolina Geological Survey: Contact Phil Bradley, Piedmont Geologist, by email at pbradley@ncdenr.gov. Both samples consist mainly of chlorite and other hydrous minerals that preserve a texture that probably formed by pyroclastic eruption.

## COMPOSITIONS OF FELSIC ROCKS

Table 2 shows average compositions of felsic rocks in both the Virgilina and Albemarle sequences. For comparison, we also include compositions of representative suites from known tectonic environments. The Water Island Formation was formed above an intra-oceanic subduction zone in the U.S. Virgin Islands. The early Andes suites were formed above a subduction zone beneath the continental margin of Chile.

Analyzed members of the Virgilina sequence have $SiO_2$ concentrations of about 70%, consistent with their classification as dacites. In addition to having slightly lower $SiO_2$ concentrations than Albemarle rocks. The Virgilina rocks have higher (and extremely variable) $Na_2O/K_2O$ ratios that average 14.3. This high average of ratios results from ratios in a

**Table 2. Average compositions of felsic rocks in Slate Belt and comparable suites**

| | Uwharrie | Tillery | Morrow Mtn. | Cid | Virgilina | Water Island | early Andes |
|---|---|---|---|---|---|---|---|
| $SiO_2$ | 77.9 | 75.7 | 76.2 | 75.5 | 71.3 | 74.0 | 71.7 |
| $TiO_2$ | 0.16 | 0.11 | 0.10 | 0.19 | 0.33 | 0.30 | 0.46 |
| $Al_2O_3$ | 11.7 | 12.8 | 12.5 | 12.6 | 13.6 | 11.2 | 13.9 |
| $Fe_2O_3$ | 1.55 | 1.36 | 1.52 | 1.88 | 2.86 | 4.66 | 1.08 |
| MgO | 0.17 | 0 | 0 | 0.28 | 0.96 | 3.37 | 0.22 |
| CaO | 0.71 | 0.35 | 0.41 | 0.62 | 1.21 | 0.89 | 2.58 |
| $Na_2O$ | 4.44 | 6.16 | 6.09 | 5.85 | 6.61 | 4.64 | 3.05 |
| $K_2O$ | 2.80 | 3.17 | 2.80 | 2.64 | 2.40 | 1.07 | 4.59 |
| $Na_2O/K_2O$ | 2.27 | 1.48 | 2.50 | 1.86 | 14.33 | 8.36 | 0.63 |
| | | | | | | | |
| Rb | 81 | 84 | 90 | 72 | 81 | 18 | 143 |
| Sr | 98 | 46 | 62 | 102 | 203 | 17 | 56 |
| Y | 39 | 63 | 64 | 65 | 39 | 0.2 | 31 |
| Zr | 145 | 174 | 167 | 239 | 226 | 203 | 195 |

Notes:
1. All values are anhydrous.
2. Major elements are in percent by weight. Trace elements are in ppm.
3. $Fe_2O_3$ is total iron calculated as $Fe_2O_3$.
4. Water Island is average of 12 samples of felsic rocks analyzed by Jolly et al. (2008).
5. Early Andes is the average composition of felsic rocks from the Lo Prado and Veta Negra Formations (Vergara et al., 1995).
6. $Na_2O/K_2O$ ratio is average of individual ratios, not the ratio of the averages.

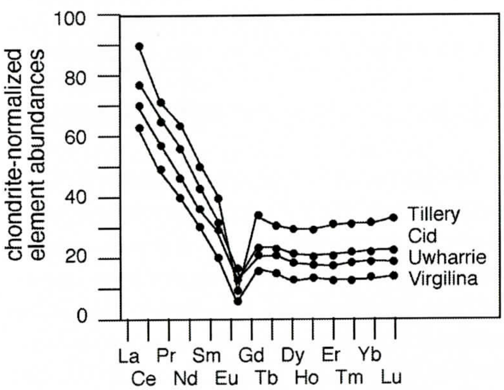


**Figure 3. REE patterns of average compositions of felsic rocks from the Albemarle and Virgilina sequences. Based on data in Steponaitis et al. (2006). Locations and identification of samples are in Table 1.**

few individual rocks as high as 250. Rare earth patterns (Figure 3) are similar to those in Albemarle rocks, with high LREE/HREE and pronounced negative Eu anomalies.

Most members of the Albemarle sequence have $SiO_2$ concentrations of 75% or greater and $Na_2O/K_2O$ ratios in the range of 1.5 to 2 (Table 2). These values and the concentrations of other major elements are consistent with petrography that classifies the Albemarle rocks as rhyodacites. Rare earth patterns (Figure 3) are steep, with high LREE/HREE and pronounced negative Eu anomalies.

## COMPOSITIONS OF MAFIC ROCKS

Table 3 shows the compositions of basaltic rocks in the Virgilina and Albemarle suites and in rocks from other suites known to have formed above subduction zones (Maricao Formation in the Caribbean and Lo Prado and Veta Negra Formations in the Andes). Figure 4 shows average REE patterns for both suites.

## ND ISOTOPE DATA FOR VIRGILINA AND ALBEMARLE SUITES

The Virgilina and Albemarle sequences

**Table 3. Average compositions of mafic rocks in Slate Belt and comparable suites**

| | Albemarle | Virgilina | Maricao | early Andes |
|---|---|---|---|---|
| $SiO_2$ | 51.1 | 49.9 | 50.2 | 50.5 |
| $TiO_2$ | 0.81 | 1.06 | 1.14 | 0.92 |
| $Al_2O_3$ | 18.5 | 19.9 | 15.3 | 20.3 |
| $Fe_2O_3$ | 11.7 | 11.3 | 11.5 | 9.8 |
| MgO | 6.85 | 6.22 | 7.87 | 4.5 |
| CaO | 5.67 | 7.21 | 11.0 | 8.8 |
| $Na_2O$ | 4.19 | 3.98 | 3.05 | 3.5 |
| $K_2O$ | 1.21 | 0.91 | 0.63 | 1.7 |
| $Na_2O/K_2O$ | 3.43 | 4.87 | 4.84 | 2.1 |
| | | | | |
| Rb | 14 | 17 | 5.9 | 56 |
| Sr | 14 | 441 | 222 | 575 |
| Y | 22 | 19 | 10.7 | 17 |
| Zr | 44 | 66 | 15.9 | 51 |
| Nb | 2.7 | 1.85 | 4.9 | 1.33 |
| Ta | 0.15 | 0.02 | 0.30 | 0.12 |

Notes:
1. All values are anhydrous.
2. Major elements are in percent by weight. Trace elements are in ppm.
3. $Fe_2O_3$ is total iron calculated as $Fe_2O_3$.
4. $Na_2O/K_2O$ ratio is average of individual ratios, not the ratio of the averages.
5. Maricao basalt of the northern Caribbean is from Jolly et al. (2001)
6. Early Andes is the average composition of mafic rocks from the Lo Prado and Veta Negra Formations of Chile (Vergara et al., 1995).

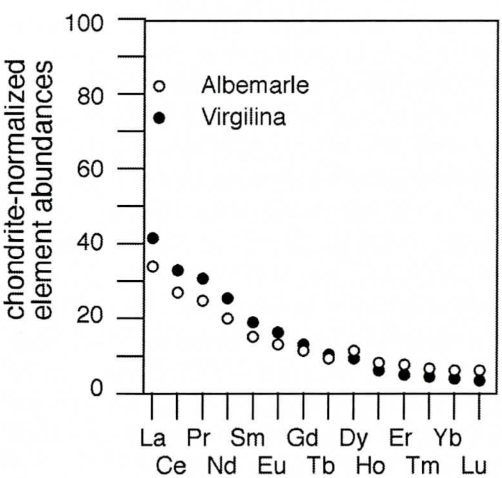


**Figure 4. Average REE patterns of mafic rocks of the Virgilina and Albemarle sequences.**

show very different relationships between $T_{DM}$ and eruption ages (Table 4). All of the Albemarle magmas were erupted at about 550 Ma, but $T_{DM}$ ages range from 750 Ma in the Uwharrie Formation up to 1050 Ma in overlying formations.

Differences between $T_{DM}$ and eruption ages are much smaller in the Virgilina suite. Most of the magmas were erupted at about 625 Ma from lithosphere with $T_{DM}$ ages about 750 Ma.

## ENVIRONMENTS OF ERUPTION OF VIRGILINA AND ALBEMARLE SEQUENCES

We use five criteria to identify the environments of formation of the Virgilina and Albemarle sequences: 1) frequency distribution of $SiO_2$; 2) $Na_2O/K_2O$ ratios of felsic rocks; 3)

**Table 4. Average $T_{DM}$ of rocks in Slate Belt**

| Suite | no. samples | $T_{DM}$ (Ma) |
|---|---|---|
| Uwharrie felsic | 9 | 1131 |
| Tillery felsic | 7 | 1057 |
| Morrow Mtn. felsic | 4 | 1104 |
| Cid felsic | 9 | 906 |
| Yadkin mafic | 2 | 1593 |
| Virgilina felsic | 24 | 769 |
| Virgilina mafic | 2 | 900 |

differences between $T_{DM}$ and eruption age; 4) concentrations of high-field-strength (HFS) elements, particularly Ti, Zr, Nb, and Ta, in mafic rocks; and 5) REE patterns in mafic rocks.

Both the Virgilina and Albemarle sequences have bimodal $SiO_2$ distributions, with subequal amounts of mafic and felsic rocks. These bimodal distributions occur in rock suites formed in primitive island arcs, in continental rifts, and during the initial stages of subduction beneath continental margins.

Average $Na_2O/K_2O$ ratios of approximately 14 in Virgilina felsic rocks are characteristic of rocks erupted in primitive intra-oceanic island arcs, and $Na_2O/K_2O$ ratios in the range of 1–3 in Albemarle felsic rocks are consistent with eruption on continental crust (Riecker, 1979; Donnelly and Rogers, 1980; Vergara et al., 1995).

The $T_{DM}$ ages about 100 million years older than eruption of the Virgilina rocks suggest that the suite was erupted on oceanic lithosphere that was still developing when the magmas formed. Conversely, $T_{DM}$ ages more than 200 million years older than eruption ages demonstrate that all of the Albemarle magmas were generated on older lithosphere (e.g., DePaolo, 1981).

Average concentrations of $TiO_2$ (1.06%), Zr (66 ppm), Nb (1.85 ppm), and Ta (0.02 ppm) in the Virgilina basalts indicate their formation above a subduction zone, apparently in a primitive island arc (Donnelly and Rogers, 1980; Tatsumi, 2005; Jolly et al., 2007, 2008). Similarly, concentrations of $TiO_2$ (0.8%), Zr (22 ppm), Nb (2.7 ppm), and Ta (0.15 ppm) in the Albemarle basalts, are also typical of basalts formed above a subduction zone, probably in a continental-margin (Xiong et al., 2005). The HFS element concentrations of Albemarle basalts are lower than any concentrations reported from basalts in modern rifts (McMillan et al., 2000; Macdonald et al., 2001).

The REE patterns of mafic rocks in both the Virgilina and Albemarle sequences are typical of rocks formed above subduction zones.

All of our five criteria suggest that The Virgilina rocks formed above an intra-oceanic subduction zone that developed a few tens of millions of years before 600 Ma. Subduction probably did not cease until after the Virgilina suite was incorporated into the slate belt and accreted to North America, but any evidence that the Virgilina arc progressed to a mature arc dominated by andesites has been destroyed by erosion.

The environment of formation of the Albemarle suite is based on the same criteria that were used for the Virgilina rocks. The low $Na_2O/K_2O$ ratios and differences of about 500 million years between $T_{DM}$ and eruption age both demonstrate that Albemarle rocks developed on continental crust (DePaolo, 1981). The bimodal $SiO_2$ distribution and absence of andesites suggests that the Albemarle suite formed during the very early stages of subduction because subduction beneath even a thin continental margin generally creates suites containing andesites with typical concentrations of 60% $SiO_2$ (Rogers and Ragland, 1980).

The proposed environment of formation of the Albemarle suite appears to be similar to an environment in which volcanism occurred during the earliest stages of development of the Andes. Although the present Andes mountains are dominated by andesitic volcanism on a thick continental crust, Vergara et al. (1995) showed that initial subduction formed basalt–rhyolite suites erupted into shallow marine basins on the continental margin. Andesites did not form until subduction continued and the crust became thicker (Kay and Ramos, 2006).

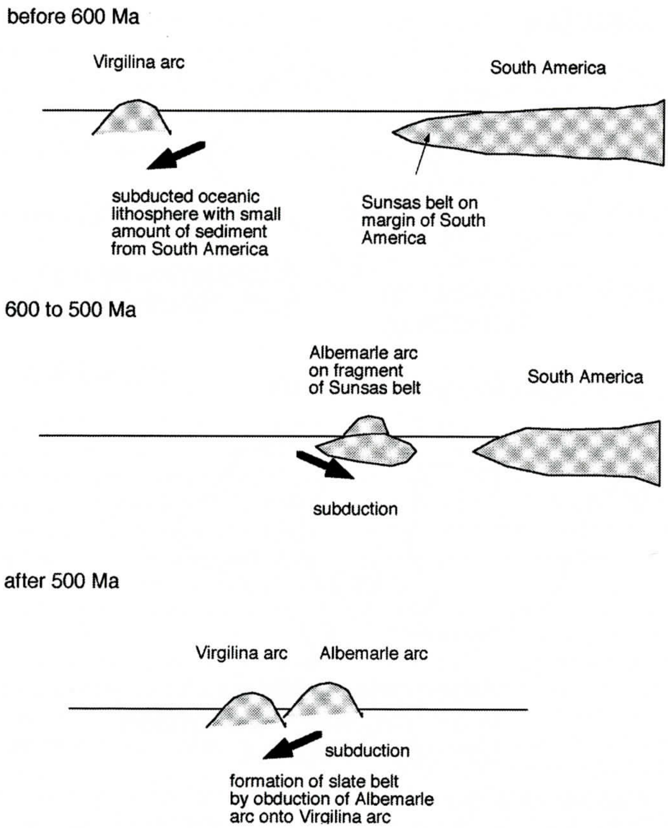


**Figure 5. Environments of evolution of the Albemarle and Virgilina sequences.**

## RELATIONSHIP BETWEEN ALBEMARLE AND VIRGILINA SEQUENCES

The contact between the Albemarle and Virgilina sequences is not exposed. Although Hibbard et al. (2007) suggested that the contact is an unconformity at the base of the overlying Albemarle sequence, Nd isotope and other compositional data show that the Albemarle rocks could not have been deposited on a Virgilina substrate. The $T_{DM}$ values of Albemarle volcanic rocks are so much older than the $T_{DM}$ values of the Virgilina sequence that Albemarle magmas must have been derived from an old source such as the continental margin of South America. Eruption on a continental margin is supported by the comparatively low $Na_2O/K_2O$ ratios of Albemarle rocks. Consequently, we interpret the Albemarle–Virgilina contact as a fault.

## MODEL FOR EVOLUTION OF THE SLATE BELT

The breakup of Rodinia created an ocean basin between eastern North America and the western edge of the Amazonian part of South America (both continents in present orientations). The margins of the separated continents were mostly along 1000-Ma orogenic belts (Grenville in North America; Sunsas in South America).

The time of separation is uncertain, but it was presumably earlier than 800 Ma because oceanic lithosphere was dense enough to subduct and create an intra-oceanic island arc shortly before 600 Ma (Figure 5). At the same time, or perhaps slightly later, subduction under the margin of Amazonia began to develop the Albemarle suite. Rifting of the Albemarle rocks and their underlying lithosphere from South America probably occurred within a few tens of million

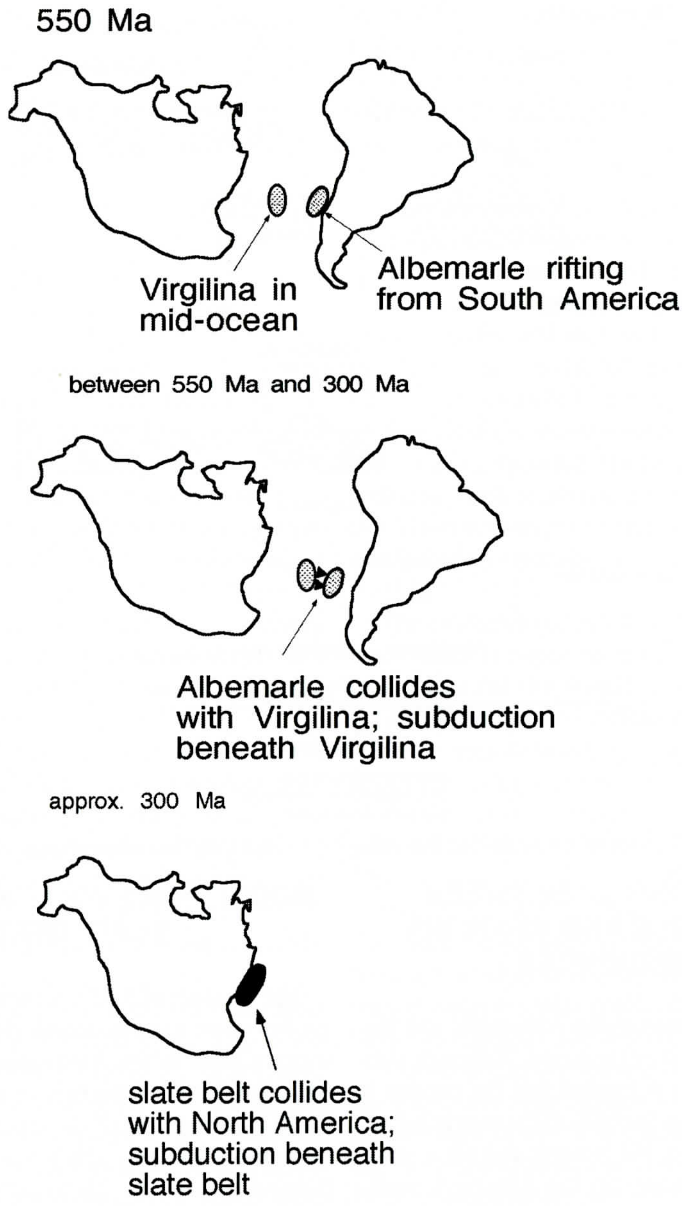


**Figure 6. Model of evolution of the Carolina slate belt. The Albemarle sequence developed on western South America. This block then drifted across the ocean toward North America and collided with the Virgilina arc by subduction beneath the arc. The merger of the Albemarle and Virgilina terranes created the slate belt, which collided with eastern North America in the middle to late Paleozoic.**

years after subduction began, but that time is not certain.

Subduction continued beneath the Virgilina arc as the Albemarle terrane approached it, and subduction may also have continued beneath the Albemarle terrane (Figure 6). At some time before 300 Ma the Virgilina and Albemarle suites fused to form the slate belt. Subduction beneath the slate belt continued until it collided with eastern North America at about 300 Ma.

By this time, the slate belt was probably covered by a thick sequence of lower Paleozoic supracrustal rocks. These rocks probably contained andesites, but details are unknown because they have all been removed by erosion.

## ACKNOWLEDGMENT

We thank Joseph Forrest for help in locating and collecting basalt samples.

## REFERENCES

Bradley, P, Gay, K., and Clark, T., 2006, An overview of new geologic mapping of the Chapel Hill, Hillsborough, and Efland 7.5-minute quadrangles, Orange and Durham Counties, Carolina Terrane, North Carolina. in Bradley, P. J., and Clark, T. W., eds., The geology of the Chapel Hill, Hillsborough, and Efland 7.5-minute quadrangles, Orange and Durham Counties, Carolina Terrane, North Carolina. Carolina Geological Society Guidebook 2006, p. 1–16.

Bradley, P. J., and Clark, T. W., eds., 2006, The geology of the Chapel Hill, Hillsborough, and Efland 7.5-minute quadrangles, Orange and Durham Counties, Carolina Terrane, North Carolina. Carolina Geological Society Guidebook 2006.

Conley, J. F, and Bain, G. L., 1965, Geology of the Carolina slate belt west of the Deep River-Wadesboro Triassic basin, North Carolina. Southeastern Geology, v. 6, p. 117–138.

Dennis, A. J., and Shervais, J. W., 1996, The Carolina Terrane in northwestern South Carolina; insights into the development of an evolving island arc. in Nance, R. D., and Thompson, M. D., eds., Avalonian and related peri-Gondwanan terranes of the Circum-North Atlantic. Geological Society of America Special Paper 304, p. 237–256.

Dennis, A. J., Shervais, J. W., Mauldin, J., Maher, H. D., and Wright, J. E., 2004, Petrology and geochemistry of Neoproterozoic volcanic arc terranes beneath the Atlantic coastal plain, Savannah River site, South Carolina. Geological Society of America Bulletin, v. 116, p. 572–593.

DePaolo, D. J., 1981, Nd isotopic studies: Some new perspectives on Earth structure and evolution. Eos, v. 14, p. 137–140.

D'Lemos, R. S., Strachan, R. A., and Topley, C. G. eds., 1990, The Cadomian orogeny. Geol. Soc. London Spec. Paper 51, 423 pp.

Donnelly, T. W., and Rogers, J. J. W., 1980, Igneous series in island arcs - The northeastern Caribbean compared with worldwide island-arc assemblages: Bulletin Volcanologique, v. 43, p. 347-382.

Feiss, P. G., 1982, Geochemistry and tectonic setting of the volcanics of the Carolina slate belt. Economic Geology and the Bulletin of the Society of Economic Geologists, v. 77, p. 273–293.

Gibson, G. G, 1989, Trace fossils from late Precambrian Carolina slate belt, south-central North Carolina. Journal of Paleontology, v. 63, p. 1–10.

Gibson, G. G, Teeter, S. A, and Fedonkin, M. A., 1984, Ediacaran fossils from the Carolina slate belt, Stanly County, North Carolina. Geology, v. 12, p. 387–390.

Glover, L., III, and Sinha, A., 1973, The Virgilina deformation, a late Precambrian to early Cambrian(?) orogenic event in thee central piedmont of Virginia and North Carolina. American Journal of Science, v. 273A, p. 234–251.

Harris, C. W, 1984, Coarse-grained submarine-fan deposits of magmatic arc affinity in the late Precambrian Aaron Formation, North Carolina, U.S.A. Precambrian Research, v. 26, p. 285–306.

Harris, C. W., and Glover, L., III, 1988, The regional extent of the ca. 600 Ma Virgilina deformation; implications for stratigraphic correlation in the Carolina Terrane. Geological Society of America Bulletin, v. 100, p. 200–217.

Hibbard, J., Stoddard, E., Secor, D., and Dennis, A., 2002, The Carolina zone: overview of Neoproterozoic to early Paleozoic peri-Gondwanan terranes along the eastern flank of the Appalachians. Earth Science Reviews., v. 57, p. 299–339.

Hibbard, J., McMenamin, M. A. S, Pollock, J., Weaver, P.G., Tacker, R. C., Miller, B. V., Samson, S., and Secor, D., 2006, Significance of a new Ediacaran fossil find in the Albemarle Group, Carolina terrane of North Carolina. in Bradley, P.J., and Clark, T. W., eds., The geology of the Chapel Hill, Hillsborough, and Efland 7.5-minute quadrangles, Orange and Durham Counties, Carolina Terrane, North Carolina. Carolina Geological Society Guidebook 2006, p. 29–34.

Hibbard, J. P., van Staal, C. R., and Rankin, D. W., 2007a, A comparative analysis of pre-Silurian crustal building blocks of the northern and southern Appalachian orogen. American Journal of Science, v. 307, p. 23–45.

Hibbard, J., van Staal, C., and Miller, B., 2007b, Links between Carolinia, Avalonia, and Ganderia in the Appalachian peri-Gondwanan Realm, in Sears, J., Harms, T., and Evenchick, C., eds., From Whence the Mountains?: Inquiries into the Evolution of Orogenic Systems: A Volume in Honor of Raymond A. Price, Geological Society of America Special Paper 433, p. 291–311.

Hibbard, J.P., Pollock, J.C., Brennan, M., Samson, S.D., and Secor, D., 2009, Significance of New Ediacaran Fossils and U?Pb Zircon Ages from the Albemarle Group, Carolina Terrane of North Carolina. Journal of Geology, v. 117, p. 487¬498.

Ingle, S., Mueller, P. A, Heatherington, A.L., and Kozuch, M., 2003, Isotopic evidence for the magmatic and tectonic histories of the Carolina terrane; implications for stratigraphy and terrane affiliation. Tectonophysics, v. 371, p. 187–211.

Jolly, W. T., Schellekens, J. H., and Dickin, A. P., 2007, High-Mg andesites and related lavas from southwest Puerto Rico (Greater Antilles island arc): petrogenetic links with emplacement of the late Cretaceous Caribbean mantle plume. Lithos, v. 98, p. 1–26.

Jolly, W. T, Lidiak, E. G., and Dickin, A. P., 2008, Bimodal volcanism in northeast Puerto Rico and the Virgin Islands (Greater Antilles island arc); genetic links with Cretaceous subduction of the Mid-Atlantic ridge Caribbean spur. Lithos, v. 103, p. 393–414

Kay, S. M., and Ramos, V. A., eds., 2006, Evolution of an Andean margin: A Tectonic and Magmatic View from the Andes to the Neuquén Basin (35°–39°S lat). Geological Society of America Special Paper 407.

Landing, E., Westrop, S. R., and Kim, D. H., 2003, First Middle Ordovician biota from southern New Brunswick; stratigraphic and tectonic implications for the evolution of the Avalon continent. Canadian Journal of Earth Sciences, v. 40, p. 715–730.

LeHuray, A. P., 1987, U–Pb and Th-Pb whole-rock isochrons from metavolcanic rocks of the Carolina slate belt. Geological Society of America Bulletin, v. 100, p. 354–361.

LeHuray, A. P., 1989, U-Pb and Th–Pb whole rock studies in the Southern Appalachian Piedmont. Southeastern Geology, v. 30, p. 77–94.

Macdonald, R., Rogers, N. W., Fitton, J. G., Black, S., and Smith, M., 2001, Plume-lithosphere interactions in the generation of the basalts of the Kenya Rift, East Africa. Journal of Petrology, v. 42, p. 877–900.

Mallard, L. D., and Rogers, J. J. W., 1997, Relationship of Avalonian and Cadomian terranes to Grenville and Pan-African events. Journal of Geodynamics, v. 23, p. 197–221.

McMenamin, M. A S., and Weaver, P. G., 2004, Middle Cambrian polymeroid trilobites and correlation of Carolina and Augusta Terranes. Southeastern Geology, v. 43, p. 21–38.

McMillan, N. J., Dickin, A, P., and Haag, D., 2000, Evolution of magma source regions in the Rio Grande rift, southern New Mexico. Geological Society of America Bulletin, v. 112, p. 1582–1593.

Milton, D. J., 1984, Revision of the Albemarle Group, North Carolina. U. S. Geological Survey Bulletin, Report: B 1537-A, p. A69-A72

Mueller, P. A., Kozuch, M., Heatherington, A. L, Wooden, J. L, Offield, T. W., Koeppen, R. P., Klein, T. L., and Nutman, A. P., Jr., 1996, Evidence for Neoproterozoic basement in the Carolina terrane and speculations on its origin; speculations on its origin. in Nance, R. D., and Thompson, M. D., eds., Avalonian and related peri-Gondwanan terranes of the Circum-North Atlantic, Geological Society of America Special Paper 304.

North Carolina Geological Survey, 1991, Geologic map of North Carolina.

Parnell, D., Blake, D. E., and Bradley, P., 2006, Geochemical correlation and tectonic setting of the northeastern Carolina zone in North Carolina. in Bradley, et al., Carolina Geological Society Guidebook, p. 47–68.

Pollock, J.G., 2007, The Neoproterozoic-Early Paleozoic tectonic evolution of the peri-Gondwanan margin of the Appalachian orogen: an integrated geochronological, geochemical and isotopic study from North Carolina and Newfoundland. Unpublished Ph.D. Dissertation, North Carolina State University.

Riecker, R. E., ed., 1979, Rio Grande rift tectonics and magmatism. Washington, DC, American Geophysical Union.

Rogers, J. J. W, 1999, History and Environment of North Carolina's piedmont. on the web at www.geosci.unc.edu/faculty/rogers.piedmont_hist_env.pdf.

Rogers, J. J. W., and Bernosky, S., 2008, Differences between Paleozoic Asia Paleozoic North America as shown by the distribution of ultra-high-pressure (UHP) terranes. Gondwana Research, v. 13, p. 428–433.

Rogers, J. J. W., and Ragland, P. C., 1980, Trace elements in continental-margin magmatism - Part I. Trace elements in the Clarno Formation of central Oregon and the nature of the continental margin on which eruption occurred: Geological Society of America Bulletin, v. 91, Part I - p. 196–198, Part II - Card 3, p. 1217–1292.

Samson, Sara, Palmer, A. R., Robison, R. A., and Secor, D. T, Jr., 1990, Biogeographical significance of Cambrian trilobites from the Carolina slate belt. Geological Society of America Bulletin, v. 102, p. 1459–1470.

Samson, Scott D., Hibbard, J P., and Wortman, G L, 1995a, Nd isotopic evidence for juvenile crust in the Carolina terrane, Southern Appalachians. Contributions to Mineralogy and Petrology, v. 121, p. 171–184.

Samson, Scott D., Coler, D. G, and Speer, J. J., 1995b, Geochemical and Nd–Sr–Pb isotopic composition of Alleghanian granites of the Southern Appalachians; origin, tectonic setting, and source characterization. Earth and Planetary Science Letters, v. 134, p. 359–376.

Secor, D. T, Jr., Samson, S. L, Snoke, A. W, and Palmer, A., 1983, Confirmation of the Carolina slate belt as an exotic terrane. Science, v. 221, p. 649–651.

Seiders, V. M., 1978, A chemically bimodal, calc-alkalic suite of volcanic rocks, Carolina volcanic slate belt, central North Carolina. Southeastern Geology, v. 19, p. 241–265.

Steponaitis, V. P., Irwin, J. D., McReynolds, T.E., and Moore, C., eds., 2006, Stone Quarries and Sourcing in the Carolina Slate Belt. Research Report 25 of the Research Laboratories of Archaeology, University of North Carolina at Chapel Hill.

Tadlock, K. A., and Loewy, S. L., 2006, Isotopic characterization of the East Farrington pluton constraining the Virgilina orogeny. in Bradley, P. J., and Clark, T. W., eds., The geology of the Chapel Hill, Hillsborough, and Efland 7.5-minute quadrangles, Orange and Durham Counties, Carolina Terrane, North Carolina. Carolina Geological Society Guidebook 2006, p. 17–22.

Tatsumi, Y., 2005, The subduction factory; how it operates in the evolving earth. GSA Today, v. 15, p.4–10.

Vergara, M., Levi, B., Nystrom, J. O., and Cancino, A., 1995, Jurassic and Cretaceous island arc volcanism, extension, and subsidence in the Coast Range of central Chile. Geological Society of America Bulletin, v. 107, p. 1427–1440.

Vick, H K., Channell, J E T., and Opdyke, N D, 1987, Ordovician docking of the Carolina slate belt; paleomagnetic data. Tectonics, v. 6, p. 573–583.

Weaver, P. G., Tacker, R. C., and McMenamin, M. A. S., 2006, Ediacaran body fossils of South–Central North Carolina; preliminary report. in Bradley, P. J., and Clark, T. W., Eds., The geology of the Chapel Hill, Hillsborough, and Efland 7.5-minute quadrangles, Orange and Durham Counties, Carolina Terrane, North Carolina. Carolina Geological Society Guidebook 2006, p. 35–42.

Whitney, J A., Paris, T A, Carpenter, R H, and Hartley, M E, III, 1978, Volcanic evolution of the southern Slate Belt of Georgia and South Carolina; a primitive oceanic island arc. Journal of Geology, v. 86, p. 173–192.

Wilson, W. F, and Allen, E. P, 1968, Spilitic amygdaloidal basalt flow rocks and associated pillow structure in Orange County, North Carolina. Southeastern Geology, v. 9, p. 133–141.

Wortman, G. L., Samson, Scott D., and Hibbard, J.P., 2000, Precise U-Pb zircon constraints on the earliest magmatic history of the Carolina Terrane. Journal of Geology, v. 108, p. 321–338.

Xiong, X. L., Adam, J., and Green, T. H., 2005, Rutile stability and rutile/melt HFSE partitioning during partial melting of hydrous basalt; implications for TTG genesis. Chemical Geology, v. 218, p. 339–359.

SOUTHEASTERN GEOLOGY
V. 47, No.1, February 2010, p. 15-26

# NATURAL OCCURRENCE OF ELEVATED ARSENIC AND SELENIUM IN GEORGIA REGOLITH: IMPLICATIONS FOR THEIR RELATIVE MOBILITY IN PIEDMONT SOILS

PAUL A. SCHROEDER

*Department of Geology*
*University of Georgia*
*Athens, Georgia 30602-2501*

## ABSTRACT

**Arsenic concentrations of >100 ppm were detected above the regional value of ~7 ppm in soils near the Georgia Brevard Zone using optical emission spectroscopy (OES). Natural, anthropogenic, and false-positive hypotheses were tested to determine a most likely explanation. Induction coupled plasma mass spectroscopy (ICP-MS), X-ray diffraction, optical microscopy, electron microprobe analysis, and historical aerial photographs were subsequently used to determine the most parsimonious hypothesis. ICP-MS results indicated positive detection and verified accuracy of the OES-measured As and concentrations of many other trace elements such as Se. Arsenopyrite is the primary As- and Se-bearing phase in the underlying mafic schist bedrock. The associated bedrock mineral assemblage suggests a fossil hydrothermal system protolith and subsequent prograde and retrograde moderate metamorphism. As/Se ratios in the 20m-thick saprolite are much higher (~2000) than regional baseline values for the SE United States (~15) and the underlying bedrock itself (~45). The high soil-saprolite As/Se ratio empirically supports a theoretical ionic potential basis for greater solubility and transport of Se (relative to As) out of the weathered zone and into rivers. Published As/Se ratios for biomonitor proxies living in rivers that drain through the Brevard Zone (~0.6) further support the idea that As in saprolites of the Piedmont in the SE United States is more conservative in fate and transport than Se.**

## INTRODUCTION

Arsenic (As) and selenium (Se) in soils of the southeastern United States (SE U.S.) have been generally mapped or delineated by low-density and shallow depth (<20 cm) soil sampling surveys of areas relatively unaffected by human activities (Shacklette and Boerngen, 1984) or by site-specific surveys of areas known to be significantly impacted by human activities (Kukier and others, 2001; Jackson, 1998). Canonical baseline values for As and Se in conterminous eastern U.S. surface soils are reported to be about 7 and 0.5 parts-per-million (ppm), respectively, resulting in an As/Se ratio of about 15 (Shacklette and Boerngen, 1984). Numerous international and national regulations and guidelines for As and Se exposure exist for air, water, and food because they are considered to cause adverse health effects when absorbed in high concentrations (Frankenberger, 2002). Examples of exposure limits include (1) the U.S. Environmental Protection Agency (EPA) recommendation of a maximum As contamination limit of 0.010 ppm for drinking water, (2) the U.S. Occupational Safety and Health Organization (OSHA) recommendation of a permissible As exposure limit of 0.01 mg/m$^3$ over an eight hour period, and (3) the U.S. Food and Drug Administration stipulation of As limits at 0.5 to 2.0 ppm for certain animal by-products treated with As-bearing drugs (Anonymous ATSDR report, 2006). The Georgia Environmental Protection Division (EPD) notes that releases resulting in As and Se concentrations in excess of 41 and 36 ppm, respectively requires notification (Georgia State rule 391-3-19-04). Concentrations of As and Se in soils are not specifically regulated by these guidelines, but are factored into the assessment of EPA's Na-

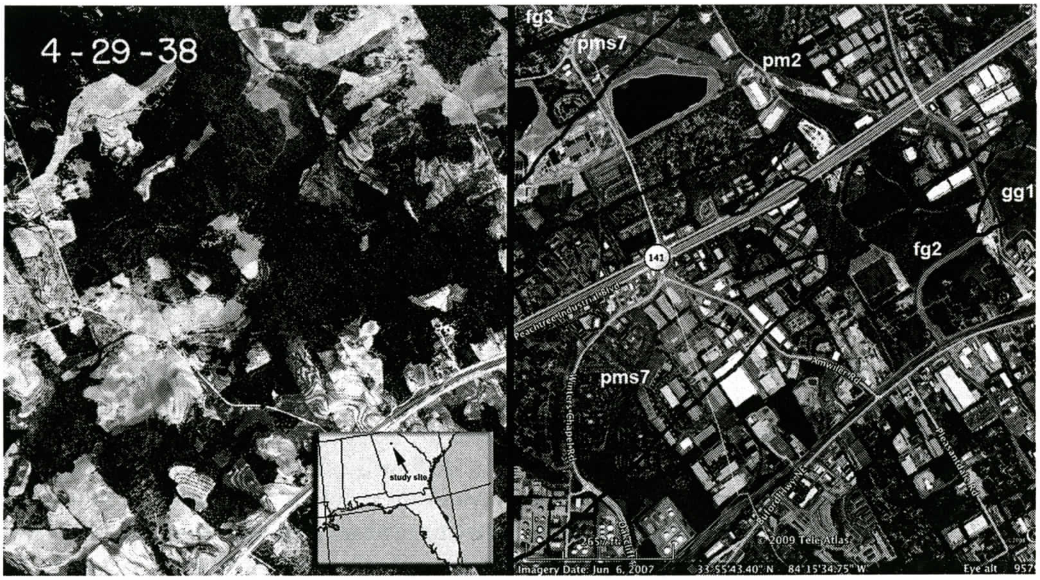


**Figure 1. Location map (inset) and aerial photographs of study site. Left image is 1938 photo showing primary land use as forested with remnants of agricultural tilling. Right photo shows 2007 use as mixed residential and industrial parks. Bold dark line in NW corner of right photo delineates SE extent of the Brevard Zone. Lines on right photo delineate formation contacts as published by (Dicken, 2005). All rocks are Precambrian-Cambrian with lithology noted by following symbols: fg2 -Biotitic Gneiss Undifferentiated; gg1 - Granitic Gneiss; pms7 - Button Mica Schist undifferentiated; fg3 - Biotitic Gneiss/Mica Schist/ Amphibolite; pm2 - Metagraywacke/ Mica Schist. Sample location is at 33° 55′ 43.40″ N, 84° 15′ 34.75″ W. Right photo modified from Google Earth © Tele Atlas.**

tional Priorities List promulgated by the 1980 U.S. Comprehensive Environmental Response, Compensation, and Liability Act (CERCLA). As part of due diligence associated with performing CERCLA-prompted Phase I and II environmental site assessments (standardized by EPA), soil As and Se concentrations in excess of regional background levels appear to be the threshold to report a potential for threat to human health and/or the environment. Georgia EPD release thresholds for reporting As and Se are about 6 and 72 times regional baseline values, respectively.

As and Se concentrations observed in excess of the regional background can be attributed to multiple factors. Anthropogenic factors and natural factors are the two main categories for explaining or finding elevated levels in soils. Human activities such as pesticide application, wood preservative production, coal fly ash production, and acid-sulfide mine tailing accumulations account for the major sources of anthropogenic As and Se contaminant sites in the SE United States (Frankenberger, 2002). The purpose of this study is to document a natural occurrence of elevated As and Se concentrations in soils and to provide empirical insights into their relative fate and transport in the near surface weathering environment of the Piedmont SE United States.

## BACKGROUND

The study site is located in the Piedmont of Georgia, Gwinnett County (Figure 1 inset) and was initially identified in response to reconnaissance work associated with a phase 1 assessment, in which As-bearing soils were noted in surface auger samples tested by optical emission spectroscopy (OES) (see more detailed comments below in methods selection). Causes for elevated As concentrations in the soil were considered with multiple working hypotheses, which included (1) a human source or (2) a natural source, or (3) false positive results. Common anthropogenic sources of As in the Georgia Piedmont include pesticide applications associated with control of the cotton boll weevil around the 1920's (Williams and others, 2005; Haney and others, 2009) and herbicide control for cotton growing, which occurred into the 1990's (Bednar and others, 2002). Historical aerial photography of the study site indicates it was utilized for agricultural purposes as far back as the 1930's, as evidenced by the plowing contours seen in Figure 1 (approximate center of left photo). The area has since rapidly developed into industrial parks and is now proximal to residential areas and major rail and road transportation lines (Figure 1, approximate center of right photo). Arsenopyrite has been reported in association with gold mining and tailings (EPA Report, 2003), the latter of which has been known to occur in north Georgia. If such tailings were transported to the site and dumped, then this represents a possible As and Se source.

Quadrangle-scale geologic mapping for this area indicates the study site is situated on lower Paleozoic metamorphic rocks with SW-NE trending structures (Higgins, 1968). These rocks have experienced numerous cycles of intrusion, folding, faulting, and deformation with the most recent influences of metamorphism associated with final stage collisions of Eurasian and North American Plates (200 to 230 Ma) and subsequent mafic dike emplacement related to cratonic rifting. Figure 1 shows approximate locations of formation contacts in the study area, as well as the trace of the Brevard Zone. The Brevard Zone is a narrow SW-NE trending feature with numerous interpretations and likely owes its origins to multiple mechanisms of thrust faulting, strike-slip faulting, overturned folding, and the development of complex features associated with prograde and retrograde metamorphism (Crawford and Kath, 2001). The study site (Figure 1) is mapped as "Button schist", a term noted by Higgins (1966) for the pattern of two distinct subparallel cleavages that appear upon weathering. These rocks occur throughout the Brevard Zone and are described as having crystalline texture resulting from metamorphic recrystallization under conditions of high viscosity, directed pressure, and some recrystallized after granulation (Reed, 1970).

## METHODS

Impetus for study was based on prior surface sampling of soils (<5 m) and using OES analysis via EPA method 6010C (Jones and others, 1987; Hassan and Loux, 1990), with some As concentrations reported above the regional baseline value of ~7 ppm. Reported OES-determined As concentrations ranged from 4 to 375 ppm. A two-point drilling program was conducted to continuously core from the surface through the saprolite and into the rock basement. Two hand-auger samples from approximately the same locations were also taken to a depth of approximately 1.5 m below the surface. The auger samples were immediately tested using Induction Coupled Plasma Mass Spectrometry (ICP-MS) because of the potential for false positive As testing by ICP-OES in the presence of Al-rich materials (Jones and others, 1987) and because the regional bedrock and soils are known to be aluminous (Higgins, 1966). ICP-MS technology is capable of simultaneous determination of up to 80 elements in a liquid sample in a single run of a few minutes. The mass-selective detector is extremely sensitive, particularly for heavier elements, giving very low, down to parts per trillion, detection limits. The detector system is also relatively immune to many of the chemical and spectroscopic interferences that plague ICP-OES systems (Hassan and Loux, 1990). Seventy-three elements were determined on individually extracted samples using a proprietary Perkin-Elmer Elan 6000 ICP-MS semi-quantitative element scan called "Total scanQuant." The instrument was also calibrated for As, Se and several other metals of environmental interest (including EPA regulated metals) and run using a proprietary calibrated technique called "fullQuant".

Cores were sampled approximately every meter (Table 1) and hand ground for ICP-MS and X-ray diffraction powder analysis (XRD) using a zirconium mortar and pestle with alcohol as a grinding agent. For soils, sediments,

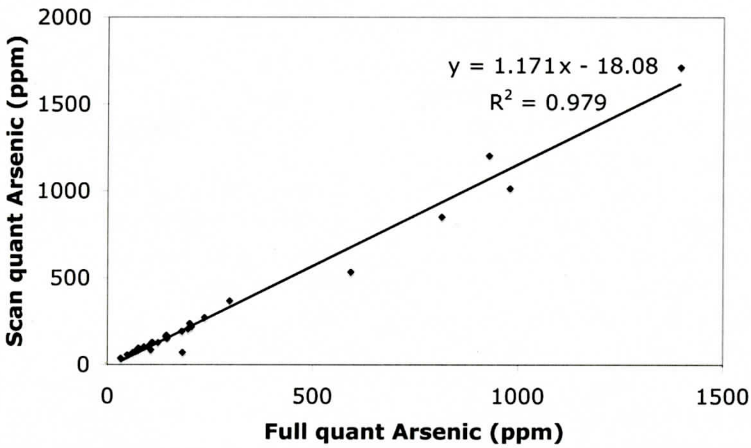


**Figure 2. Quantitative analysis of As concentration in cores #1 and #2 sampled in Gwinnett County, GA. Axes depict duplicate analyses using two different proprietary quantification schemes. Line represents least-squares minimization fit to the data assuming a linear model. Cross plot using Se values produces similar coefficients.**

rocks and organics, a boiling nitric acid digest was used to extract metals (EPA method 3050A). This involves digestion of the sample in concentrated nitric acid on a hot plate, followed by hydrogen peroxide to further oxidize organics and solubilize metals (Edgell, 1988). This works less well for soils and rock material and very well for highly organic samples (e.g., plant tissue). The concentrations reported herein therefore, may reflect slightly varied values relative to the total mass of the soil or rock because less soluble silica and aluminum oxide phases may not be totally dissolved. The hand auger near-surface soil samples measured by ICP-MS showed similar arsenic values to those measured by ICP-OES. It was therefore concluded that the measured arsenic concentrations using ICP-OES are accurate and grounds for nullifying the false positive hypothesis is justified.

The powdered bedrock material for XRD analysis was transferred to 30 x 30 mm mount and pressed to minimize transparency and preferred orientation. Data were collected using a Scintag diffractometer, with Co K$\alpha$ radiation, a 250 mm goniometer circle, 2°/4° primary and scattering slits, 0.5°/0.3° scattering and receiving slits, 40 kV and 35 mA, a step size of 0.01°, and a scan rate of 2° per minute. Selected pieces of the bedrock schist from the unweathered portion of the core were cut, polished, and prepared for electron microprobe analysis (EMPA) using wavelength dispersive spectroscopy (WDS) and backscatter secondary electron imaging (BSE). A representative thick section was cut perpendicular to foliation and fractures in the schist. The polished mount was carbon coated for EMPA-WDS using a JEOL JXA-8600 Superprobe. Beam current was 15 nA and accelerating voltage was 15 keV. Grains were analyzed for Fe, As, and, Se using natural and synthetic mineral standards.

## RESULTS

Coring resulted in the retrieval of 23 and 25m of continuous sampling for cores #1 and #2, respectively (Table 1). Saprolite thicknesses for each core are approximately 20m and 22m, respectively and approximately 3m of solid bedrock core were recovered from each drill hole. Foliations of the core are oriented with a dip of about 25°, which is slightly less than the regional dips of 36°-40° SE, published by Higgins and Crawford (2007). Table 1 includes depths sampled for ICP-MS analysis, with the solid line indicating sampling above and below the bedrock-saprolite interface.

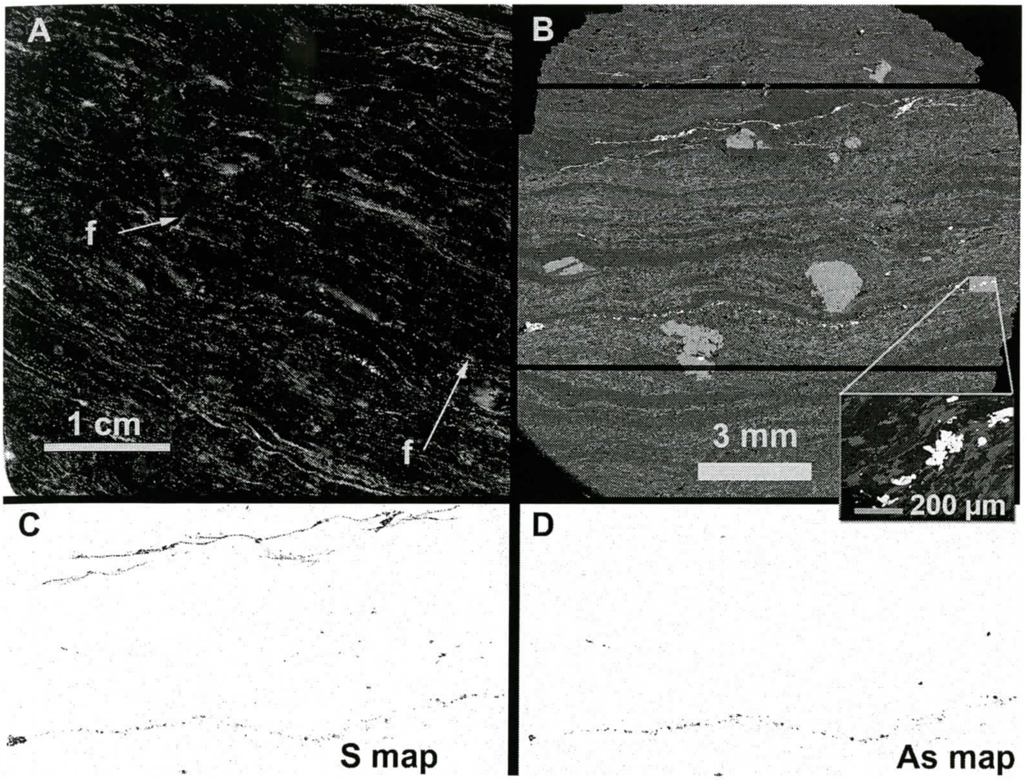


**Figure 3. Micrographic images of schist from core #2 (depth 21.8 m). A) Reflective light image of polished core section cut perpendicular to dipping foliations. With exception to occasional cross-cutting brittle fractures (f), all primary mineral fabrics appear to follow the foliation, B) BSE image reveals electron dense (brighter) minerals following foliation trends. Horizontal lines depict mapped areas shown below. Inset shows higher magnification view of arsenopyrite grains. C) Sulfur WDS map of same area shown above in BSE. Two dark bands (one in the top and other in bottom) highlight concentrations of pyrite (top) and arsenopyrite (bottom), D) Arsenic WDS map of same area shown above in BSE, but only lower dark band highlights concentration of arsenopyrite. Note As blebs follow foliations, while S follows both blebs in foliations and pyrite in fractures.**

ICP-MS duplicate analyses for As using the different quantitative approaches reveals values are reproducible over the range from 37 to 1710 ppm and having near unity correlation (Figure 2). A plot using Se scanQuant and fullQuant values (not shown) reveals linear trend coefficients similar to As, with the main difference being the concentration range, which varied from 0.03 to 6.12 ppm for Se. Semi-quantitative scanQuant ICP-MS results in Table 1 are reported to three significant figures. The focus of this study is the source and relative fate of As and Se, therefore discussion of other elemental trends is beyond the study scope, however data are provided for future workers.

XRD and optical analyses of the bedrock schist from the core hole bottom reveals a mafic minerals assemblage, with quartz, biotite, muscovite, garnet, clinochlore, albite, laumontite, and pyrite occurring as major phases (Figures 3 and 4). Foliation and fracture fabrics dominate the rock's texture. Included in the foliations are most all the above mineral grains, which appear to follow slight undulating mm-scale waves (Figures 3A and 3B). Cross-cutting brittle fractures comprises a fabric that is often filled with pyrite and laumontite. These fracture-fills clearly post-date the foliation and are indicative of retrograde metamorphism of a fossil hydrothermal system (Deer and others, 2004). Sulfur and

Table 1. ICP-MS FullQuant results for elemental concentrations using EPA extraction method 3010A. Concentrations are reported as ppm (mgkg).Solid line marks samples from above and below the saprolite/bedrock contact.

Core 1

| Depth (m) | Sc | Ti | V | Cr | Mn | Fe | Co | Ni | Cu | Zn | Ga | Ge | As | Se | Br | Rb | Sr | Y | Zr | Nb | Mo | Pd | Ag | Cd | In | Sn | Sb |
|---|---|---|---|---|---|---|---|---|---|---|---|---|---|---|---|---|---|---|---|---|---|---|---|---|---|---|---|
| 0.6 | 2.54 | 733 | 139 | 44.6 | 257 | 43200 | 13 | 27 | 22 | 115 | 15 | 0.14 | 70 | 0.92 | 0.52 | 119 | 4.5 | 43.9 | 14.6 | 0.07 | 0.19 | 0.03 | 0.02 | 0.04 | 0.08 | 1.05 | 0.01 |
| 1.8 | 1.35 | 555 | 102 | 42.4 | 732 | 48244 | 12 | 24 | 102 | 50 | 12 | 0.13 | 237 | 0.82 | 0.38 | 125 | 2.3 | 32.2 | 22.3 | 0.08 | 0.00 | 0.89 | 0.04 | 0.07 | 0.05 | 0.37 | 0.01 |
| 3.1 | 1.13 | 470 | 79 | 38.4 | 669 | 42964 | 23 | 26 | 49 | 68 | 10 | 0.12 | 163 | 0.61 | 0.27 | 84 | 3.0 | 21.3 | 15.9 | 0.07 | 0.14 | 0.01 | 0.03 | 0.07 | 0.04 | 0.45 | 0.00 |
| 4.3 | 2.50 | 648 | 155 | 50.5 | 1446 | 45588 | 29 | 39 | 20 | 123 | 15 | 0.15 | 130 | 0.68 | 0.94 | 106 | 4.7 | 32.1 | 16.7 | 0.05 | 0.00 | 0.04 | 0.05 | 0.14 | 0.07 | 0.19 | 0.01 |
| 5.8 | 2.68 | 732 | 122 | 62.8 | 334 | 39349 | 12 | 31 | 5 | 145 | 15 | 0.12 | 56 | 0.58 | 0.82 | 123 | 4.7 | 20.1 | 14.2 | 0.05 | 0.14 | 0.03 | 0.02 | 0.05 | 0.07 | 0.22 | 0.00 |
| 7.6 | 0.30 | 234 | 37 | 20.5 | 67 | 26473 | 5 | 9 | 44 | 40 | 4 | 0.07 | 97 | 0.51 | 0.46 | 196 | 3.3 | 14.0 | 12.6 | 0.11 | 0.38 | 0.01 | 0.02 | 0.08 | 0.01 | 0.11 | 0.00 |
| 8.5 | 0.81 | 534 | 66 | 30.4 | 298 | 36390 | 11 | 24 | 45 | 91 | 9 | 0.06 | 103 | 0.30 | 0.37 | 81 | 7.7 | 10.6 | 19.6 | 0.11 | 0.22 | 0.71 | 0.04 | 0.15 | 0.03 | 0.23 | 0.00 |
| 10.1 | 0.82 | 509 | 86 | 40.1 | 424 | 46291 | 18 | 35 | 38 | 39 | 9 | 0.07 | 162 | 0.42 | 0.44 | 103 | 7.3 | 11.6 | 14.2 | 0.12 | 0.19 | 0.44 | 0.06 | 0.23 | 0.03 | 0.23 | 0.01 |
| 11.6 | 1.97 | 746 | 158 | 32.0 | 666 | 45844 | 24 | 20 | 111 | 149 | 13 | 0.11 | 110 | 0.40 | 0.48 | 109 | 9.4 | 11.6 | 11.6 | 0.06 | 0.35 | 0.49 | 0.08 | 0.17 | 0.07 | 0.40 | 0.00 |
| 13.7 | 2.20 | 482 | 164 | 40.4 | 1057 | 72604 | 22 | 34 | 64 | 180 | 13 | 0.25 | 271 | 0.94 | 0.49 | 84 | 10.3 | 31.3 | 11.3 | 0.05 | 0.61 | 0.40 | 0.13 | 0.99 | 0.06 | 0.15 | 0.02 |
| 15.3 | 1.20 | 546 | 118 | 47.8 | 282 | 48175 | 25 | 29 | 53 | 61 | 10 | 0.10 | 218 | 0.54 | 0.31 | 97 | 10.1 | 17.4 | 9.9 | 0.09 | 0.65 | 0.03 | 0.07 | 0.27 | 0.04 | 0.38 | 0.01 |
| 19.2 | 0.77 | 412 | 88 | 39.7 | 86 | 33720 | 21 | 37 | 48 | 26 | 7 | 0.07 | 534 | 0.79 | 0.46 | 82 | 4.6 | 13.4 | 5.8 | 0.10 | 1.48 | 0.25 | 0.14 | 0.06 | 0.03 | 0.46 | 0.02 |
| 20.7 | 1.07 | 509 | 95 | 53.7 | 62 | 36521 | 31 | 41 | 68 | 38 | 10 | 0.04 | 1203 | 0.73 | 0.71 | 97 | 2.8 | 6.2 | 8.6 | 0.16 | 0.91 | 0.01 | 0.28 | 0.10 | 0.04 | 0.65 | 0.05 |
| 21.4 | 0.30 | 143 | 29 | 40.0 | 81 | 245774 | 20 | 177 | 132 | 70 | 7 | 0.14 | 86 | 3.13 | 0.84 | 9 | 44.0 | 13.6 | 11.6 | 0.21 | 1.16 | 0.10 | 0.24 | 1.73 | 0.04 | 0.83 | 0.87 |
| 21.8 | 0.80 | 69 | 9 | 8.5 | 18 | 37004 | 20 | 99 | 6 | 16 | 23 | 1.39 | 37 | 6.16 | 2.30 | 3 | 242.0 | 383.7 | 4.1 | 0.01 | 0.48 | 0.08 | 0.12 | 0.08 | 0.01 | 0.05 | 0.12 |

Core 2

| Depth (m) | Sc | Ti | V | Cr | Mn | Fe | Co | Ni | Cu | Zn | Ga | Ge | As | Se | Br | Rb | Sr | Y | Zr | Nb | Mo | Pd | Ag | Cd | In | Sn | Sb |
|---|---|---|---|---|---|---|---|---|---|---|---|---|---|---|---|---|---|---|---|---|---|---|---|---|---|---|---|
| 0.6 | 1.64 | 415 | 118 | 45.1 | 206 | 48436 | 15 | 35 | 85 | 50 | 12 | 0.08 | 86 | 0.79 | 0.62 | 31 | 2.6 | 9.3 | 9.2 | 0.21 | 0.58 | 0.02 | 0.13 | 0.04 | 0.05 | 0.43 | 0.03 |
| 1.8 | 2.53 | 633 | 160 | 109.2 | 673 | 43796 | 21 | 22 | 48 | 55 | 14 | 0.08 | 152 | 0.91 | 1.28 | 40 | 0.6 | 27.6 | 13.9 | 0.12 | 0.15 | 0.47 | 0.03 | 0.06 | 0.07 | 0.60 | 0.01 |
| 3.1 | 1.96 | 332 | 88 | 35.4 | 621 | 34396 | 8 | 9 | 36 | 64 | 12 | 0.06 | 1014 | 0.60 | 0.36 | 44 | 0.3 | 35.5 | 21.2 | 0.11 | 0.00 | 0.81 | 0.02 | 0.10 | 0.06 | 0.29 | 0.01 |
| 4.3 | 2.47 | 838 | 215 | 77.9 | 1094 | 59365 | 20 | 30 | 50 | 160 | 15 | 0.09 | 852 | 0.64 | 0.52 | 88 | 0.8 | 47.2 | 16.3 | 0.06 | 0.00 | 0.01 | 0.03 | 0.24 | 0.10 | 0.37 | 0.01 |
| 5.5 | 0.41 | 62 | 8 | 6.7 | 116 | 34848 | 7 | 25 | 20 | 58 | 3 | 0.04 | 72 | 0.64 | 0.51 | 12 | 6.4 | 10.3 | 8.2 | 0.05 | 0.00 | 0.03 | 0.03 | 0.30 | 0.02 | 0.26 | 0.23 |
| 6.7 | 1.02 | 531 | 66 | 34.2 | 292 | 34264 | 7 | 14 | 51 | 144 | 9 | 0.08 | 368 | 0.39 | 0.30 | 123 | 1.1 | 15.7 | 14.0 | 0.14 | 0.31 | 0.00 | 0.02 | 0.09 | 0.03 | 0.65 | 0.02 |
| 8.2 | 0.88 | 138 | 45 | 18.1 | 444 | 25501 | 4 | 11 | 7 | 181 | 9 | 0.04 | 170 | 0.52 | 0.23 | 27 | 2.4 | 21.8 | 16.1 | 0.03 | 0.06 | 0.02 | 0.02 | 0.41 | 0.05 | 0.11 | 0.00 |
| 9.8 | 0.43 | 17 | 62 | 9.9 | 1883 | 40494 | 29 | 11 | 64 | 105 | 7 | 0.05 | 193 | 0.67 | 0.19 | 16 | 5.1 | 28.8 | 7.7 | 0.01 | 0.26 | 0.27 | 0.03 | 0.24 | 0.02 | 0.03 | 0.01 |
| 11.9 | 1.32 | 131 | 116 | 31.7 | 620 | 48508 | 18 | 19 | 51 | 129 | 9 | 0.12 | 1712 | 0.71 | 0.54 | 26 | 13.6 | 46.3 | 12.1 | 0.02 | 0.00 | 0.06 | 0.25 | 1.76 | 0.03 | 0.08 | 0.02 |
| 14.3 | 0.64 | 343 | 59 | 27.2 | 511 | 28994 | 14 | 11 | 84 | 153 | 7 | 0.04 | 206 | 0.34 | 0.25 | 50 | 6.4 | 9.6 | 13.4 | 0.13 | 0.16 | 0.03 | 0.07 | 0.19 | 0.03 | 0.12 | 0.01 |
| 16.5 | 1.87 | 530 | 115 | 46.9 | 671 | 36045 | 27 | 23 | 41 | 90 | 9 | 0.06 | 128 | 0.31 | 0.25 | 58 | 5.2 | 14.5 | 13.5 | 0.11 | 0.31 | 0.03 | 0.03 | 0.14 | 0.04 | 0.29 | 0.01 |
| 23.2 | 1.11 | 431 | 102 | 50.9 | 208 | 50735 | 23 | 50 | 118 | 64 | 11 | 0.08 | 89 | 0.92 | 0.39 | 38 | 3.4 | 8.7 | 5.6 | 0.17 | 0.49 | 0.03 | 0.16 | 0.05 | 0.04 | 0.51 | 0.03 |

**Table 1 continued. ICP-MS results for elemental concentrations using EPA extraction method 3010A. Concentrations are reported as ppm (mg/kg). Solid line marks samples from above and below the saprolite/bedrock contact.**

**Core 1**

| Depth (m) | Te | I | Cs | Ba | La | Ce | Pr | Nd | Sm | Eu | Gd | Tb | Dy | Ho | Er | Tm | Yb | Lu | Hf | Ta | W | Hg | Tl | Pb | Bi | Th | U |
|---|---|---|---|---|---|---|---|---|---|---|---|---|---|---|---|---|---|---|---|---|---|---|---|---|---|---|---|
| 0.6 | 0.03 | 0.53 | 9.2 | 508 | 66.6 | 16.3 | 16.0 | 62.0 | 12.8 | 3.0 | 13.5 | 2.0 | 11.3 | 2.1 | 5.7 | 0.8 | 4.9 | 0.7 | 0.7 | 0.02 | 0.08 | 0.00 | 0.85 | 12.8 | 0.19 | 6.65 | 0.70 |
| 1.8 | 0.03 | 0.28 | 8.4 | 212 | 43.4 | 41.6 | 11.3 | 45.0 | 9.5 | 2.1 | 10.0 | 1.5 | 8.2 | 1.5 | 4.2 | 0.6 | 3.8 | 0.6 | 0.9 | 0.02 | 0.09 | 0.01 | 1.02 | 16.8 | 0.37 | 6.90 | 1.57 |
| 3.1 | 0.05 | 0.16 | 8.1 | 255 | 31.5 | 31.9 | 8.3 | 34.1 | 6.9 | 1.6 | 7.2 | 1.0 | 5.7 | 1.0 | 2.9 | 0.4 | 2.6 | 0.4 | 0.6 | 0.01 | 1.32 | 0.03 | 0.80 | 21.9 | 0.37 | 8.27 | 1.39 |
| 4.3 | 0.01 | 0.23 | 4.7 | 526 | 54.4 | 105.6 | 14.7 | 61.6 | 12.5 | 2.7 | 12.2 | 1.6 | 8.6 | 1.6 | 4.3 | 0.6 | 3.7 | 0.6 | 0.7 | 0.02 | 0.10 | 0.03 | 0.90 | 29.5 | 0.24 | 7.26 | 0.00 |
| 5.8 | 0.02 | 0.27 | 5.2 | 543 | 24.9 | 32.0 | 6.9 | 29.3 | 6.1 | 1.6 | 6.1 | 0.9 | 4.8 | 0.9 | 2.5 | 0.3 | 2.1 | 0.3 | 0.6 | 0.01 | 0.08 | 0.01 | 0.82 | 8.2 | 0.15 | 6.94 | 0.61 |
| 7.6 | 0.03 | 0.06 | 4.0 | 148 | 40.1 | 82.2 | 10.7 | 43.3 | 8.4 | 1.7 | 8.1 | 1.1 | 5.0 | 0.8 | 1.9 | 0.3 | 1.7 | 0.3 | 0.6 | 0.01 | 0.06 | 0.00 | 1.11 | 8.9 | 0.37 | 6.56 | 1.60 |
| 8.5 | 0.06 | 0.03 | 4.4 | 311 | 14.0 | 33.1 | 4.3 | 17.5 | 3.6 | 0.7 | 3.6 | 0.5 | 2.8 | 0.5 | 1.5 | 0.2 | 1.4 | 0.2 | 0.8 | 0.01 | 0.05 | 0.01 | 0.64 | 13.7 | 0.35 | 8.41 | 0.00 |
| 10.1 | 0.04 | 0.08 | 4.3 | 297 | 13.9 | 37.4 | 4.8 | 19.5 | 4.2 | 1.0 | 3.9 | 0.6 | 3.4 | 0.7 | 1.8 | 0.3 | 1.8 | 0.3 | 0.6 | 0.01 | 0.06 | 0.03 | 0.68 | 17.6 | 0.19 | 11.28 | 2.19 |
| 11.6 | 0.04 | 0.04 | 5.9 | 500 | 32.1 | 75.3 | 9.0 | 36.3 | 7.7 | 1.3 | 6.9 | 0.8 | 3.8 | 0.6 | 1.4 | 0.2 | 1.1 | 0.2 | 0.5 | 0.01 | 0.14 | 0.02 | 0.78 | 14.4 | 0.36 | 5.90 | 0.00 |
| 13.7 | 0.05 | 0.07 | 10.6 | 444 | 174.8 | 320.4 | 34.1 | 138.7 | 27.6 | 4.7 | 27.2 | 2.9 | 11.3 | 1.7 | 4.0 | 0.5 | 3.3 | 0.5 | 0.5 | 0.02 | 1.31 | 0.03 | 0.52 | 75.0 | 0.54 | 5.48 | 3.65 |
| 15.3 | 0.04 | 0.04 | 5.7 | 264 | 76.4 | 137.7 | 15.5 | 63.2 | 12.1 | 2.3 | 11.8 | 1.5 | 6.2 | 0.9 | 2.0 | 0.2 | 1.4 | 0.2 | 0.4 | 0.01 | 0.40 | 0.03 | 0.73 | 20.1 | 0.75 | 9.04 | 0.00 |
| 19.2 | 0.09 | 0.01 | 4.0 | 165 | 51.3 | 114.3 | 13.7 | 55.2 | 10.6 | 2.1 | 10.1 | 1.2 | 5.3 | 0.7 | 1.5 | 0.2 | 0.9 | 0.1 | 0.3 | 0.01 | 2.21 | 0.02 | 0.63 | 9.9 | 1.09 | 10.93 | 2.84 |
| 20.7 | 0.16 | 0.00 | 4.2 | 240 | 15.2 | 34.3 | 4.2 | 16.8 | 3.4 | 0.7 | 3.2 | 0.4 | 2.2 | 0.3 | 0.8 | 0.1 | 0.5 | 0.1 | 0.4 | 0.01 | 0.12 | 0.04 | 0.76 | 9.1 | 1.81 | 11.23 | 2.61 |
| 21.4 | 0.00 | 0.01 | 4.9 | 26 | 62.4 | 133.9 | 16.1 | 67.3 | 13.5 | 2.8 | 13.6 | 1.7 | 6.6 | 0.9 | 1.8 | 0.2 | 1.3 | 0.2 | 0.5 | 0.00 | 5.09 | 0.27 | 0.65 | 20.7 | 0.60 | 43.78 | 1.40 |
| 21.8 | 0.01 | 0.00 | 18.2 | 50 | 2218.8 | 4963.0 | 589.4 | 2307.9 | 348.7 | 68.5 | 322.1 | 36.0 | 137.8 | 18.3 | 37.4 | 4.1 | 25.4 | 3.0 | 1.2 | 0.13 | 0.30 | 0.13 | 0.58 | 18.6 | 0.17 | 37.79 | 15.70 |

**Core 2**

| Depth (m) | Te | I | Cs | Ba | La | Ce | Pr | Nd | Sm | Eu | Gd | Tb | Dy | Ho | Er | Tm | Yb | Lu | Hf | Ta | W | Hg | Tl | Pb | Bi | Th | U |
|---|---|---|---|---|---|---|---|---|---|---|---|---|---|---|---|---|---|---|---|---|---|---|---|---|---|---|---|
| 0.6 | 0.03 | 0.42 | 1.9 | 87 | 10.4 | 36.0 | 3.0 | 12.7 | 2.8 | 0.6 | 3.3 | 0.5 | 2.6 | 0.5 | 1.3 | 0.2 | 1.0 | 0.1 | 0.4 | 0.01 | 0.34 | 0.02 | 0.50 | 16.0 | 0.34 | 8.90 | 1.16 |
| 1.8 | 0.04 | 1.24 | 3.0 | 255 | 40.3 | 69.4 | 12.6 | 53.7 | 11.1 | 2.4 | 10.0 | 1.4 | 7.8 | 1.5 | 4.0 | 0.6 | 3.8 | 0.5 | 0.7 | 0.02 | 0.69 | 0.16 | 0.46 | 34.0 | 0.25 | 12.74 | 1.41 |
| 3.1 | 0.34 | 0.94 | 2.1 | 243 | 40.2 | 41.1 | 10.8 | 43.9 | 9.9 | 2.2 | 10.5 | 1.6 | 9.6 | 1.8 | 5.3 | 0.8 | 4.9 | 0.7 | 1.0 | 0.01 | 0.09 | 0.01 | 0.34 | 28.3 | 0.78 | 9.58 | 1.75 |
| 4.3 | 0.05 | 0.80 | 4.6 | 388 | 45.0 | 44.3 | 12.3 | 51.6 | 11.8 | 2.9 | 12.9 | 2.1 | 12.7 | 2.4 | 6.8 | 0.9 | 6.0 | 0.9 | 0.7 | 0.02 | 0.18 | 0.02 | 0.61 | 33.3 | 0.57 | 8.57 | 1.84 |
| 5.5 | 0.01 | 0.06 | 1.2 | 50 | 18.6 | 35.3 | 5.1 | 20.9 | 4.5 | 0.9 | 4.5 | 0.6 | 3.0 | 0.5 | 1.3 | 0.2 | 1.1 | 0.2 | 0.3 | 0.01 | 0.92 | 0.03 | 0.15 | 10.0 | 0.15 | 8.10 | 0.00 |
| 6.7 | 0.10 | 0.16 | 6.0 | 203 | 21.5 | 21.3 | 6.1 | 26.0 | 5.7 | 1.2 | 5.3 | 0.8 | 4.5 | 0.8 | 2.3 | 0.3 | 2.0 | 0.3 | 0.6 | 0.01 | 0.11 | 0.02 | 0.66 | 22.7 | 0.47 | 8.49 | 1.89 |
| 8.2 | 0.02 | 0.10 | 0.9 | 120 | 28.9 | 28.8 | 7.9 | 33.0 | 7.1 | 1.5 | 7.2 | 1.1 | 6.3 | 1.2 | 3.1 | 0.4 | 2.6 | 0.4 | 0.7 | 0.01 | 0.05 | 0.02 | 0.16 | 65.6 | 0.45 | 6.21 | 3.35 |
| 9.8 | 0.05 | 0.23 | 0.7 | 156 | 39.4 | 163.6 | 10.1 | 40.1 | 8.0 | 1.9 | 8.9 | 1.3 | 7.7 | 1.4 | 3.8 | 0.5 | 3.1 | 0.4 | 0.3 | 0.01 | 0.34 | 0.03 | 0.49 | 56.3 | 0.26 | 6.59 | 2.80 |
| 11.9 | 0.09 | 0.08 | 1.2 | 267 | 108.8 | 162.8 | 27.5 | 106.5 | 21.5 | 4.0 | 19.2 | 2.7 | 14.6 | 2.6 | 6.8 | 0.9 | 5.5 | 0.7 | 0.6 | 0.03 | 0.08 | 0.02 | 0.14 | 60.3 | 0.82 | 7.12 | 3.71 |
| 14.3 | 0.03 | 0.02 | 2.1 | 302 | 10.7 | 29.2 | 3.6 | 15.6 | 3.6 | 0.7 | 3.6 | 0.5 | 3.0 | 0.6 | 1.5 | 0.2 | 1.3 | 0.2 | 0.6 | 0.01 | 0.04 | 0.00 | 0.32 | 28.0 | 0.27 | 8.46 | 1.70 |
| 16.5 | 0.00 | 0.01 | 4.5 | 452 | 29.4 | 70.0 | 8.6 | 36.1 | 7.8 | 1.4 | 7.4 | 1.0 | 5.1 | 0.8 | 2.0 | 0.3 | 1.5 | 0.2 | 0.7 | 0.01 | 0.51 | 0.02 | 0.45 | 8.0 | 0.16 | 7.71 | 1.27 |
| 23.2 | 0.04 | 0.00 | 2.2 | 105 | 10.9 | 24.4 | 3.0 | 12.3 | 2.7 | 0.6 | 3.1 | 0.4 | 2.6 | 0.4 | 1.1 | 0.1 | 0.8 | 0.1 | 0.2 | 0.00 | 0.16 | 0.02 | 0.64 | 6.7 | 0.29 | 9.48 | 1.17 |

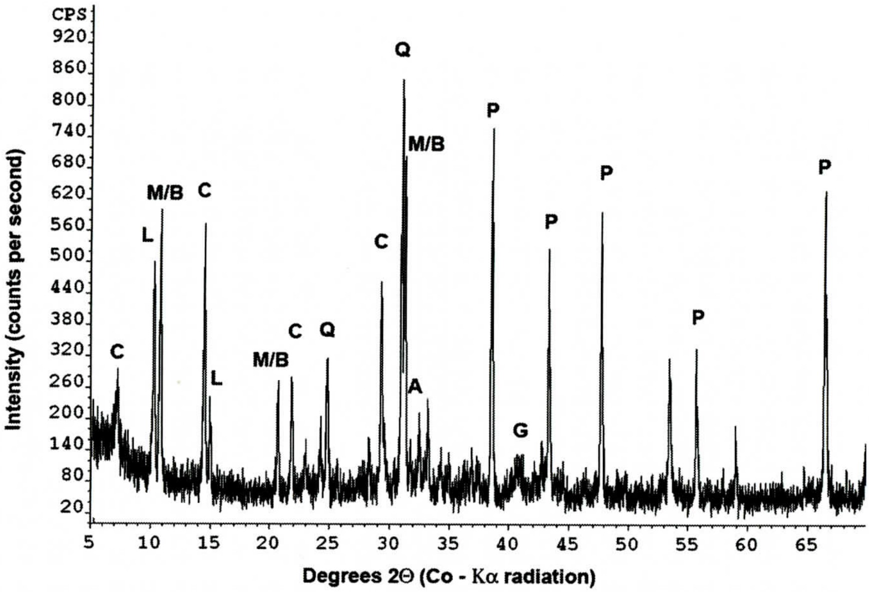


**Figure 4. X-ray powder diffractogram of schist from core #2 (depth 21.8 m). Major minerals detected in pattern are noted by letters placed near strong reflections (Q) quartz, (B) biotite, (M) muscovite, (G) garnet, (C) clinochlore, (A) albite, (L) laumontite, and (P) pyrite.**

As WDS maps of the same area seen in BSE (Figures 3C and 3D) show bands that trend with the foliation. The band in Figures 3B and 3C upper field of view highlights a concentration of pyrite (top). The band in Figures 3B, 3C, and 3D bottom field of view highlights arsenopyrite. The arsenopyrite blebs (Figure 3B inset) follow foliations, while pyrite continuously occurs in both foliations and in fractures.

Certain metals (e.g., Co, Ni, Mn, Cu, Pb, Zn) are known to isomorphously substitute into arsenopyrite structures (Wuensch, 1974; Morimoto and Clark, 1961). Some of these metals were detected by ICP-MS in the extractions (Table 1), however they were not specifically measured on the grains using WDS. It is possible these elements are present in the arsenopyrite structure but only As and Se were measured for the focus of this study. Analysis of nine different pyrite and arsenopyrite grains each, using WDS, reveals the following average percent concentrations and standard deviations: Pyrite Fe: 46.51 +/- 0.25, S: 53.49 +/-0.25, As: 0.00 +/- 0.00, Se: 0.00 +/- 0.00; Asenopyrite Fe: 33.21+/ -0.45, S: 20.54 +/-0.84, As: 46.15 +/-1.12, Se: 0.10 +/-0.01. Assuming Fe, As, S, and Se occur in their reduced states, these compositions yield structural formulae of $Fe_{0.998}S_2$ and $Fe_{0.938}As_{0.962}Se_{0.002}S_{0.998}$ for pyrite and arsenopyrite, respectively.

Saprolite and soil mineralogy are typical of the region, with soils being classified as Pacolet sandy loams (Tate, 1967). Optical examination of hand samples recovered from near the surface reveals the remnants of (Fe-rich) garnet and biotite. Their hydrolysis and oxidation products hematite ($Fe_2O_3$) and manganite (MnOOH) stain portions of the schist-saprolite red (Munsell 10R 5/4) and dark brown (10R 2.5/1), respectively. Also observed are goethite stains that appear as yellowish brown (7.5YR 5/6) in fractures. Goethite is a common hydrolysis product generated from oxidation of ferrous minerals, such as garnet, biotite, and pyrite ($FeS_2$), under slightly acidic conditions. Fine-grained sulfides are not observed in saprolite, however it is not uncommon to find pseudomorphic casts. Trace abundances of isometric casts can be found in the saprolite. The presence of these casts is consistent with pyrite being a trace component of the parent rock of the saprolite.

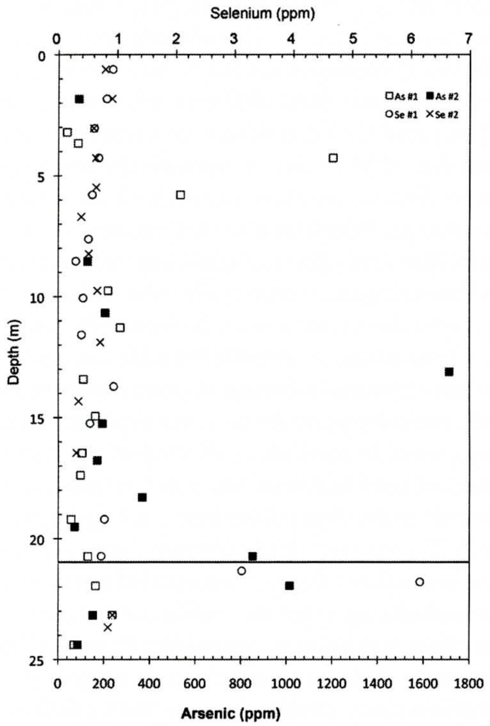


**Figure 5. Arsenic and selenium concentrations of soil and rock samples of two core samples from Gwinnett County, GA. Concentrations are in ppm (mg per kg$^{-1}$) based on extractions using EPA method 3050A (Edgell, 1988) and subsequent measurement by ICP-MS (Hassan and Loux, 1990). Horizontal line at ~21m depth is approximate bedrock-saprolite boundary. Legend on upper right portion of graph shows respective symbols for arsenic (lower scale) and selenium (upper scale).**

## DISCUSSION

The large saprolite thickness of the study site and retrieval of the underlying bedrock allows for a meaningful context to evaluate natural versus anthropogenic origins of the high As values measured during the initial phase of the study as well as the co-existing Se in the arsenopyrite. Figure 5 shows a plot of As and Se concentrations versus depth in the two profiles. The first noticeable trend is the highly variable As concentrations that persist through both cores, with many values one to two orders of magnitude greater than the regional baseline value of 7 ppm. Arsenic values in the saprolite exceed those in the bedrock. In contrast the Se values are much higher in the bedrock when compared to the saprolite. In part, some of the variability can be attributed to compositional inhomogeneities of the schist as the evidence for moderately dipping foliations seen in the bedrock core and regional studies by Higgins and Crawford (2007). If a simplified assumption is made about the maximum availability of As and Se in the saprolite potentially coming from Brevard Zone bedrock, then the relative mobility of these two elements can be assessed for weathering conditions in this region of the Piedmont in the SE United States.

Model bedrock As and Se concentrations can be derived using the arsenopyrite stoichiometry measured in this study, assuming its volume abundance of 0.1% in the schist (Figure 3B), and densities of 2.7 and 6.2 g/cm$^3$ for the schist and arsenopyrite, respectively. These estimates result in bedrock concentrations of 1055 ppm for As and 23 ppm for Se and a relative As/Se for the bedrock of about 46. The measured ICP-MS values for the bedrock are somewhat lower with the greatest values being 75 ppm for As and 4 ppm for Se. These lower values can be attributed to incomplete extraction from the bedrock (see methods section) and inaccurate estimates in the model assumptions. The relative measured As/Se ratio is about 19, which is similar to regional values (Shacklette and Boerngen, 1984) and slightly less than the model estimate above. In contrast, the highest ICP-MS saprolite concentrations are 1396 ppm for As and 0.7 ppm for Se, which result in an As/Se ratio of 1990. The saprolite As value is very similar to the bedrock As value, even with correction for density differences due to silicate mass loss from hydrolysis. Most notable is the much lower value of Se in the saprolite, which is an order of magnitude less than the bedrock. The As/Se ratio is also notably orders of magnitude larger in the saprolite. This observation supports two important aspects regarding the fate and transport of As and Se in Piedmont weathered environments of the SE United States. Firstly, As appears to be relatively conserved during weathering and secondly, Se appears to be mobile and subject to transport away from the weathering zone.

The behavior of naturally occurring As in arsenopyrite and its oxidized forms can be understood in terms of location within the bedrock/saprolite/soil profile and available electron acceptors in the weathering profile. The oxidation from $As^{(III)}$ in arsenopyrite to $As^{(V)}$ is a well-studied process with associations to microbially mediated lithotrophy during weathering (Ehrlich, 1964; Strawn and others, 2002; Yu Yunmei and others, 2004). An important consequence of this oxidation reaction is the generation of acidity and the production of arsenate complexes (Walker and others, 2005). The latter of which behave much like soil phosphate complexes that are know to associate with Fe-oxide surfaces. (Qafoku and others, 1999; Filippi and others, 2007; Neel and others, 2003). Given the abundance of hematite and goethite in these piedmont soils, the retention of As relative to bedrock concentrations in this study can be parsimoniously explained as a natural occurrence related to the original bedrock. The heterogeneous vertical distribution As and its concordance of mass balance between bedrock and weathered horizons are in contrast to known studies of anthropogenic As occurrences. For example, Kukier and others (2001) amended similar Georgia Piedmont Cecil soils with As-bearing fly ash. In this anthropogenic case, a signature distribution of As is characterized by a high near the surface followed by a gradational decrease at depth to an order of magnitude lower level.

The behavior of naturally occurring Se, as it is released during arsenopyrite oxidation, is not as well documented as As. Se in arsenopyrite most likely occupies sulfur sites in arsenopyrite as a reduced selenide form. Upon exposure to electron acceptors such as oxygenated ground waters, the Se reacts to form the oxidized states of $Se^{(IV)}$ and $Se^{(VI)}$, with the latter selenate form being more common in weathering environments (Strawn and others, 2002). Comparison of As and Se ionic potentials [IP = defined as the ratio of ionic charge (Z) to ionic radius (r)] predicts their solubility behavior to be different (Pauling, 1948). Assuming the respective values of $r_{As(V)} = 0.46Å$ and $r_{Se(VI)} = 0.42$, then respectively $IP_{As(V)} = 10.9$ and $IP_{Se(VI)} = 14.2$. These IP values indicate that both As and Se should complex as soluble radicals. The greater IP value of $Se^{(VI)}$ indicates it is more soluble than As, which is consistent with the observations of this study. Studies of both As and Se for the Georgia Piedmont are not extensive, however Peltier and others (2008) have indirectly evaluated heavy metal abundance in watersheds by using the Asiatic clam (*Corbicula fluminea*) as a biomonitor. The studies specific interest is the contributions of trace elements associated with different point sources and land uses in a large river. In particular they studied the tributaries of the Chattahoochee River, whose main channel in the Georgia Piedmont is largely controlled by the trace of the Brevard Zone. Realizing that the Chattahoochee integrates a watershed larger than the Brevard Zone, analysis of As and Se in nine samples from each of fifteen river sites reveals an As/Se ratio of 0.6, which is much smaller than the ratios of about ~40 for the bedrock and ~2000 for the saprolite at the study site. If the primary As and Se signature of the Georgia Piedmont is controlled by arsenopyrite similar to that in this study area, then both the saprolite and the river waters (as proxied by a biomonitor of Peltier and others, (2008)) provide a good model for the partitioning of the two elements in the Piedmont of SE United States.

## CONCLUSIONS

Pyrite and arsenopyrite occur in a mafic schist of the Piedmont of Gwinnett County, Georgia associated with a fossil hydrothermal system and the Brevard Zone. The pyrite is texturally associated with late stage retrograde metamorphic laumontite, which occurs along brittle fractures and within foliations. Arsenopyrite appears as discreet grains within and associated with foliations formed or retained during prograde metamorphism. Analysis of the As and Se in the bedrock shows they reside in the arsenopyrite resulting in bulk rock concentrations above regional baseline values. Analysis of the As and Se in overlying saprolite and soil indicates they are weathered from the arsenopyrite but have different fates. Arsenic is conserved most likely as arsenate complexes adsorbed to abundant Fe-oxyhydroxide surfaces in the saprolite/soil. Selenium is transported out of the weathering profile and presumed to be carried off by the rivers. This scenario is directly supported by the high As/Se ratios measured in the saprolite of this study and indirectly by the very low As/Se ratios measured in biomonitor proxies of river waters draining the Brevard Zone (Peltier and others, 2008). Ascribing high concentrations of As and Se to anthropogenic, natural, or false-positive factors requires analysis of bedrock, saprolite, soil, and methodology (in aluminous terrains). In cases where As concentrations are high at the surface and decrease to regional baseline values, then an anthropogenic cause might be ascribed. In the case of this study, where there are no discrete vertical trends and mass balancing of underlying bedrock can account for saprolite concentrations, naturally elevated As levels are possible on small spatial scales in the Piedmont soils of the SE United States.

## ACKNOWLEDGEMENTS

The author is indebted to Chris Fleisher (EMPA) and Sayed Hassan (ICP-MS) for their expert skills and friendly demeanors. Thanks are given to the University of Georgia Departments of Geology and Crop and Sciences for access to their analytical facilities. The review of David Leigh significantly improved the manuscript.

## REFERENCES

Bednar, A.J., Garbarino, J.R., Ranville, J.F. and Wildeman, T.R., 2002. Presence of Organoarsenicals Used in Cotton Production in Agricultural Water and Soil of the Southern United States. Journal of Agricultural and Food Chemistry, 50(25): 7340-7344.

Crawford, T.J. and Kath,.R.L., 2001. The Brevard Zone: A literature Review. In: T.J. Kath R. L. and Crawford (Editor), Across the Brevard Zone: The Chattahoochee Tunnel, Cobb County, Georgia. Georgia Geological Society Guidebooks, pp. 1-16.

Deer, W.A., Howie, R.A., Wise, W.S. and Zussman, J., 2004. Rock-forming minerals: Framework Silicates, Volume 4B. Geological Society, London, 982 pp.

Dicken, C.L., Nicholson, Suzanne W., Horton, John D., Foose, Michael P. and Mueller, Julia A.L., 2005. Preliminary integrated geologic map databases for the United States. U.S. Geological Survey, pp. 44.

Edgell, K., 1988. USEPA method study 37-SW-846 method 3050 acid digestion of sediments, sludges and soils. In: E.C. 68-03-3254. (Editor), pp. 12.

Ehrlich, H.L., 1964. Bacterial oxidation of arsenopyrite and enargite. Economic Geology, 59(7): 1306-1312.

EPA Report 2003, U.S. EPA Workshop on Managing Arsenic Risks to the Environment: Characterization of Waste, Chemistry, and Treatment and Disposal, EPA/625/R-03/010: Denver, Colorado, National Risk Management Research Laboratory Office of Research and Development U.S. Environmental Protection Agency, Cincinnati, OH 45268, 107 pp.

Filippi, M., Dousova, B. and Machovic, V., 2007. Mineralogical speciation of arsenic in soils above the Mokrsko-west gold deposit, Czech Republic. Geoderma, 139(1-2): 154-170.

Frankenberger, W.T., 2002. Environmental chemistry of arsenic. Books in soils, plants, and the environment. Marcel Dekker, New York, xiii, 391 pp.

Haney, P.B., W.J. Lewis, and W.R. Lambert. 2009. Cotton production and the boll weevil in Georgia: History, cost of control, and benefits of eradication. Univ. of Georgia Agric. Exp. Stn. Research Bulletin 428, 34 pp.

Hassan, S.M. and Loux, N.T., 1990. Elimination of spectral interference in inductively coupled plasma atomic emission spectroscopy using orthogonal ploynomials. Spectrochemica Acta, 45B: 719 - 729.

Higgins, M.W., 1966. Geology of the Brevard Lineament near Atlanta. In: M. Georgia Department of Mines, and Geology. Geological Survey Bulletin 77, Atlanta, GA, 49 pp.

Higgins, M.W. 1968. Geologic map of the Brevard fault zone near Atlanta, Georgia, Miscellaneous geologic investigations map I-511. U.S. Geological Survey, Washington, D.C.

Higgins, M.W. and.Crawford, Ralph F., 2007. Geologic Map of the Atlanta 30' x 60' Quadrangle, GA. Version 4.1.0. Geologic Mapping Institute and Atlanta Geological Society, Clayton, GA.

Jackson, B.P. 1998. Trace element solubility from land application of fly ash/organic waste mixtures with emphasis on arsenic and selenium speciation. Thesis (PhD), University of Georgia, 151 pp.

Jones, C.L., Hodge, V. F., Schoengold, D. M., Biesiada H., and Starks, T. H., 1987. An Interlaboratory Study of Inductively Coupled Plasma Atomic Emission Spectroscopy Method 6010 and Method 3050. In: U.S. Environmental Protection Agency (Editor), Las Vegas. Nevada., 34 pp.

Kukier, U., Sumner, M.E. and Miller, W.P., 2001. Distribution of exchangeable cations and trace elements in the profiles of soils amended with coal combustion by-products. Soil science, 166(9): 585-597.

Morimoto, N. and Clark, L.A., 1961. Arsenopyrite crystal-chemical relations. American Mineralogist, 46(11-12): 1448-1469.

Neel, C., Bril, H., Courtin-Nomade, A. and Dutreuil, J.P., 2003. Factors affecting natural development of soil on 35-year-old sulphide-rich mine tailings. Geoderma, 111(1-2): 1-20.

Pauling, L., 1948. The nature of the chemical bond, and the structure of molecules and crystals: An introduction to modern structural chemistry. H. Milford, Oxford University Press, Ithaca, N.Y. London, 450 pp.

Peltier, G.L., Meyer, J.L., Jagoe, C.H. and Hopkins, W.A., 2008. Using trace element concentrations in Corbicula fluminea to identify potential sources of contamination in an urban river. Environmental Pollution, 154(2): 283- 290.

Qafoku, N.P., Kukier, U., Sumner, M.E., Miller, W.P. and Radcliffe, D.E., 1999. Arsenate displacement from fly ash in amended soils. Water, air, and soil pollution, 114(1/2): 185-198.

Reed, J.C., 1970. The Brevard Zone: A re-interpretation. In: G.W. Fisher, Pettijohn, F.J., Reed, J.C. Jr., and Weaver, K.N. (Editors), Studies of Appalachian geology: central and southern. Interscience Publishers, New York, pp. 261-269.

Shacklette, H.T., and Boerngen, J.G., 1984. Element concentrations in soils and other surficial materials of the conterminous United States, U.S. Geological Survey Professional Paper 1270. Professional Paper, 105 pp.

Strawn, D., Doner, H., Zavarin, M. and McHugo, S., 2002. Microscale investigation into the geochemistry of arsenic, selenium, and iron in soil developed in pyritic shale materials. Geoderma, 108(3-4): 237-257.

Tate, R.J., 1967. Soil Survey, Gwinnett County, Georgia. In: U.S. Department of Agriculture, Washington, DC.

Walker, S.R., Jamieson, H.E., Lanzirotti, A., Andrade, C.F. and Hall, G.E.M., 2005. The Speciation Of Arsenic In Iron Oxides In Mine Wastes From The Giant Gold Mine, N.W.T.: Application Of Synchrotron Micro-Xrd And Micro-Xanes At The Grain Scale. Canadian Mineralogist, 43(4): 1205-1224.

Williams, P.N. and others, 2005. Variation in Arsenic Speciation and Concentration in Paddy Rice Related to Dietary Exposure. Environmental Science & Technology, 39(15): 5531-5540.

Wuensch, B.J., 1974. Sulfide crystal chemistry. Mineralogical Society of America Short Course Notes, 1: 24.

Yu Yunmei, Zhu Yongxuan, Williams-Jones, A.E., Gao Zhenmin and Li Dexian, 2004. A kinetic study of the oxidation of arsenopyrite in acidic solutions; implications for the environment. Applied Geochemistry, 19(3): 435-444.

SOUTHEASTERN GEOLOGY
V. 47, No.1, February 2010, p. 27-39

# GEOMORPHOLOGY AND PEDOLOGY OF A MIXED ALLUVIAL-COLLUVIAL DEPOSIT IN CENTRAL WEST VIRGINIA: NEW INSIGHT INTO APPALACHIAN LANDSCAPE EVOLUTION

TODD GROTE[1] AND J. STEVEN KITE

*Department of Geology and Geography*
*West Virginia University*
*PO Box 6300, Morgantown, West Virginia, 26505*
*[1] Now at: Department of Geology, Allegheny College, 520 N. Main Street, Meadville, Pennsylvania, 16335*

## ABSTRACT

**Sediments exposed within the banks of a low-order tributary in central West Virginia reveal that alluvial and colluvial systems were both geomorpologically active from late middle Wisconsin (OIS 3) through more recent time. This complex deposit records distinct depositional episodes including a lower sediment package containing organic-bearing slackwater deposits and alluvial deposits unconformably underlying an upper package consisting of co-alluvium, a variant of colluvium and alluvium, with pedogenic overprinting. Geomorphologic reconstruction suggests the lower sediment package is largely alluvium deposited in high-energy streams bracketed by two distinct periods of slackwater deposition and associated organic matter accumulation. The upper sediment package was deposited under co-alluvial conditions with both colluvial and alluvial processes contributing sediment.**

**Radiometric dating of the lowermost and topmost organic-bearing units indicates that sedimentation and hollow infilling commenced prior to 39,320 $^{14}C$ years before present (YBP) and ceased by approximately 33,800 $^{14}C$ YBP. Geomorphologic responses to changing environmental conditions, possibly related to the occasional intrusion of warm tropical air into the area, during the late phases of OIS 3 and the transition to OIS 2 are responsible for deposition of the lower sediment package. Deposition of the upper co-alluvial package occurred from subsequent to 33,800 $^{14}C$ YBP by both high-energy stream and colluvial processes. Furthermore, the weak degree of pedogenic development above a paleosol at the upper sediment package base suggests the upper portion of the deposit may be significantly younger than the underlying sediments and possibly emplaced by geomorphic instability linked to the OIS 2-OIS 1 transition.**

## INTRODUCTION

Unconsolidated colluvial and alluvial deposits commonly occupy mountain hillslopes and footslopes throughout the Appalachian region of North America. The Appalachians have a landscape history that dates back as far as the late Mesozoic with significant modification throughout the Cenozoic (Poag and Sevon, 1989; Pazzaglia and Brandon, 1996). Eocene-Oligocene (35-30 million years ago) climatic cooling initiated the beginning of icehouse climatic conditions, ultimately leading to global Quaternary glacial and interglacial fluctuations (Frakes and others, 2005) and final sculpting of the Appalachian landscape (Braun, 1989; Poag and Sevon, 1989; Braun and others, 2003).

During peak glacial times, sea level may have been as much as 120 meters lower than present, thus influencing regional and global atmospheric circulation (Conners, 1986; Bull, 1991). Regional paleoclimate in the central Appalachians would have been dramatically different due to the compression of the polar frontal zone (PFZ) to the south of West Virginia (Conners, 1986; Kochel, 1987). North of the PFZ, atmospheric circulation would have maintained a West to East zonal flow (Knox, 1983). The zonal flow likely would disallow interactions between warm moist air from the south

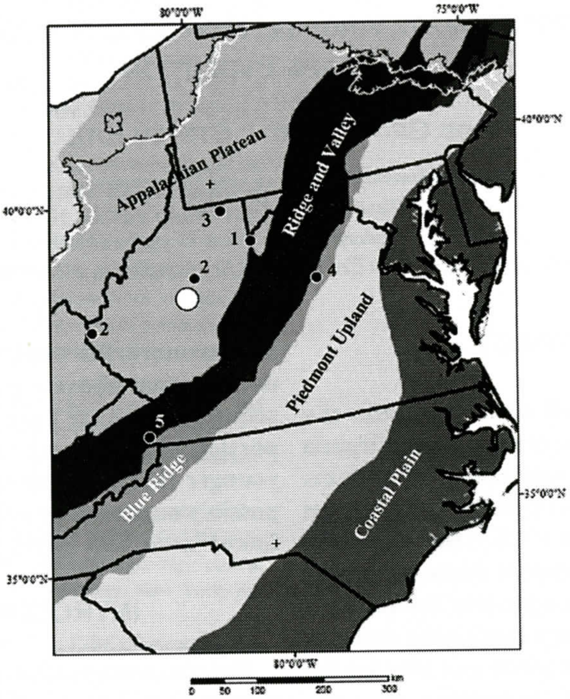


**Figure 1: Location of study area (large white dot) on the Appalachian Plateau in central West Virginia. Black dots denote other studies conducted by (1) Jordan, 1992, Behling et al. (1993); (2) Cremeens et al. (2003); (3) Jacobson et al. (1989); (4) Eaton et al. (2003), Litwin et al. (2004); and (5) Whittecar et al.(2007). Glacial margins from Fullerton et al., 2003: Black = Late Wisconsin, White = Illinoian or Pre-Illinoian.**

and cold dry air from the north that many times causes intense and catastrophic storms in the Appalachian region (Conners, 1986; Kochel, 1987). In the periglacial zone south of the glacial border, environmental conditions would have been cold, dry, and windy (Watts, 1979). Periglacial botanical communities during glacial times in much of the central Appalachians would have consisted of a mixture of boreal forest and herbaceous tundra depending on elevation, and climatic and topographic gradients (Maxwell and Davis, 1972; Watts, 1979; Pewe, 1983; Whittecar and others, 2007).

During interglacial times, a more temperate climatic regime would have been in place due to the intrusion of warmer air as the PFZ migrated northward with the retreating ice sheets (Kochel, 1987). A more meridianal atmospheric flow would allow the incursion of warm moist air into the region increasing seasonal precipitation patterns (Delcourt, 1985). These milder climatic times may have been conducive to more temperate vegetation species. Conner (1986) suggested that interglacial climates, such as the present Holocene climate, may be characteristic for about 10% of the total Pleistocene glacial-interglacial cycles. Examination of middle and late Pleistocene composite ice core records available at www.quaternary.stratigraphy.org.uk/correlation/chart.html suggest that only a few interglacial times may have had a warmer climate, notably Oxygen Isotope Stage (OIS) 5e, 9e, and 11.

Hillslope soils and fill deposits may provide valuable information about terrestrial paleoenvironments and processes through time (Pederson and others, 2000) that are only now being realized in the central Appalachian region (e.g. Eaton and others, 2003; Whittecar and others, 2007). Much of the colluvial sediment that

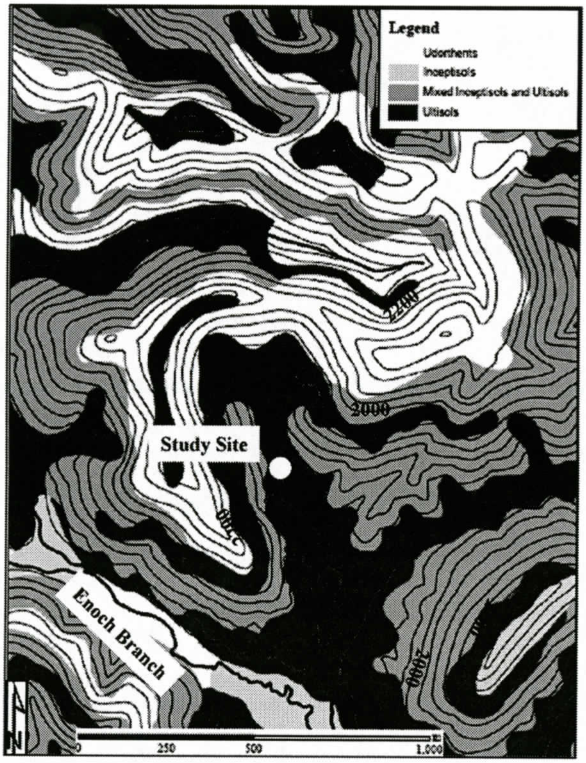


**Figure 2: Digital line graphic of the study site showing topographic contours, generalized soil orders, and major drainageways. Study site (white dot) coordinates: UTM 17S; NAD 27 0514459E 4248375N). Contour interval is 40 feet.**

blankets the Appalachian hillslopes appears to be relict and generated during Pleistocene paleoperiglacial conditions (Clark and Ciolkosz, 1988; Braun, 1989; Mills, 2005). Several investigations into the depositional history of surficial deposits throughout the central Appalachians suggest that much of the deposition along mountain footslopes has occurred during glacial to interglacial transitions during the Quaternary (Delcourt, 1985; Larabee, 1986; Whittecar and Duffy, 2000; Eaton and others, 2003). However, studies of Quaternary geomorphology and paleoenvironments within the central Appalachians suffer from rapid oxidation and decomposition of organic matter, thus sparse chronostratigraphic control, and thick vegetation cover (Mills and Delcourt, 1991; Mills, 2005). A storm struck central West Virginia during the summer of 2003 exposing a unusual alluvial-colluvial deposit that included two beds containing abundant wood fragments, charcoal and finely disseminated organic matter in distinct stratigraphic positions on the unglaciated Appalachian Plateau. The goals of this paper are (1) to describe and interpret the depositional processes and geomorphologic history of this unique deposit south of the glacial border on the Appalachian Plateau of Eastern North America, and (2) to integrate this new data into what is currently known about the late Quaternary geomorphology of the region (Figure 1).

## STUDY AREA AND METHODS

The study site is located on a second order, unnamed tributary to Enoch Branch in central West Virginia (Figures 1 and 2). The stream gradient measured at the site is approximately 12%. This part of West Virginia lies within the unglaciated portion of the Appalachian Plateau Physiographic Province that is underlain by slightly tilted and folded Pennsylvanian sand-

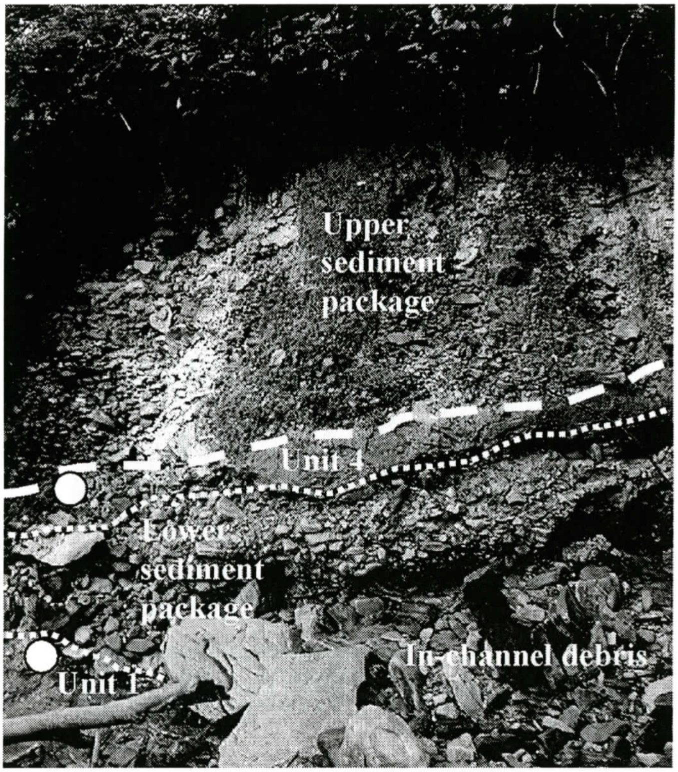


**Figure 3: Looking upstream at the study site exposed within the left streambank. White dots denote $^{14}C$ sample locations. See figure 2 and text for detailed stratigraphic and sedimentologic information.**

stone, siltstone, shale, and coal beds of the Allegheny and Conemaugh formations (Reger, 1921). The topography in and around the site is steep to very steep with hillslopes consisting of a patchwork of colluvial and residual soil types of Ultisol and Inceptisol soil orders, and Udorthents occurring on previously mined or disturbed lands (Carpenter, 1992) (Figure 2). Precipitation gradients for the Appalachian Plateau of West Virginia increase eastward from approximately 101 cm/yr in the western portion of the state to greater than 152 cm/yr in central West Virginia, approaching the Allegheny Front, the boundary between the Appalachian Plateau and the Ridge and Valley physiographic provinces (Messinger and Wiley, 2004). Central West Virginia in the vicinity of the study site receives approximately 118 cm of precipitation that is evenly distributed throughout the year and has an annual average air temperature of 10.3° C (Carpenter, 1992). Approximately 55% of the annual precipitation falls during April to September (Carpenter, 1992).

Lithologic and pedologic descriptions were made of the stream bank exposure in the field along with photo-documentation of channel and bank conditions along the impacted length of stream (Figures 3 and 4). Due to the ephemeral nature of the site, no detailed laboratory analyses were conducted. However, a field rating scale based on the degree of pedologic development was applied using five morphological properties (color, texture, structure, boundaries, and clay films) originally described in Bilzi and Ciolkosz (1977). Soil profile development indices compare the morphological development of a soil horizon to adjacent horizons (Bilzi and Ciolkosz, 1977) or to the soil parent material (Bilzi and Ciolkosz, 1977; Harden, 1981). Using the Bilzi and Ciolkosz method hereafter referred to as relative profile development (RPD), soil horizons are compared to the underlying


**Figure 4: Stream channel and bank characteristics observed post flood event. A: photo looking upstream towards the study site on left bank (photo left). B: Photo looking upstream showing in-channel lags and bank erosion. C: Photo looking downstream at in-channel debris jam, water ponding, and bank erosion. D: In-channel head cut with large woody debris and sandstone boulder denoting head cut location.**

parent material and morphological and physical changes numerically quantified. For example, a change in soil color (rubification) from a Munsell color of 10YR 5/6 parent material to a B horizon with 7.5YR 5/8 color would yield a three unit change (1 point increase from 10YR to 7.5YR hue; no unit change in value 5 vs. 5 and two unit changes in chroma 6 to 8), and a textural change from loam to silt loam would yield a one unit change since they are adjacent to one another on the textural triangle. For a full description of all indices the reader is referred to the original article by Bilzi and Ciolkosz (1977). For the purposes of this study, five properties were determined in the field to develop a RPD for the study site soil and they are summarized in Appendix 1. Since stratified parent materials were identified in the field, each overlying soil horizon was compared to the lowermost parent material horizon as suggested by Bilzi and Ciolkosz (1977). Furthermore, the lowermost parent material properties were also used as a surrogate to examine the buried soil material identified in this study since all soil horizons below this horizon are gleyed and not representative of a well-drained and oxidizing soil environment.

Bulk samples were collected from each organic-bearing units within the exposed stream bank (Figure 3) and transported to the West Virginia University Quaternary Geology Laboratory where they were subsequently frozen and stored. Organic samples were then delivered to Beta Analytic, Inc for radiometric analyses. Radiometric analyses were completed using conventional and accelerator mass spectrometer

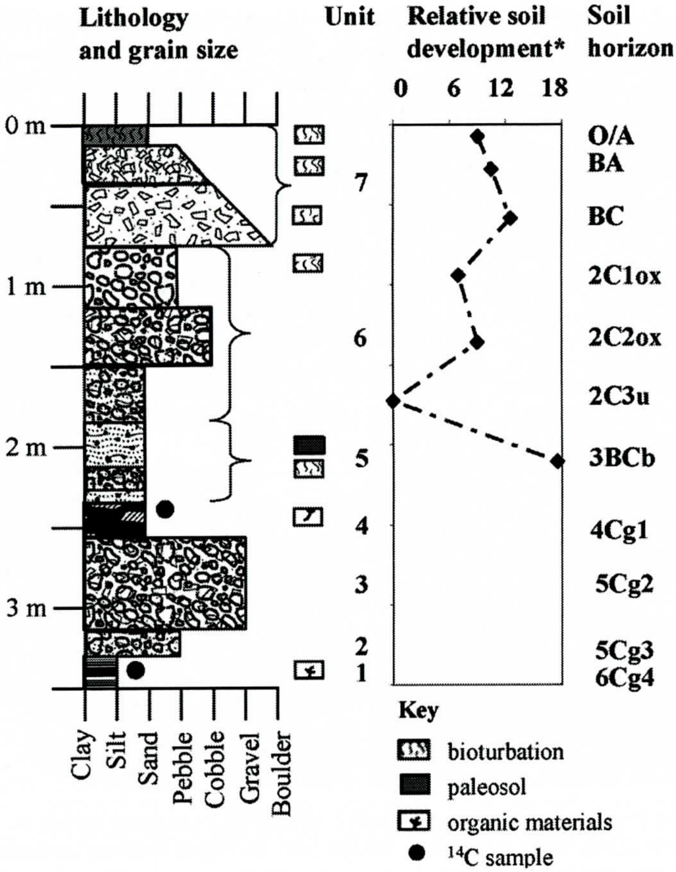


**Figure 5: Sediment stratigraphy and pedology of cut bank exposure. Note: grain size shown is maximum for each stratigraphic interval as interpreted in the field. Gravel designation shown on figure denotes poorly-sorted diamicton with no dominant particle size. See text for detailed sedimentologic descriptions.**
*** = Relative Profile Development (RPD) is based on five observed field characteristics and quantified using the method of Bilzi and Ciolkosz (1977). Data are plotted at the midpoint of each soil horizon. Gleyed soil horizons below the 3BCb horizon were not quantitatively evaluated. See Appendix 1 for full RPD calculation.**

(AMS) radiometric dating of wood and charcoal samples from the uppermost and lowermost organic-bearing beds respectively.

## RESULTS

A storm event during the summer of 2003 triggered considerable geomorphologic activity within this low-order drainage basin in central West Virginia ephemerally exposing an unusual alluvial-colluvial deposit (Figures 3, 4, and 5). Flooding associated with this storm reworked channel substrate by concentrating larger sandstone clasts in some localities, scouring to bedrock in others, and creating in-channel obstructions with a high concentration of large woody debris behind which slackwater conditions were created (Figure 4). The geomorphologic effectiveness of this rainfall event is also evident by the creation of the study site and numerous other new stream bank cuts and slumps adjacent to the stream channel and in adjacent hollows by mass wasting processes.

Stratigraphic, sedimentologic, and pedologic examination of the deposit exposed within the study site stream banks indicates distinctly different depositional processes between the lower and upper sediment packages (Figures 3 and 5). The lower sediment package consists of lithostratigraphic units 1 through 4 and ranges in grain size from pebbly sand and gravel to organic-bearing silt and clayey sand. The upper sediment package consists of lithostratigraphic units 5 through 7 that is a series of clast-supported pebble through boulder diamictons with sandy and silty matrix. Units 5 through 7 have been pedogenically modified to express a basal paleosol remnant underlying the modern surface soil (Figures 3 and 5).

## Lithostratigraphy and Sedimentology

The lowermost lithostratigraphic unit is Unit 1 (> 350-330 cm; 6Cg4 on Figure 5) that is a dark gray (Munsell 5YR 4/1) weakly bedded to massive, gleyed organic-bearing silt. This unit was firm and sticky throughout. Organic-bearing beds occur as 2-5 mm thick very dark grayish brown (10YR 3/2) partially laminated silts with abundant wood and finely disseminated organic matter along bedding planes. Analysis of wood fragments (BETA sample # 221999) from Unit 1 yielded a conventional radiocarbon age of > 39,320 radiocarbon years before present ($^{14}C$ YBP) with a $^{13}C/^{12}C$ ratio of -26.6 o/oo relative to the PDB-1 international standard (PDB) (see Figures 3 & 5 for location). No root remains or traces were observed in Unit 1.

Unit 2 (330-316 cm) is a gray (10YR5/1) matrix-supported pebble diamicton with a loamy sand matrix (5Cg3 on Figure 5). Sub-rounded and sub-angular sandstone clasts within this unit are well-weathered with significant rind development present, > 3mm in many instances. This unit is gleyed and well indurated throughout with many redoximorphic accumulations (strong brown: 7.5YR 5/6) and depletions (grayish brown: 10YR 5/2) throughout. Some finely disseminated organic matter is also present throughout the diamicton matrix. Root remains or traces were not observed in Unit 2.

Unit 3 (316-255 cm) is a gleyed grayish brown (10YR 5/2) sandy gravel with a loamy sand matrix (5Cg2 on Figure 5). Sub-rounded to sub-angular sandstone clasts within this unit are weakly imbricated in places and intermixed with finely disseminated organic matter. Common redoximorphic accumulations (strong brown: 7.5YR 5/6) and depletions (brown: 10YR 5/3) are abundant within the top 20 cm of the exposure, and less abundant, but present, throughout the unit. Sandstone clasts within Unit 3 are highly weathered with weathering rinds typically > 2 mm. No root remains or traces were observed within Unit 3.

Unit 4 (255-236 cm) is a dark grayish brown (10YR 4/2) massive silty sand to silt loam that also contains abundant charcoal, finely disseminated organic matter and interbedded, rounded sandstone pebbles (4Cg1 on Figure 5). No large wood fragments were observed within this unit. Unit 4 is gleyed throughout and contains numerous low chroma black and dark gray depletions (colors not determined). Analysis of charcoal (BETA sample # 221998) from Unit 4, the topmost organic-bearing unit, yielded an AMS radiocarbon age of 33,800 +/- 380 $^{14}C$ YBP with a $^{13}C/^{12}C$ ratio of -28.1 o/oo PDB (see Figures 3 & 5 for location). Sandstone pebbles within Unit 4 are moderately to highly weathered with weathering rinds commonly > 2mm with some pebbles disintegrating to the touch. No root remains or traces were observed within this unit. Unit 4 is in unconformable contact with the overlying Unit 5.

Unit 5 (236-185 cm) is a matrix-supported sandy clay deposit that is strong brown (7.5YR 6/8) at the base that gradually transitions to light yellowish brown (2.5Y 6/4) in the middle and top with strong brown (7.5YR 5/6) patches and oxidation mottles throughout. The basal contact with the underlying sediment package is abrupt and erosive. A 20-30 cm thick concentration of crudely stratified gravels and cobbles is present within the deposit. Sandstone clasts within Unit 5 are highly weathered with weathering rinds > 3 mm common, and silt and clay films coating some clast surfaces. Clay films are also present on matrix sand grains. Field-based soil morphological descriptions included moderately developed coarse subangular blocky structure, soil reddening (rubification), a somewhat sticky consistency, and clay bridges on sand grains are apparent within Unit 5 and consistent with a buried soil horizon (3BCb on Figure 5).

Unit 6 (185-76 cm) consists of three subunits of variable texture and color. The lower unit (A) is a pale olive (5Y 6/3) gravelly sand that is overlain by a middle unit (B) of variegated brownish yellow (10YR 6/3), brownish yellow (10YR 6/8), and light gray (2.5Y 7/2) cobble and pebble diamicton. The top of the unit (C) is capped by a yellowish brown (10YR 5/6) pebble diamicton with a wavy erosive contact with the overlying Unit 7. The low chroma light gray (2.5Y 7/2) and brownish yellow (10YR 6/3) colors appear to be concentrated within the coarsest grained middle (B) member of Unit 6. Sandstone clasts within Unit 6 are moderately decomposed with some weathering rinds < 2mm with others > 2 mm. The degree of cement dissolution does not appear to be as great as the underlying lithostratigraphic units. Fine and medium roots have penetrated into Unit 6 with the finer roots extending to greater depths. Unit 6 is a parent material sequence (2C1ox-2C2ox-2C3u in Figure 5) of the current surface soil.

Uppermost lithostratigraphic Unit 7 (76-0 cm) fines upward from a yellowish brown (10YR 5/6) cobble and boulder diamicton at the base to a pebble to cobble diamicton in the middle, and a sandy and silty loam at the land surface. The whole of Unit 7 has been pedogenically modified, overprinting the original sediment fabric. Sandstone clasts within this unit are moderately weathered throughout with many weathering rinds > 2mm, but with some rinds < 1 mm or non-existent. Oxidation colors are common throughout the unit with no evidence of gleying and poor water drainage. Pedogenesis has altered Unit 7 into a O/A-BA-BC soil profile from the ground surface downward (Figure 5). The degree of soil structure development determined in the field is very weak, with only the lower 41-76 cm (BC) showing moderate coarse subangular blocky structure with clay films coating some ped surfaces and sandstone clasts. The overlying 41 cm (O/A & BA) has a weak fine granular to fine subangular blocky soil structure. Fine through coarse roots are present throughout the entire unit with fine and medium sizes being very common. Decomposing roots and other organic matter are also present within Unit 7. Translocated clays are present as discontinuous films and coating on some sandstone clasts, and around weakly developed ped and sand grain surfaces. Unit 7 also shows abundant bioturbation from both floral and faunal activity.

## DISCUSSION

### Appalachian Plateau Geomorphology

It has long been recognized that the Appalachian landscape experienced tremendous amounts of regolith generation under paleoperiglacial conditions during the Quaternary (e.g. Clark and Ciolkosz, 1988; Braun, 1989; Middlekauff, 1991; Mills and Delcourt, 1991). Some workers in the Appalachians have shown that much of the geomorphologic work on steep Appalachian hillslopes occurs in association with rare, high-magnitude events (Kochel, 1987; Jacobson and others, 1989; Eaton and others, 2003). The series of deposits exposed within the unnamed tributary stream banks in central West Virginia suggest that late Quaternary climatic perturbations have interacted with various geomorphologic and sedimentologic processes. Thus, this deposit is separated into a lower sediment package overlain by an upper sediment package emplaced by differing geomorphologic processes.

The lower sediment package consists of units 1 through 4 and is interpreted as alluvium deposited in high-energy streams (units 2 and 3) that is bounded on the bottom (Unit 1) and top (Unit 4) by low-energy slackwater deposits. The deposition of the lower sediment package occurred during the waning phases of the middle Wisconsin, Oxygen Isotope Stage 3 (OIS 3), and straddles the transition to OIS 2, the Late Wisconsin glacial. Delcourt and Delcourt (1981) suggested that the summertime PFZ was generally situated south of West Virginia during the middle Pleistocene. This would set up a situation that would only occasionally allow the intrusion of warm moist air into the region and allowing intense rain events capable of triggering the geomorphologic activity documented here and in other studies throughout the Appalachians. Changes in environmental conditions (i.e. cooling climate, decline in vegetation cover, position of the polar front) likely triggered geomorphologic instability on the Appalachian Plateau and can be linked to alternating alluvial and slackwater deposition. The cause of slackwater deposition within this geomorphologic setting is unknown at this time but could have been created by either debris flow/landslide activity or possibly impoundments associated with beaver (*Caster sp.*) dam construction and blockage in the downstream direction. Geomorphologic activity shown in figures 3 and 4 associated with the summer 2003 storm event could argue that rainfall-induced hillslope mass-wasting events occurring today may be analogies for the past and would be the more plausible cause of slackwater deposition. This type of mass wasting and associated temporary slackwater conditions is a natural part of hillslope geomorphologic processes. Whatever the cause of slackwater ponding, the preservation of wood fragments, charcoal, and finely disseminated organic matter indicates low redoximorphic (oxygen deficient) slackwater conditions within the environment associated with saturation of the mineral substrate. The preservation of organic materials in slackwater units 1 and 4 and low-chroma colors throughout the entire sediment package suggest that the redoximorphic state was variable through time and was likely controlled by hillslope-stream channel hydrology and biogeochemical processes. Coarser alluvial deposits occur between the two slackwater deposits suggesting high-energy stream flow conditions returned once termination of the slackwater conditions ceased sometime subsequent to 39,320 $^{14}$C YBP until renewed slackwater deposition around 33,800 $^{14}$C YBP. The degree of weathering of sandstone clasts within alluvial units 2 and 3 suggests that they were deposited close in time and have weathered under similar environmental conditions.

The upper sediment package consisting of units 5 through 7 is interpreted to be co-alluvial and deposited under both high-energy alluvial and colluvial (debris flow?) environments. Coalluvium is a variant of colluvium and alluvium occurring in low-order drainage basins where fluvial processes have not sorted the material more typical of other alluvial deposits (Cremeens and Lothrop, 2001). Cremeens and others (2003) studied similar, but younger, coalluvial deposits on other hillslopes in central and western West Virginia, showing the Appalachian Plateau has been geomorphologically active during the much of the late Quaternary.

Based on brighter (rubified) soil colors, texture, and intact soil structure, Unit 5 is interpreted as the remnants of a truncated and buried paleosol (3BCb on Fig. 5). The degrees of pedogenic development of the 3BCb horizon is an indicator of a prior phase of pedogenesis as some amount of time must be allowed to develop a hue of 7.5 YR. This paleosol must have developed during the late Wisconsin and possibly prior to the late Wisconsin glacial maximum (LGM), though sufficient data to confirm this is lacking. In contrast to the radiometrically-constrained lower sediment package, the weak degree of pedogenic overprinting of the sediment above the paleosol suggests the remainder of the deposit may be significantly younger and highly influenced by late Wisconsin hillslope processes (Figure 5). Units 6 and 7 represent cyclic sedimentation likely in relation to late Quaternary climatically-driven geomorphologic events. The degree of weathering of sandstone clasts within the upper units and RPD values significantly higher than 0 (the baseline datum of unweathered parent materials) indicate much of the material was likely weathered and reworked prior to the latest phase of soil formation as previously suggested for steep colluvial hillslopes of the unglaciated Appalachians (e.g. Mills, 2005). Low chroma colors within the upper sediment package are likely lithochromic (inherited from parent materials) in origin and not gleying associated with poor drainage and redoximorphic conditions. The overall coarser grain size upward through the profile, up to boulders in Unit 7, may be the product of debris flow/avalanche deposition in a largely colluvial geomorphologic regime under a periglacial climate. Weak soil horizonation, a lack of well defined soil structure, and a lack of rubification and clay accumulation suggest that the surface soil may only be several thousand years old and possibly linked to geomorphic instability caused by environmental changes as the northward migration of the PFZ associated with the late Wisconsin (OIS 2)-Holocene (OIS 1) transition initiated the cessation of periglacial conditions.

Similar colluvial deposits have also been studied and dated to between 28,700 +/- 190 $^{14}C$ YBP and 21,780 +/- 1500 $^{14}C$ YBP in the Pendleton Creek Valley in northern West Virginia to the northeast of this study (Jordan, 1992) (Figure 1). Additional work in the same area as Jordan (1992) indicates that the onset of colluviation may have been as early as 31,140 +/- 380 $^{14}C$ YBP, pre-dating LGM (Behling and others, 1993) and is interpreted to have ceased in the Pendleton Creek valley by approximately 16,000 YBP (Jordan, 1992). Colluviation commencing approximately 31,000 $^{14}C$ YBP supports the onset of co-alluvial deposition occurring during the OIS 3-2 transition. Similar to the co-alluvial deposits of this study, Conner (1986) and Kochel (1987) have suggested that many debris flow events within the central and southern Appalachians may coincide with climatic fluctuations associated with the northerly migration of the PFZ and the intrusion of warmer tropical air masses into the region.

Jacobson and others (1989) showed additional evidence of ancient hillslope colluviation and debris fan formation in the Buffalo Creek basin in northern West Virginia to the north-northeast of this study (Figure 1). They estimated that the oldest buried paleosols within the colluvial diamictons developed during the early Wisconsin or an earlier time, thus pre-dating deposits of this study, and suggesting prolonged climatically-driven regional hillslope instability throughout Wisconsin time, and likely throughout the Quaternary.

## The Blue Ridge Story

In the Blue Ridge physiographic province of Virginia to the east of this study, Eaton and others (2003) have documented debris flow activity starting more than 50,000 $^{14}C$ YBP with an average of one event every 2500 years for approximately the last 25,000 $^{14}C$ YBP (Figure 1). Eaton and others (2003) also demonstrate that the Blue Ridge hillslopes were colluviated under periglacial conditions with reduced vegetation cover from 27,410 through 18,800 $^{14}C$ YBP. Data presented in Eaton and others (2003) and Kochel (1987) suggest a debris flow recurrence interval of ~2500-4000 years for the Blue Ridge Province. Preliminary paleoclimatic reconstructions based on palynological evidence and modern vegetation distributions suggests a minimum range of mean annual temperature (MAT) of 1.5 °C to 13 °C over the past 45,000 years in that part of the Blue Ridge (Litwin and others, 2004). The Blue Ridge paleobotanical study also suggested that vegetation shifted largely in-phase with regional climatic fluctuations (Litwin and others, 2004) and would have influenced and likely enhanced late Pleistocene hillslope geomorphologic processes throughout the region. This chronology of widespread dated colluvial/debris flow deposition from the Blue Ridge to the east, also demonstrates that geomorphologic systems in the unglaciated central Appalachians were active and responding to regional periglacial and cool-temperate climatic conditions during middle and late Wisconsin time.

## A Brief Glimpse from the Ridge and Valley

Recently another unique Quaternary site has been reported on from the Ridge and Valley Province of Virginia (Whittecar and others, 2007) (Figure 1). The site also documents middle and late Wisconsin geomorphologic activity (debris flows and interbedded standing water deposits) and also demonstrates that the central Appalachians to the south of central West Virginia experienced boreal climatic conditions in the late middle Wisconsin and late Wisconsin prior to the LGM (> 44,000 $^{14}C$ YBP to 29,000 $^{14}C$ YBP) (Whittecar and others, 2007). Ages and geomorphologic data reported by Whittecar and others (2007) are similar to data reported herein and from other locations in West Virginia. Whittecar and others' data also closely resemble both geomorphologic and paleoenvironmental data from the Blue Ridge region indicating periods of geomorphologic instability attributed to occasional northward migration of the PFZ and the intrusion of tropical air masses in an overall periglacial, boreal environment.

## CONCLUSIONS

Even though there have been relatively few dates on surficial deposits within the Appalachians, data discussed herein paint a picture of regional geomorphologic processes, both alluvial and colluvial, responding to climate variations throughout glacial-interglacial cycles of the late Quaternary in the central Appalachians. The unique alluvial-colluvial deposit reported on in this study and a synthesis of pre-existing regional data broadens our knowledge and confirms that during the late middle Wisconsin, (OIS 3) through the Holocene, both alluvial and colluvial geomorphologic processes appear to have been operating on Appalachian hillslopes, and likely have operated in similar fashion during the whole of the Pleistocene. Data from this co-alluvial deposit from central West Virginia show that from sometime prior to 39,320 $^{14}$C YBP to 33,800 $^{14}$C YBP in central West Virginia, geomorphologic processes in the form of slackwater deposition interrupted high energy stream processes varied in response to local environmental conditions and appear to have left a reasonable record of hillslope activity. Erosional and deposition features produced by the summer storm of 2003 may be modern analogs for the depositional environment responsible for slackwater conditions documented in this study and are a natural part of hillslope processes. From about 33,800 $^{14}$C YBP to the present, the dominant geomorphologic regime appears to have switched to one dominated by colluvial (debris flow?) activity intermixed with alluvial processes creating the co-alluvial upper sediment package. The weak degree of pedogenesis may indicate units 6 and 7 of the upper sediment package may have been deposited during the late Wisconsin-Holocene transition as the PFZ migrated northward and warm and moist air masses could once again enter the region. Geomorphologic instability recognized in this study and a review of others suggest that geomorphologic processes have likely varied in relation to regional climate fluctuations and the location of the PFZ associated with glacial advances and retreats during the late Quaternary.

## ACKNOWLEDGEMENTS

We thank Bob Shumaker and the West Virginia University Department of Geology Shumaker Fund for financial support of this project. Hugh Mills provided a critical review of the manuscript that significantly improved the final product. Bob Behling, Milan Pavich, Frank Pazzaglia, and Noel Potter provided many useful discussions concerning on the Quaternary geomorphology of the Appalachians.

## REFERENCES

Behling, R. E., Kite, J. S., Springer, T. C., Cenderelli, D. A., and Stuckenrath, R., 1993. Buried organic-rich sediments in the unglaciated Appalachian Highlands: a stratigraphic model for finding pre-Late Wisconsin paleoenvironmental data: Geological Society of America Abstracts with Programs, v. 25, p. 60.

Bilzi, A. F., and Ciolkosz, E. J., 1977. A field morphology rating scale for evaluating pedological development: Soil Science, v. 124, p. 45-48.

Braun, D. D., 1989. Glacial and periglacial erosion of the Appalachians: Geomorphology v. 2, p. 233-256.

Braun, D. D., Pazzaglia, F. J., and Potter, N., Jr., 2003. Margin of Laurentide Ice to the Atlantic Coastal Plain: Miocene-Pleistocene landscape evolution in the Central Appalachians. In: Easterbrook, D. J., (Ed.), Quaternary Geology of the United States: INQUA 2003 Field Guide Volume, Desert Research Institute, Reno, Nevada. pp. 219-244.

Bull, W. B., 1991. Geomorphic Responses to Climatic Change. Oxford University Press, New York, 326 p.

Carpenter, S. G., 1992. Soil Survey of Nicholas County, West Virginia. United States Department of Agriculture, Natural Resource Conservation Service, 138 p.

Clark, G. M. and Ciolkosz, E. J., 1988. Periglacial geomorphology of the Appalachian Highlands and Interior Highlands south of the glacial border – a review: Geomorphology v.1, p. 191-220.

Conners, J. A., 1986. Quaternary geomorphic processes in Virginia. In: McDonald, J. N., and Bird, S. O., (Eds.), The Quaternary of Virginia – a symposium volume, Charlottesville, Virginia, pp. 23-35.

Cremeens, D. L., and Lothrop, J. L., 2001. Geomorphology of upland regolith in the Unglaciated Appalachian Plateau: Implications for prehistoric archaeology. In: Sullivan, L. and Prezzano, S., (Eds.),. Archaeology of the Appalachian Highlands. University of Tennessee Press, Knoxville, pp. 31-48.

Cremeens, D. L., MacDonald, D. H., and Lothrop, J. C., 2003. Holocene colluvial soils and geoarchaeology in the Unglaciated Appalachian Plateau: Two examples from West Virginia, USA: Geoarchaeology v. 18, p. 799-826.

Delcourt, P. A., 1985. The influence of late-Quaternary climatic and vegetational change on paleohydrology in unglaciated eastern North America: Ecologia Mediterranea Tome v. 11, p. 17-26.

Delcourt, P.A., and Delcourt, HR., 1981. Vegetation maps for eastern North America: 40,000 yr BP to the present. In: Romans, R.C. (Ed.), Geobotany II. Plenum.

Eaton, L. S., Morgan, B. A., Kochel, R. C., and Howard, A. D., 2003. Quaternary
deposits and landscape evolution of the central Blue Ridge of Virginia: Geomorphology v. 56, p. 139-154.

Frakes, L. A., Francis, J. E., and Syktus, J. I., 2005. Climate modes of the Phanerozoic. Cambridge University Press, New York, 274 p.

Fullerton, D. S., Bush, C. A., and Pennell, J. N., 2003. Map of surficial deposits and materials in the Eastern and Central United States (East of 102° Longitude): U.S. Geological Survey Geologic Investigation Series I-2787, 46 p.

Harden, J. W., 1981. A quantitative index of soil development from field descriptions: Examples from a chronosequence in central California: Geoderma, v. 28, p. 1-28.

Jacobson, R. B., Miller, A. J., and Smith, J. A., 1989. The role of catastrophic geomorphic events in central Appalachian landscape evolution: Geomorphology v. 2, p. 257-284.

Jordan, M. K., 1992. Late Quaternary history and characterization of deposits in Pendleton Creek valley, Tucker County, West Virginia, unpublished masters thesis, West Virginia University, Morgantown, West Virginia.

Knox, J. C., 1983. Responses of rivers systems to Holocene climates. In: Wright, H. E., Jr., (Ed.), Late-Quaternary Environments of the United States, vol. 2, pp. 26-41.

Kochel, R. C., 1987. Holocene debris flows in central Virginia. In: Costa, J. E., and Wirczorak, G. F., (Eds.), Debris flows/avalanches: Process, recognition, and mitigation, Reviews in Engineering Geology vol. 3, Geological Society of America, Boulder, pp.139-155.

Larabee, P. A., 1986. Late-Quaternary vegetational and geomorphic history of the Allegheny Plateau at Big Run Bog, Tucker County, West Virginia. unpublished masters thesis, University of Tennessee, Knoxville.

Litwin, R. J., Morgan, B. A., and Eaton, L. S., 2004. Proxy climate trends in the Blue Ridge of Virginia, 0-45 KA, and comparison to the Greenland ice core record. Geological Society of America Abstracts with Programs, v. 36, p. 114.

Maxwell, J. A., and Davis, M. B., 1972. Pollen evidence of Pleistocene and Holocene vegetation on the Allegheny Plateau, Maryland: Quaternary Research 17, 93-104.

Messinger, T. and Wiley, J. B., 2004. Regional relations in bankfull channel characteristics determined from flow measurements at selected stream-gaging stations in West Virginia, 1911-2002. U. S. Geological Survey Water-Resources Investigations Report 13-4276, 43 p.

Middlekauff, B. D., 1991. Probable paleoperiglacial morphosequences in the Northern Blue Ridge: Physical Geography v. 12, p. 19-36.

Mills, H. H., 2005. Relative-age dating of transported regolith and application to study of landform evolution in the Appalachians: Geomorphology v. 67, p. 63-96.

Mills, H. H., and Delcourt, P. A., 1991. Quaternary geology of the Appalachian Highlands and Interior Low Plateaus, In: Morrison, R. B., (Ed.), Quaternary non-glacial geology; Conterminous U.S.: Boulder, Colorado, Geological Society of America, The Geology of North America, vol. K-2, pp. 611-628.

Pazzaglia, F. J., and Brandon, M. T., 1996. Macrogeomorphic evolution of the post-Triassic Appalachian mountains determined by deconvolution of the offshore basin sedimentary record: Basin Research v. 8, p. 255-278.

Pederson, J, Pazzaglia, F., and Smith, G., 2000. Ancient hillslope deposits: missing links in the study of climate controls on sedimentation: Geology v. 28, p. 27-30.

Pewe, T., L., 1983. The periglacial environment in North America during Wisconsin time. In: Porter, S. C., (Ed.), Late-Quaternary environments of the United States, vol 1, The late Pleistocene, University of Minnesota Press, Minneapolis, pp. 157-189.

Poag C. W., and Sevon, W. D., 1989. A record of Appalachian denudation in postrift Mesozoic and Cenozoic sedimentary deposits of the U. S. middle Atlantic Continental margin: Geomorphology v. 2, p. 119-157.

Reger, D. B., 1921. Nicholas County [County Report]. West Virginia Geological and Economic Survey, Morgantown, West Virginia, 847 p.

Watts, W. A., 1979. Late Quaternary vegetation of central Appalachia and the New Jersey coastal plain: Ecological Monographs v. 49, p. 427-469.

Whittecar, G. R., and Duffy, D. F., 2000. Geomorphology and stratigraphy of Late Cenozoic alluvial fans, Augusta County, Virginia, USA: Southeastern Geology v. 39, p. 259-279.

Whittecar, G. R., Wann, T. C., and Bartlett Jr., C. S., 2007. Paleoenvironmental analysis of a middle Wisconsinan biota site, southwestern Virginia, U.S.A.: Quateranry Research, v. 68, p. 133-140.

**Appendix 1: Soil Profile Morphology Data**

| Criteria: | Thickness | Color | | | Texture | Structure | | | Boundaries | Clay Films | SUM |
|---|---|---|---|---|---|---|---|---|---|---|---|
| Horizon: | (cm) | *Hue* | *Value* | *Chroma* | | *Type* | *Grade* | *Size* | | | |
| O/A | 15 | 10YR | 5 | 6 | sil-sl | gr | w | f | d | | |
| | | 2 | 1 | 3 | 0.5 | | 1 | 1.5 | 0 | 0 | 9 |
| BA | 26 | 10YR | 5 | 6 | sil | gr | w | f | g | | |
| | | 2 | 1 | 3 | 1 | | 1 | 1.5 | 1 | 0 | 10.5 |
| BC | 35 | 10YR | 5 | 6 | sil | pl | w | f | g | c | |
| | | 2 | 1 | 3 | 1 | | 1 | 1.5 | 1 | 2 | 12.5 |
| 2C1ox | 36 | 10YR | 5 | 6 | sl | m | N/A | N/A | d | f | |
| | | 2 | 1 | 3 | 0 | | 0 | 0 | 0 | 1 | 7 |
| 2C2ox | 48 | 10YR | 6 | 8 | sil | m | N/A | N/A | d | f | |
| | | 2 | 0 | 5 | 1 | | 0 | 0 | 0 | 1 | 9 |
| 2C3u | 25 | 5Y | 6 | 3 | sl | m | N/A | N/A | g | none | |
| | | 3 | 0 | 5 | 2 | | 2 | 0.5 | 3 | 2 | 17.5 |
| 3BCb | 51 | 7.5YR | 6 | 8 | sc | sab | m | c | a | c | |

**Key:**

Texture: l = loam; sl = sandy loam; sil = silt loam; scl = silty clay loam; sc = silty clay

Structure:

type: gr = granular; pl = platy; sab = subangular blocky; m = massive

grade: w = weak; m = moderate; s = strong

size: vf = very fine; f = fine; m = medium; c = coarse

Horizon boundaries: d = diffuse; g = gradual; w = wavy; a = abrupt

Clay films: f = few; c = common; m = many

SOUTHEASTERN GEOLOGY
V. 47, No.1, February 2010, p. 41-47

# Mazon Creek Style Soft-Tissue Preservation In The Mississippian Nancy Member Of The Borden Formation, Northeastern Kentucky: Evidence For Early Siderite Precipitation

**Bradley Deline**

*Department of Geosciences*
*University of West Georgia*
*Carrollton, GA 30118*
*bdeline@westga.edu*

**James J. Zambito IV**

*Department of Geology*
*University of Cincinnati*
*Cincinnati, OH 45221*

## ABSTRACT

**Exposures of the Mississippian Nancy Member of the Borden Formation in northeastern Kentucky contain a diverse marine delta fauna preserved within siderite nodules. In most cases initial siderite precipitation began relatively early, following burial but before sediment compaction. A new discovery of soft tissue preservation of a polychaete annelid indicates that the precipitation of siderite can occur rapidly (days to weeks) following burial and that the Nancy Member of the Borden Formation can display exceptional fossil preservation reminiscent of the Pennsylvanian Mazon Creek lagerstätte of northeastern Illinois.**

## INTRODUCTION

At first glance, polychaete worms have a surprisingly long and extensive fossil record with representatives known from almost every stage throughout the Phanerozoic. However, the paleontological record of poychaetes is diminished when two facts are taken into consideration. First, polychaete worms are one of the most diverse and abundant components of modern marine faunas (Rouse and Pleijel, 2001). For example, Grassle (1973) identified 103 species and 1441 individual polychaetes from a single coral fragment weighing only a few kilograms. In many shallow marine environments polychaetes represent approximately 2/3 of the species of macrofauna (Grassle, 1973) and their diversity has been used as a proxy for overall biodiversity within marine communities (Olsgard et al., 2004). Secondly, the vast majority of reported fossil polychaetes are based on the ichnofossil record, consisting of mud burrows (Nara, 1995) and epibiont borings (Brett, 1978), as well as isolated jaw pieces referred to as scolecodonts (Szaniawski, 1996). Body fossils of polychaete worms are rare in the fossil record (Briggs and Kear, 1993, and references therein) and occur in a variety of depositional environments, though their preservation normally occurs in anoxic black shale.

One exception to this mode of preservation is the Pennsylvanian Mazon Creek Fauna in northeastern Illinois. Amongst other flora and fauna, Mazon Creek deposits contain exceptionally preserved, abundant, and diverse polychaete worms preserved within siderite nodules. The Mazon Creek is a freshwater to marine estuarine environment with steady influxes of sediment and freshwater which buried the animals and the resulting decay may have produced a chemical microenvironment that promoted siderite precipitation (Baird, 1997a; 1997b; 1997c).

The Mississippian Nancy Member of the Borden Formation has a somewhat analogous depositional setting and previous studies have reported a similar mode of preservation that is limited to skeletonized fauna (Lierman and Mason, 1992). Herein we reevaluate the taphonomy of the Nancy Member fauna and report the

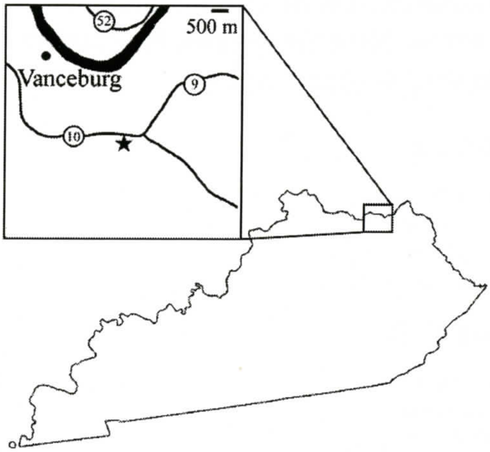


**Figure 1. Locality map of the AA Highway Section of the Nancy member, Borden Formation near Vanceburg, Kentucky.**

discovery of soft tissue preservation of a polychaete annelid worm and the implications this has on the precipitation of siderite nodules within the Borden Formation.

## GEOLOGICAL SETTING

The Nancy Member of the Borden Formation in northeastern Kentucky, has been dated as early Osagean in age based on conodonts, corresponding to the lower Ivorian Stage of the Belgian upper Tournaisian succession (Lower Mississippian; see Work and Mason, 2005). The sediments of the Borden Formation were deposited in the central Appalachian Basin following the fourth tecto-phase of the Acadian Orogeny, during an overall regressive period as the rate of sediment influx was higher than that of subsidence (Ettensohn, 1992, and references therein). The Nancy Member is dominated by highly bioturbated bluish-gray to greenish-gray silty shale containing nodular and concretionary siderite-cemented siltstones, which is interbedded with silt and fine sandstones of turbiditic origin (Weir et al., 1966; Lierman and Mason, 1992; Lierman et al., 1992a; Lierman et al., 1992b). Lithologic, paleoecologic, and taphonomic features of the Nancy Member suggest that it records change from dysoxic to oxic conditions in a pro-delta to slope setting (Mason and Kammer, 1984; Kammer and Cox, 1985; Kammer et al., 1986; Lierman and Mason, 1992; Lierman et al., 1992a; Lierman et al., 1992b).

**Figure 2. The AA Highway Section of the Nancy member, Borden Formation showing distinctive horizons of siderite-rich siltstones and isolated siderite nodules.**

## STRATIGRAPHIC AND PALEONTOLOGIC SUCCESSION

The section investigated in this study is located on the southside of the AA Highway (KY Routes 9, 546, and 10) a few km east of Vanceburg, Kentucky (Figure 1). In general, the section studied represents a shale-dominated, coarsening-upward (shallowing) succession (Figure 2). The lowest ~4.5 meters of the section consists of gray shales containing siderite concretions interbedded with tabular to nodular siderite cemented siltstones (Figure 3). Above this, siderite, though still present, decreases in abundance up through the section, while the abundance and thickness of siltstones increases. These siltstones commonly display scoured soles with tool-marks, load casts, and in one case, channelized bedding features, which we interpret as distal pro-delta and slope turbidite and distributary channel deposits, resulting from sediment exported down-ramp from shallower environments.

Paleoecological patterns through the section also suggest an overall, however, slight, shallowing. Throughout the section, common ichnogenera include *Chondrites, Scalarituba,* and *Zoophycos*. In the Vanceburg, Kentucky area, Chaplin (1982) has placed such trace-fossil assemblages in the *Nereites* ichnofacies. The lowest ~4.5 meters is a probable correlative with the upper portion of the Cave Run Lake interval of Mason and Kammer (1984) and Kammer et al. (1986). This dysoxic environment interval is typically found in the lowest portion of the Nancy Member and contains a low diversity, diminutive fauna, similar to other localities in which this unit has been recognized.

In the section studied, we did not observe the pyrite replaced and mollusk-dominated faunas typical of this interval, and, therefore, we assume the section outlined in this study does not contain the lowest portions of the Cave Run Lake interval. We do, however, observe an in-

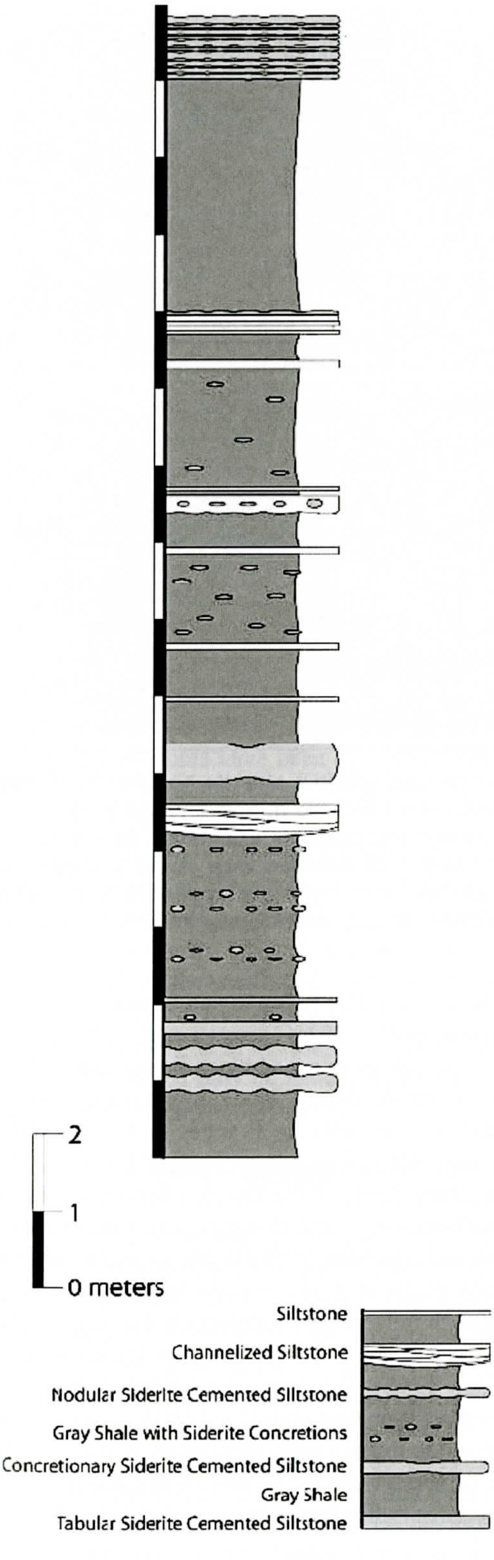


**Figure 3. Stratigraphic section of the exposure of the middle to upper Nancy Member of the Borden Formation near Vanceburg, Kentucky.**

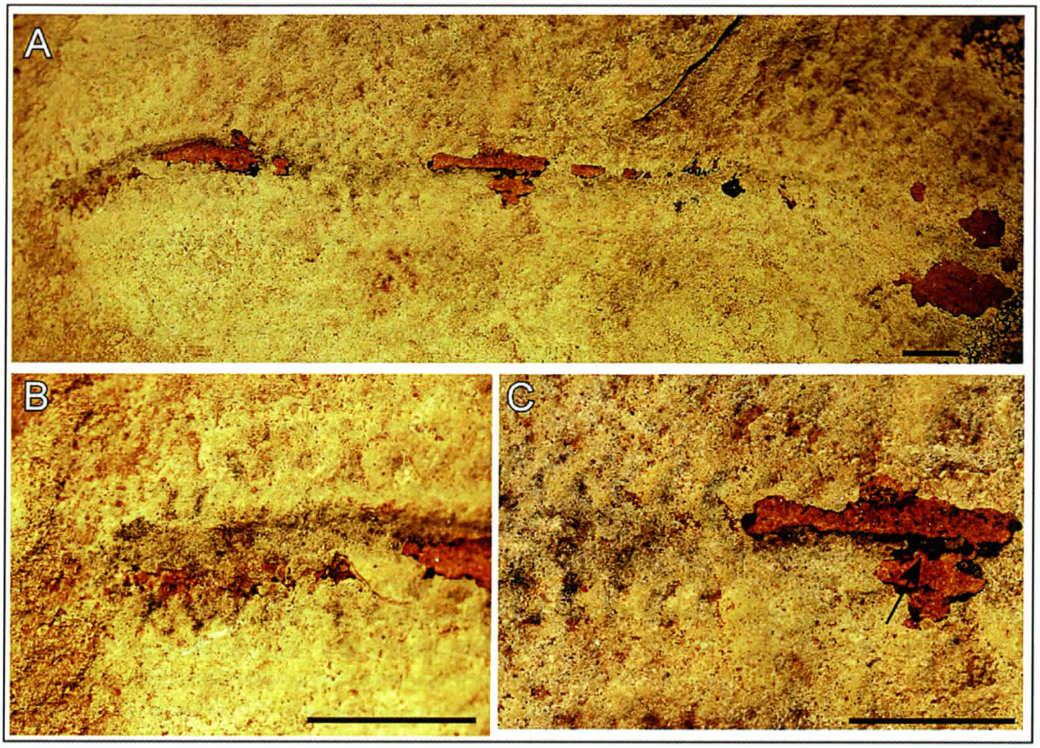


**Figure 4. A. Body fossil of a polychaete annelid preserved within a siderite nodule (Cincinnati Museum Center IP54522). Though the surface is weathered and the mineralized features of the animal are absent (jaw features and chaetae), the anterior and posterior orientation can be distinguished as well as the parapodia and sections of the gut. B. Detailed view of the prostomium (anterior margin) showing parapodia and dark areas that could represent eye spots. C. Detailed view of the medial trunk showing parapodia and preserved gut, indicated by an arrow. All scale bars are 5 millimeters.**

crease in diversity through the succession that is typically associated with the transition from the Cave Run Lake interval into the upper portions of the Nancy Member. In particular, the middle portion of our section (8 to 10 meters above section base) contains a diverse oxic fauna, including abundant spiriferid, orthid, and strophonemid brachiopods, common disarticulated crinoid ossicles, trilobites, orthoconic cephalopods, goniatites, and rare gastropods, bryozoans, solitary rugose corals, and conularids. The increase in diversity is interpreted as representing the transition from dysoxic to oxic conditions through the section. This succession is similar to that observed in previous studies of the Nancy Member of the Borden Formation in both eastern and western Kentucky (Mason and Kammer, 1984; Kammer and Cox, 1985; Kammer et al., 1986; Lierman and Mason, 1992; Lierman et al., 1992a; Lierman et al., 1992).

Though there are obvious faunal similarities between the Nancy fauna in eastern Kentucky and sections near St. Frances in western Kentucky, there are also significant differences. The western flank of the Borden delta contains a well-preserved and diverse crinoid and bryozoan fauna preserved as calcitic skeletons within silty shales and siltstone and lacks the diversity and abundance of cephalopods that can be observed in the eastern exposures (Kammer and Cox, 1985). This east-west variation in faunal composition may reflect a shift in preservational mode from more typical shallow marine calcitic preservation to preservation within siderite nodules rather than a true ecological shift.

## DESCRIPTION OF THE POLYCHAETE ANNELID

The newly discovered polychaete worm is preserved within a siderite nodule from the Nancy Member of the Borden Formation and clearly shows soft-tissue preservation (Figure 4). The nodule had split naturally on the outcrop and was already heavily weathered when collected. The specimen is bilaterally symmetrical and preserved dorsoventrally flattened. The specimen is 55 millimeters in length with a 2.25 millimeters wide trunk and 1 millimeter long laterally projecting parapodia. The specimen has between 40 and 50 sets of parapodia with no preserved traces of chaeta. The anterior is slightly broader and does not appear to bear any cirri, but does contain dark areas that could indicate eye spots (Figure 4b). The specimen also shows portions of the gut that runs throughout the trunk of the specimen and is approximately 0.9 millimeters wide (Figure 4c). The specimen is too weathered to preserve the jaw apparatus and no scolecodonts have been described from this unit. The trunk has a slight taper to the posterior end of the organism.

The systematics of polychaete annelids has been the subject of discussion and close morphologic scrutiny (Rouse and Fauchald, 1997; Fauchild and Rouse, 1997; Rouse and Pleijel, 2001), but given the weathered condition of the current specimen it would be difficult to decidedly place it into one of the known Carboniferous families based only on general body shape (J. K. Fitzhugh, personal communication).

## TAPHONOMY

Fossils from the Nancy Member typically occur within siderite concretions, which form around organisms soon after burial. The decay of the animals results in chemical reactions that create a microenvironmental halo at shallow depths under the sediment water interface. The precipitation of siderite ($FeO+CO_2 \rightarrow FeCO_3$) took place in the absence of free oxygen through bacterial-mediated reactions that create hard cement that entombs and protects the animal remains and prevents further decay (Baird, 1997b). Siderite concretions commonly contain uncompacted body fossils and burrows preserved as molds, casts, and/or mineralized replacements, typically infilled with barite, sphalerite, and minor amounts of galena (Lierman and Mason, 1992). This type of preservation suggests that siderite concretions and cemented beds were formed by early diagenetic cementation prior to sediment compaction (Lierman et al., 1992a). The presence of soft-tissue preservation also indicates that the timing of siderite precipitation must be much earlier than compaction. Laboratory studies of the decay of modern polychates indicate that regardless of conditions (temperature, oxygen, or disturbance) the volatile tissues (including muscle and cuticle), which compose the gut and body wall, disintegrate within a few weeks (Briggs and Kear, 1993), such that the precipitation of the siderite preserving the polychaete must have occurred extremely rapidly within the sediment. Most fossils within the Nancy Member of the Borden Formation are preserved as internal (cephalopods and gastropods), external (bryozoans and rugose coral), or composite molds (brachiopods), or as casts (crinoids and conularids) with no trace of soft tissue preservation indicating that though possible, most siderite preservation occurred after the decay of the most volatile tissues. Since the polychaete fossil was collected as float, it cannot be placed exactly within the stratigraphic column. Approximately one hundred in place concretions were collected and split using the methods described by Sroka and Baird (1997). However, no other instances of soft tissue preservation were observed. Nevertheless, the Nancy Member has the potential to preserve a high proportion of the original Mississippian fauna that are normally lost in the fossilization process and needs to be further sampled and studied.

## DISCUSSION

Konservat-Lagerstätten, defined as fossil deposits that preserve the traces of volatile tissues (Seilacher, Reif, and Westphal, 1985; Allison and Briggs, 1993), are important in the reconstruction of fossil communities beyond the skeletonized components. These deposits are rare and are not randomly distributed through time, being over-represented during the Cambrian and Jurassic (Allison and Briggs, 1993). Therefore, the identification of a deposit that has the potential to preserve volatile tissues during the carboniferous in a bioturbated shallow marine environment offers a glimpse into the composition of the community that is rarely preserved.

A strong parallel exists between the Nancy Member of the Borden Formation and the Mazon Creek (Francis Creek Shale) deposits in northeastern Illinois. The Mazon Creek contains a much wider range of environments from fresh water to marine (Baird, 1997c) and has a much higher proportion of soft bodied fossils, but within the Mazon Creek there is a strong gradient in preservation potential. The quality of preservation and abundance of soft bodied fossils decreases across the onshore-offshore gradient, possibly due to an increase in scavenging and bioturbation or a shift in pore water chemistry (Baird, 1997a; 1997b). The Nancy Member represents an offshore continuation of this gradient compared with the more parallic Mazon Creek facies. The Nancy member contains a fully marine fauna, indicated by common crinoids and cephalopods, as well as abundant *Chondrites, Scalarituba,* and *Zoophycos* trace fossils. Compared with the Mazon creek, the Nancy Member is more oxygenated, has lower preservation quality, and fossilized volatile tissues are extraordinarily rare. Environmentally, the siderite concretion bearing Late Devonian Chagrin Shale of northeastern Ohio may be a better analog. Though there is no report of soft tissue preservation, the fully marine Chagrin Shale has a well preserved and diverse arthropod fauna (Feldman and McKenzie, 1981; Weidner and Feldman, 1985) which also indicated early precipitation of siderite following burial.

Though the preservation of non-skeletonized organisms is expected to be an extremely rare event within the Nancy Member, the discovery of a body fossil of a polychaete annelid indicates that in some cases the precipitation of siderite occurs very soon after burial yielding exceptional preservation. The fossil record allows few clear windows into the soft bodied fauna of Late Paleozoic Delta communities, and, as such, the Nancy Member of the Borden Formation represents an important and understudied fossil-bearing deposit of siderite concretion preservation of soft parts in an open marine deposit.

## ACKNOWLEDGEMENTS

We would like to thank Nick Bose for field assistance as well as Carlton Brett and Kees Dejong for bringing the rocks to our attention. We would also like to thank J. Kirk Fitzhugh for advice regarding polychaete classification. This content and clarity of the manuscript was improved through the suggestions of Gordon Baird and Thomas Kammer.

## REFERENCES

Allison, P.A. and Briggs, D.E.G., 1993, Exceptional fossil record: Distribution of soft-tissue preservation through the Phanerozoic: Geology, v. 21, p. 527-530.

Baird, G.C., 1997a, Fossil Distribution and Fossil Association: *in* Shabica, C.W. and Hay, A.A., eds., Richarson's Guide to the Fossil Fauna of Mazon Creek, Northeastern Illinois University, Chicago. p. 21-26.

Baird, G.C., 1997b, Francis Creek Diagenetic Events: *in* Shabica, C.W. and Hay, A.A., eds., Richarson's Guide to the Fossil Fauna of Mazon Creek, Northeastern Illinois University, Chicago. p. 30-34.

Baird, G.C., 1997c, Paleoenvironmental Setting of the Mazon Creek Biota: *in* Shabica, C.W. and Hay, A.A., eds., Richarson's Guide to the Fossil Fauna of Mazon Creek, Northeastern Illinois University, Chicago. p. 35-51.

Brett, C.E., 1978, Host-specific pit-forming epizoans on Silurian crinoids: Lethaia, v. 14, p. 217-232.

Briggs, D.E.G. and Kear, A.J., 1993, Decay and preservation of polychaetes: taphonomic threshold in soft-bodied organisms: Paleobiology, v. 19, p. 107-135.

Chaplin, J.R., 1982, Annual Field Conference - Society for Sedimentary Geology: Field guidebook to the paleoenvironments and biostratigraphy of the Borden and parts of the Newman and Breathitt formations (Mississippian-Pennsylvanian) in northeastern Kentucky: Society of Economic Paleontologists and Mineralogists, Great Lakes Section, 196 p.

Ettensohn, F.R., 1992, General Mississippian Paleogeographic and Tectonic Framework for Kentucky: *in* Ettensohn, F.R., ed., Miscellaneous Report No. 5 - Changing Interpretations of Kentucky Geology - Layer-cake, Facies, Flexure, and Eustacy: Ohio, Division of Geological Survey, Columbus, p. 40-42.

Fauchald, K. and Rouse, G., 1997, Polychaete systematics: Past and present: Zoologica Scripta, v. 26, p. 71-138.

Feldman, R. M. and McKenzie, S., 1981, *Echinocaris multispinosis*, a new echinocarid (Phyllocarida) from the Chagrin Formation (Late Devonian) of Ohio. Journal of Paleontology, v. 55, p. 383-388.

Fitzhugh, K., Sroka, S.D., Kruty, S., Henderson, M.D., and Hay, A.A., 1997, Polychaete Worms: *in* Shabica, C.W. and Hay, A.A., eds., Richardson's Guide to the Fossil Fauna of Mazon Creek, Northeastern Illinois University, Chicago. p. 64-83.

Grassle, J.F., 1973, Variety in coral reef communities: *in* Jones, O. A. and Endean, R., eds., Biology and Geology of Coral Reefs, Vol. 2: Biology 1, Academic Press, New York, p. 247-270.

Kammer, T.W., Brett, C.E., Boardman, D.R., and Mapes, R.H., 1986, Ecologic stability of the dysaerobic biofacies during the late Paleozoic: Lethaia, v. 19, p. 109-121.

Kammer, T.W. and Cox, K.D., 1985, Paleoecology of a delta slope community from the lower Mississippian Borden Formation in central Kentucky: Southeastern Geology, v. 26, p. 39-46.

Lierman, R.T. and Mason, C.E., 1992, Farmers, Nancy, and Cowbell members of the Borden Formation (Lower Mississippian) along Kentucky State Highway 546 in northeastern Kentucky: *in* Ettensohn, F.R., ed., Miscellaneous Report No. 5 - Changing Interpretations of Kentucky Geology - Layer-cake, Facies, Flexure, and Eustacy: Ohio, Division of Geological Survey, Columbus, p. 138-142.

Lierman, R.T., Mason, C.E., Pashin, J.C., and Ettensohn, F.R., 1992a, Cleveland Shale-through-lower Borden Sequence (Devonian-Mississippian) and Implications: *in* Ettensohn, F.R., ed., Miscellaneous Report No. 5 - Changing Interpretations of Kentucky Geology - Layer-cake, Facies, Flexure, and Eustacy: Ohio, Division of Geological Survey, Columbus, p. 77-81.

Lierman, R.T., Mason, C.E., Pashin, J.C., and Ettensohn, F.R., 1992b, Cowbell Member, Nancy Member, Farmers Member and Henley Bed of the Borden Formation, Sunbury Shale, and Bedford-Berea sequence along State Route 546 in northeastern Kentucky, *in* Ettenson, F.R., ed. Miscellaneous Report No. 5 - Changing Interpretations of Kentucky Geology - Layer-cake, Facies, Flexure, and Eustacy: Ohio, Division of Geological Survey, Columbus, p. 142-145b.

Mason, C.E. and Kammer, T.W., 1984, Dysaerobic faunas of the Mississippian Borden Formation in Kentucky and Indiana: Abstracts with Programs - Geological Society of America, v. 16, p. 178.

Nara, M., 1995, *Rosselia socialis*: a dwelling structure of a probable terebellid polychaete: Lethaia, v. 28, p. 171-178.

Olsgard, F., Brattegard, T., and Holthe, T., 2003, Polychaetes as surrogates for marine biodiversity: lower taxonomic resolution and indicator groups: Biodiversity and Conservation, v. 12, p. 1033-1049.

Rouse, G.W. and Fauchald, K., 1997, Cladistics and polychaetes: Zoologica Scripta, v. 26, p. 139-204.

Rouse, G.W. and Pleijel, F., 2001, Polychaetes. Oxford University Press, New York. p. 354.

Seilacher, A., Reif, W.E., and Westphal, F. 1985, Sedimentological, ecological and temporal patterns of fossil Lagerstätten: Philosophical Transactions of the Royal Society of London, Biology, v. 311, p. 5-23.

Sroka, S.D. and Baird, G.C., 1997, Freeze-thawing technique for opening nodules: *in* Shabica, C.W. and Hay, A.A., eds., Richarson's Guide to the Fossil Fauna of Mazon Creek, Northeastern Illinois University, Chicago. p. 281-282.

Szaniawski, H., 1996, Scolecodonts: *in* Jansonius, J. and McGregor, D.C., eds., Palynology: Principles and Applications, Vol. 1, American Association of Stratigraphic Palynologists Foundation, Pittsburgh, PA, p. 337-354.

Weidner, W.E. and Feldman, R.M., 1985, Paleoecological interpretation of echinocarid arthropod assemblages in the Late Devonian (Famennian) Chagrin Shale, Northeastern Ohio. Journal of Paleontology, v. 59, p. 986-1004.

Weir, G.W., Gualtieri, J.L., and Schlanger, S.O., 1966, Borden Formation (Mississippian) in south- and southeast-central Kentucky: U. S. Geological Survey Bulletin, p. F1-F38.

Work, D.M. and Mason, C.E., 2005, Mississippian (early Osagean) Cave Run Lake ammonoid fauna, Borden Formation, northeastern Kentucky: Journal of Paleontology, v. 79, p. 719-725.

SOUTHEASTERN GEOLOGY
V. 47, No. 1, February 2010, p. 49-59

# PRODELTAIC QUARTZ-SAND TURBIDITES IN THE UPPER PENNINGTON FORMATION (MISSISSIPPIAN) AT DOUGHERTY GAP, WALKER COUNTY, GEORGIA (U.S.A.)

CARL R. FROEDE JR.

*U.S. Environmental Protection Agency, Region 4,*
*61 Forsyth Street, SW*
*Atlanta, Georgia 30303-8960*

## ABSTRACT

**Approximately 4.0 m of interbedded fine-grained quartz sandstone and shale layers are exposed laterally for 100 m along a sidewall at Dougherty Gap, Georgia (U.S.A.). These strata have been interpreted as crevasse-splay deposits suggestive of deltaic infill near the close of the Mississippian Period. However, another depositional setting is possible. The multiple sandstone layers within this interval are not bioturbated, have no obvious internal bedding or sedimentary features, exhibit predepositional convex hypichnial traces along the bed soles, and have postdepositional asymmetric linguoid ripples across the top surfaces of the sandstones. Collectively, these features are indicative of turbidites. The limited nature and scale of these siliciclastic deposits suggest emplacement in association with storm events along an unstable delta front. This "sandy turbidite–mud" cycle was repeated more than 20 times at this locale.**

## INTRODUCTION

Eustatic position during the Carboniferous is typically defined by changes in lithofacies and biofacies consistent with Walther's Law. In northwestern Georgia (U.S.A.), Mississippian marine limestone is overlain by Mississippian and Pennsylvanian prodeltaic/deltaic clastic sediments (Thomas and Cramer, 1979). Assigning these Carboniferous strata to specific depositional settings can be problematic as exemplified by the stratigraphic section exposed at Dougherty Gap.

The Pennington Formation (upper Mississippian) is exposed along a sidewall at Dougherty Gap, Georgia (Figure 1). The silts and clays of the Pennington Formation are recognized as prodeltaic clastics (Ferm and others, 1967; Ferm and others, 1972; Thomas and Cramer, 1979; Bergenback and others, 1980; Luther and Smith, 1980; Sheehan, 1988). A small interval toward the top of the formation contains interbedded sandstone and shale layers that have been interpreted as marginal-marine, shallow-water, crevasse-splay deposits (Sheehan, 1988; Rindsberg and Martin, 2007). However, this interpretation introduces unnecessary eustatic changes and requires a completely different depositional setting from the prodeltaic sediments that both under- and overlie this small stratigraphic interval. Based on more recent work on isolated sandstone bodies in prodeltaic silts and clays (Røe, 1995; Mutti and others, 1999; Milli and Moscatelli, 2000; Mutti and others, 2000; Mutti and others, 2003; Budillon and others, 2005; Pattison, 2005a) it is more likely that this same interval of interbedded sandstone and shale represents pulses of quartz-sand-rich turbidity currents deposited across scoured, bioturbated mud under storm-induced conditions along an unstable delta front.

## AREA OF STUDY AND STRATIGRAPHY

The Mississippian and Pennsylvanian strata in this region are part of the Appalachian fold and thrust belt within the Valley and Ridge province (Thomas and Cramer, 1979). Dougherty Gap provides a moderate descent from the top of Lookout Mountain to McLemore Cove.

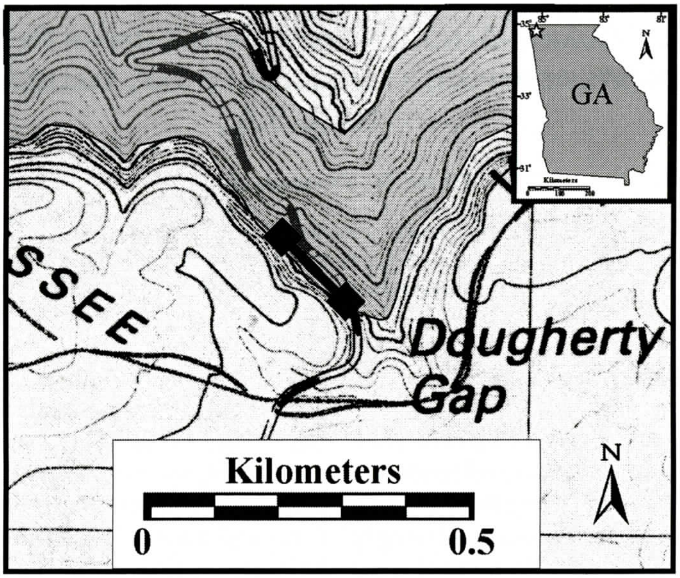


**Figure 1. An interbedded sandstone and shale section is exposed along a portion of Lookout Mountain at Dougherty Gap, Georgia. The shaded area represents the Pennington Formation outcrop (modified from Crawford, 1989) and the section of interest is highlighted as a heavy black line bounded by two black boxes near the top of the formation. Contours are in five-meter intervals.**

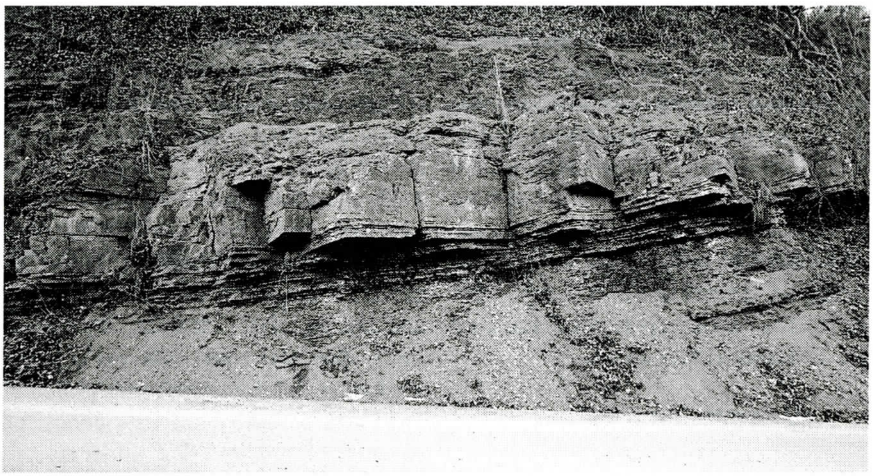

**Figure 2. A portion of the exposure along the sidewall of Lookout Mountain at Dougherty Gap. The section of interest is approximately 4.0 m of interbedded sandstones and shales. The fine-grained sandstone layers do not readily exhibit graded bedding, sedimentary structures, depositional features, or evidence of bioturbation. Scale in 15-cm divisions.**

A portion of the eastern sidewall of Lookout Mountain is exposed and Mississippian and Pennsylvanian strata can be readily examined.

Sheehan (1988) was the first to investigate an interval of alternating quartz sandstone and shale in an upper section of the Pennington Formation exposed along Dougherty Gap. His work also included a full description of the Mississippian and Pennsylvanian stratigraphic units exposed at this location. With the exception of a carbonate layer near the bottom of the section, Sheehan (1988) described the majority


**Figure 3. Sheehan (1988) envisioned the shales as being deposited in an interdistributary bay with the sand layers being derived from crevasse-splay events. Modified from Sheehan (1988, Figure 40, p. 148).**

of the prodeltaic Pennington Formation (moving from the base to the top of the section) as composed of homogeneous yellow-brown siltshale, dark-gray, carbonaceous clayshale, and maroon, light-brown, and olive-green siltshales. Near the top of the Pennington Formation, Sheehan (1988) identified a 4.0 m exposure of interbedded sandstone and shale that extends laterally along the outcrop for approximately 100 m (Figure 2). Above this interval are additional prodeltaic silts and clays, described as brown, maroon, and olive-green siltshale, that continue an additional 15 m before reaching the base of the Raccoon Mountain Formation (lower Pennsylvanian) [Sheehan, 1988].

## CREVASSE-SPLAY DEPOSITS

The primary goal of Sheehan's (1988) study was to document and interpret the suite of trace fossils within the 4.0 m interval of interbedded sandstones and shales. Subordinate attention was given to a description of the outcrop, reconstruction of the depositional environment, and the interpretation of the paleocommunity. As a result of this study, Sheehan (1988) identified a total of 16 ichnotaxa of the *Cruziana* ichnofacies on the bed soles of the many sandstone layers. These trace makers were deposit feeders horizontally mining the organic-rich silts and clays. Sheehan (1988) envisioned the depositional environment as a partially anoxic interdistributary bay, occasionally infilled by organic-rich mud from overbank flooding (Figure 3). In a similar manner, Rindsberg and Martin (2007) interpreted the depositional setting as an interdistributary bay succeeded by an interdistributary channel, both brackish but with some tidal influence. The high oxygen levels in the silts and clays enabled an opportunistic (r-selected) community of dysaerobic animals to exploit food resources across the bay floor (Sheehan, 1988). Within this setting, Sheehan (1988) proposed that pulses of sand were deposited by density currents formed by flood-generated crevasse splays. Noting the abrupt contact between the base of the sandstone layers and underlying shales, Sheehan (1988, p. 26) stated:

> ...the gently undulose to flat soles of the sandstones are interpreted to have been deposited upon erosional surfaces. This interpretation is further evidenced by scour-and-fill structures and long, straight toolmarks which infrequently punctuate these otherwise completely burrowed horizons.

Regarding the location and preservation of the ichnofossils, Sheehan (1988, p. 31) stated:

> Nearly all ichnofossils within the study interval are located at depositional interfaces. Most are preserved as convex hypichnia at sandstone – shale interfaces, with sandstone acting as the medium through which they are cast.

Sheehan (1988) also noted asymmetric linguoid ripples on the top surfaces of many of the sandstone layers and suggested they formed concomitantly with the emplacement of each of the sand layers.

In summary, the Mississippian section exposed at Dougherty Gap (moving bottom-to-top) consists of approximately 70 m of prodeltaic silts and clays, followed by approximately

4.0 m of interbedded sandstones and shales, which is covered by 15 m of prodeltaic silts and clays. To accommodate a change from the prodeltaic to an interdistributary-bay/interdistributary-channel depositional setting, sea level must have rapidly dropped. During this purported lowstand, sand-rich crevasse-splay events scoured bioturbated muds casting the exposed traces as convex hypichnia. These splay events occurred over 20 times. Following the development of this 4.0 m interval of alternating sands and clays, sea level then rapidly rose and prodeltaic deposition continued until reaching the base of the Raccoon Mountain Formation (lower Pennsylvanian). Does this small interval of interbedded sandstone and shale require such abrupt changes in eustacy and depositional setting or can this interval be defined within the context of the entire Pennington Formation prodeltaic section?

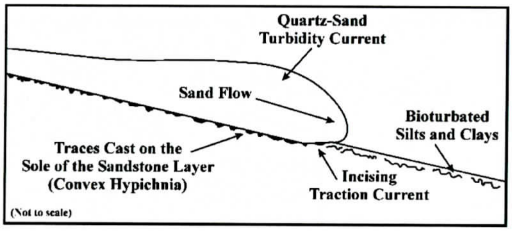


**Figure 4. Sandy turbidity currents would have proceeded under gravity from the delta front down across prodeltaic silts and clays, scouring the semi-lithified mud. Exposed traces within the mud would have been rapidly filled by quartz sands and preserved as convex hypichnial trace fossils. Not to scale.**

## PREDEPOSITIONAL TRACE FOSSILS

Fuchs (1895) was the first to identify impressions and markings on the undersides of sedimentary layers. The study of these bed sole features began when Kuenen (1957) linked them to predepositional traces in flysch beds (i.e., turbidites). Shortly thereafter, Seilacher (1962) expanded on the likely depositional conditions for turbidite deposits in Spain, differentiating between pre- and postdepositional traces. In the Polish Carpathian Mountains, Kern (1980) noted quartz-sand turbidite sole casts of predepositional ichnofauna dominated by horizontal traces. Many of the reported traces are similar to those found in the 4.0 m interval at Dougherty Gap.

Seilacher (1962) described the formation of predepositional trace fossils, linking them to the passing of sandy turbidity currents across the surface of a bioturbated mud. The turbidity current strips off the uppermost mud layer down to sediments sufficiently compact to resist the erosive force of the current. This horizontal planation typically occurs over a large area, remarkably at or very near the same depth of erosion. The traces of former life-forms that mined the mud are partially excavated and quickly filled with quartz sand from the turbidity current (Figure 4). The result is a sand sheet with convex hypichnial trace fossils cast as bed sole marks (Figures 5a and 5b). This understanding of turbidity current deposition across predepositional, bioturbated mud is consistent with the 4.0 m interval of interbedded sandstone and shale exposed at Dougherty Gap (Figures 6 and 7).

## PRODELTAIC SILTS AND CLAYS

The traces exposed on the bottom of the many sandstone layers at Dougherty Gap convey important information about the pre-turbidite conditions along the prodelta. Leszczyński (1991) documented the correlation between well-oxygenated sediments and an abundance of predepositional trace fossils, and anaerobic (anoxic) conditions and nonbioturbated sediments. Every sandstone layer at the study site exhibits convex hypichnial trace fossils, suggesting that the organic-rich silts and clays were both an excellent food source and well-oxygenated. However, some caution is warranted because of the stratigraphic position of the convex hypichnia traces in the shale layer. The sole casts were created in the upper centimeters of the silt/clay sediments. Due to compaction, the aerobic/anaerobic condition of the entire thickness of the individual shale layers cannot be fully ascertained despite the occurrence of lighter-colored shales that possibly reflect aerobic con-

**Figure 5a. The bed sole of one of the many sandstone layers. Sheehan (1988) identified a total of 16 ichnotaxa in the *Cruziana* ichnofacies. These traces are all convex hypichnia cast in sandstone. The high level of bioturbation suggests an abundance of organic food materials and a well-oxygenated substrate in the former underlying silts and clays. Scale in cm and in.**

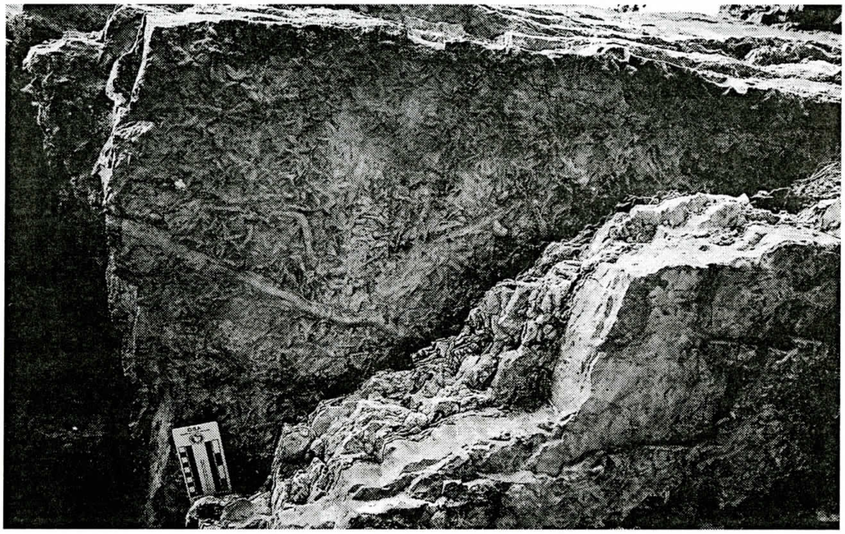

**Figure 5b. The bed sole of one of the many sandstone layers. Each of the sandstone layers examined had trace fossils on the sole of the sandstone bed. According to Rindsberg and Martin (2007), one species of bivalve made most of the traces seen in this image and in Figure 4a. Scale in cm and in.**

ditions in the subsurface (see Leszczyński, 1991).

## TURBIDITY CURRENT DEPOSITIONAL SETTING

At what water depth did these turbidites form? Turbidity currents can operate in both shallow and deep water creating deposits that

**Figure 6. The fine-grained sandstone layers have convex hypichnial traces along their soles and are separated by shales of varying thickness. The thinner sandstone layers did not penetrate deeply into the underlying silts and clays and they do not exhibit the same level of sole cast relief as is found in the thicker sandstone layers. This difference in relief might be confused with the levels of oxygen and food available to the trace makers or possible predepositional tiering and so no attempt was made to define the paleoenvironmental conditions of the mud below the sole casts. Scale in cm and in.**

are similar in sedimentary composition and structure—but different in thickness. Since trace fossils cannot be used as accurate bathymetric recorders (Ekdale, 1988; Frey and others, 1990; Goldring, 1993), other geologic tools must be used to determine possible water depths in which these turbidites formed. While it is possible that this 4.0 m interval of sand and clay was deposited in deep water (see Fenton and Wilson, 1985), the close proximity of this interval (within 15 m) to the top of the prodeltaic Mississippian section suggests that it formed within storm-wave base. The reworking of the individual sand layer surfaces within the shallow subsurface is consistent with other locales where this has been reported (Field and others, 1981; Fenton and Wilson, 1985; Weir and others, 1988; Viana and others, 1998; Milli and Moscatelli, 2000; Pattison, 2005b).

If the Dougherty Gap deposits are turbidites, where did they occur? In their examination of the trace fossils in the Italian Alps, Tunis and Uchman (1992) assigned the predepositional turbidite sandstone sole casts to the proximal portion of the turbidite deposit and assigned tiering to the hypichnial trace fossils based on bed soles and toponomic data. While tiering is not clearly present at Dougherty Gap, it is likely that these sand layers were deposited on the proximal portion of a prodelta.

The sedimentary fabric of each of the sandstone layers is reflective of the efficiency of the turbidity current (Mutti and others, 2000, p. 176):

> ...very poorly efficient flows can only partly segregate their different grain-size populations, thus producing a more limited number of facies types generally characterized by poor textural sorting and less distinctive internal structures.

The individual fine-grained sandstone layers exposed at Dougherty Gap are poorly sorted and have no distinct internal structure. This type of featureless sandstone is attributed to turbidites (Walker, 1984). According to Kneller and Branney (1995, p. 607):

> In some cases the lack of internal stratification may be a result of post-depositional liquefaction or intense

**Figure 7. A stacked sequence of sandstones all exhibiting convex hypichnial traces along the soles of the beds. In some instances, the shale between the sandstone layers can be measured in mm. Scale in cm and in.**

> bioturbation, but in many, if not most examples, the massive sand divisions appear to be the products of discrete depositional events from one or more gravity currents.

A problem in identifying these flood-generated delta-front sandstone layers is due to their formation from processes that are not observed in the present (Mutti and others, 2003, p. 736):

> Clearly, most ancient flood-dominated fluvio-deltaic systems can only be viewed in terms of catastrophic processes that were able to transport large amounts of gravel, sand and mud to delta-front and shelfal regions—a setting that is probably difficult to perceive from what we know from the Recent.

These flood-generated delta-front sandstones have only recently been recognized in the stratigraphic record (Mutti and others, 1996; Mutti and others, 1999; Mutti and others, 2003; Plink-Björklund and Steel, 2004; Mutti and others, 2009). Ongoing field work continues to define the initiating processes and resulting sedimentary deposits from these historic events along basin margins.

Figure 8. Two layers of sandstone exhibiting asymmetric linguoid ripples across their top surfaces. These features could have formed by tidal, storm, or even bottom/slope currents following the deposition of the sandy turbidites. This type of ripple mark is viewed as a mature, stable form and indicates that some period of time passed, allowing the top of the sands to be reworked before burial by mud. Scale in cm and in.

## ASYMMETRIC LINGUOID RIPPLES

Once deposited, the sandy turbidite surface can be subjected to water currents generated by storm waves and delta-front slope/bottom currents. This can result in the development of ripple marks on the surface of the sands. Ripple mark development on sandy turbidite surfaces has been documented along prodelta slopes, fans, and in the abyssal depths (Heezen and Hollister, 1964; Hsu, 1964; Bouma, 1972; Stow and Piper, 1984; Ito, 1996). Stanley (1993) interpreted ripple marks on sandy turbidite surfaces as evidence of bottom currents likely related to basin circulation or density flows from basin margins. Howe and Humphery (1995) photographically documented asymmetric linguoid ripples formed by slope currents along the Hebrides Slope.

Ripple marks can also develop on sandy turbidite surfaces in shallow water due to passing storms (Field and others, 1981; Fenton and Wilson, 1985; Weir and others, 1988; Viana and others, 1998). Storm waves with sufficient bottom orbital velocities can rework loose sand grains and create ripple marks. The resulting shape of the ripple would be a function of time, current direction, and water velocity.

The top surfaces of the many turbidite sandstones examined at Dougherty Gap exhibit asymmetrical linguoid ripple marks (Figure 8). This form of ripple mark reflects the final stage in ripple development (Baas and others, 1993) and suggests that the sandy turbidite surface was exposed for some period of time allowing the sands to be reworked by storm and possibly even slope/bottom currents before being covered by silts and clays.

## DISCUSSION

The preservation of the many turbidite sand layers suggests that they could have formed in deep water (greater than 200 m) well below storm-wave base, consistent with the model of Fenton and Wilson (1985). However, it is more likely that the volume of fine-grained sediments being discharged from the prograding delta buried and preserved the sandstone layers in a shallower marine setting, especially considering the proximity to overlying strata interpreted as Pennsylvanian coal-forming deltaic deposits (Horne and others, 1978; Crawford, 1989).

The convex hypichnial traces occur along a near flat surface which is consistent with Seilacher's (1962) concept of turbidity current erosion down to a semi-lithified substrate dominated by mining trace makers. Differences in the size of the hypichnia likely relate to the depth of turbidity current penetration into the substrate and possible tiering of the trace makers within that substrate. The thicker sandstone layers exhibit a more pronounced sole mark relief compared to the thinner layers. The presence of convex hypichnia on every sandstone layer examined indicates that oxygen and food must have been readily available to trace makers in each of the underlying mud layers.

The individual sand layers are generally featureless with no evidence of any bioturbation, suggesting emplacement by a succession of inefficient turbidity currents. None of the sandstone layers exhibit any sedimentary structures indicative of escape structures. This suggests that the sands did not bury and preserve any living predepositional trace makers. The absence of any trace fossils in the many sandstone layers suggests that the original sand contained insufficient amounts of oxygen and nutrients to promote bioturbation by trace makers.

Asymmetrical ripple marks across the top surfaces of the many turbidite quartz-sand layers indicate that they were reworked by water currents before burial. The development of this form of ripple mark suggests that the sandy surface was exposed to moving water for a period of time sufficient to reach ripple-mark maturity. Further analysis of these features could prove valuable in understanding possible paleocirculation patterns in the former basin (see Fenton and Wilson, 1985).

## CONCLUSIONS

The original assessment of this exposure as multiple crevasse-splay deposits is not consistent within the larger stratigraphic context of a prodeltaic depositional setting. The combination of convex hypichnia as sole casts on the base of the many fine-grained sandstone layers; the lack of any sedimentary sorting, bedding, or bioturbation within the sandstones; and the undisturbed and nonbioturbated ripple-marked sandstone surfaces are consistent with turbidity current deposition. The interbedded sandstones and shales suggest that pulses of sandy turbidity currents moved from an unstable delta front down across well-oxygenated, bioturbated, prodeltaic silts and clays. Following deposition, the surfaces of the sand layers were reworked by water currents into a mature and stable form of ripple mark before being buried by additional silts and clays. Likely, storm events generated the energy necessary to move the quartz sands from their source to the proximal portion of the prodelta where they were eventually deposited. This episodic turbidity current cycle was repeated more than 20 times at this locale before returning to prodeltaic deposition.

## ACKNOWLEDGMENTS

I am indebted to E.L. Williams for introducing me to this locale. Ichnologist J.H. Cowart (*deceased*) provided helpful technical assistance. Gratitude is expressed to A.J. Akridge, J.K. Reed, and M. Bennett for their helpful and constructive reviews. Appreciation is expressed to the two anonymous reviewers for their comments. Excellent reference assistance was provided by P. Vierheller and K. Piselli. This work neither represents the views or opinions of the U.S. Environmental Protection Agency, nor was this investigation conducted in any official capacity. Any mistakes that may remain are the responsibility of the author.

## REFERENCES

Baas, J.H., Oost, A.P., Sztano, O.K., de Boer, P.L., and Postma, G., 1993, Time as an independent variable for current ripples developing towards linguoid equilibrium morphology: Terra Nova, v. 5, p. 29-35.

Bouma, A.H., 1972, Fossil contourites in lower Niesenflysch, Switzerland: Journal of Sedimentary Petrology, v. 42, p. 917-921.

Budillon, F., Violante, C., Conforti, A., Esposito, E., Insinga, D., Iorio, M., and Porfido, S., 2005, Event beds in the recent prodelta stratigraphic record of the small flood-prone Bonea Stream (Amalfi Coast, Southern

Italy): Marine Geology, v. 222-223, p. 419-441.

Crawford, J., 1989, Geology of the Pennsylvanian System of Georgia: Atlanta, Georgia, Geologic Atlas 2, Georgia Geologic Survey.

Ekdale, A.A., 1988, Pitfalls of paleobathymetric interpretations based on trace fossil assemblages: Palaios, v. 3, p. 464-472.

Fenton, M.W., and Wilson, C.J.L., 1985, Shallow water turbidites: an example from the Mallacoota Beds, Australia: Sedimentary Geology, v. 45, p. 231-260.

Ferm, J.C., Ehrlich, R., and Neatherly, T.L., 1967, A field guide to carboniferous detrital rocks in northern Alabama: University, Alabama, Alabama Geological Society.

Ferm, J.C., Milici, R.C., Eason, J.E., 1972, Carboniferous depositional environments in the Cumberland Plateau of southern Tennessee and northern Alabama: Nashville, Tennessee, Report of Investigation 33, Tennessee Division of Geology.

Field, M.E., Nelson, C.H., Cacchione, D.A., and Drake, D.E., 1981, Sand waves on an epicontinental shelf: Northern Bering Sea: Marine Geology, v. 42, p. 233-258.

Frey, R.W., Pemberton, S.G., and Saunders, T.D.A., 1990, Ichnofacies and bathymetry: A passive relationship: Journal of Paleontology, v. 64, p. 155-158.

Fuchs, T., 1895, Studien über Fucoiden und Hieroglyphen: Akademie der Wissenschaft in Wien, Mathematisch-naturwissenschaftliche Classe, v. 62, p. 369-448.

Goldring, R., 1993, Ichnofacies and facies interpretation: Palaios, v. 8, p. 403-405.

Heezen, B.C., and Hollister, C.D., 1964, Deep-sea current evidence from abyssal sediments: Marine Geology, v. 1, p. 141-174.

Horne, J.C., Ferm, J.C., Caruccio, F.T., and Baganz, B.P., 1978, Depositional models in coal exploration and mine planning in Appalachian Region: American Association of Petroleum Geologists Bulletin, v. 62, p. 2379-2411.

Howe, J.A., and Humphery, J.D., 1995, Photographic evidence for slope-current activity, Hebrides Slope, NE Atlantic Ocean: Scottish Journal of Geology, v. 31, p. 107-115.

Hsu, K.J., 1964, Cross-laminations in graded bed sequences: Journal of Sedimentary Petrology, v. 34, p. 379-388.

Ito, M., 1996, Sandy contourites of the lower Kazusa Group in the Boso Peninsula, Japan: Kuroshio-current-influenced deep-sea sedimentation in a Plio-Pleistocene forearc basin: Journal of Sedimentary Research, v. 66, p. 587-598.

Kern, J.P., 1980, Origin of trace fossils in Polish Carpathian flysch: Lethaia, v. 13, p. 347-362.

Kneller, B.C., and Branney, M.J., 1995, Sustained high-density turbidity currents and the deposition of thick massive sands: Sedimentology, v. 42, p. 607-616.

Kuenen, Ph. H., 1957, Sole markings of graded graywacke beds: Journal of Geology, v. 65, p. 231-258.

Leszczyński, S., 1991, Oxygen-related controls on predepositional ichnofacies in turbidites, Guipuzcoan Flysch (Albian-Lower Eocene), northern Spain: Palaios, v. 6, p. 271-280.

Luther, E.T., and Smith, G.E., 1980, Depositional environments of a part of the southern Appalachian coal fields, in Frey, R.W., ed., Excursions in southeastern geology, v. I: Falls Church, Virginia, American Geological Institute, p. 103-148.

Milli, S., and Moscatelli, M., 2000, Facies analysis and physical stratigraphy of the Messinian turbidic complex in the Valle del Salto and Val di Varri (central Apennines): Giornale di Geologia, v. 62, p. 57-77.

Mutti, E., Davoli, G., Tinterri, R., and Zavala, C., 1996, The importance of ancient fluvio-deltaic systems dominated by catastrophic flooding in tectonically active basins: Memorie di Scienze Geologiche, v. 48, p. 233-291.

Mutti, E., Tinterri, R., Remacha, E., Mavilla, N., Angella, S., and Fava, L., 1999, An introduction to the analysis of ancient turbidite basins from an outcrop perspective: Tulsa, Oklahoma, Note Series #39, American Association of Petroleum Geologists.

Mutti, E., Tinterri, R., di Biase, D., Fava, L., Mavilla, N., Angella, S., and Calabrese, L., 2000, Delta-front facies associations of ancient flood-dominated fluvio-deltaic systems. Revista de la Sociedad Geológica de España, v. 13, p. 165-190.

Mutti, E., Tinterri, R., Benevelli, G., di Biase, D. and Cavanna, G., 2003, Deltaic, mixed and turbidite sedimentation of ancient foreland basins: Marine and Petroleum Geology, v. 20, p. 733-755.

Mutti E., Tinterri R., Bernoulli D., and Lucchi F.R., 2009, Turbidites and turbidity currents from Alpine 'flysch' to the exploration of continental margins: Sedimentology, v. 56, p. 267-318.

Pattison, S.A.J., 2005a, Storm-influenced prodelta turbidite complex in the lower Kenilworth member at Hatch Mesa, Book Cliffs, Utah, U.S.A.: Implications for shallow marine facies models. Journal of Sedimentary Research, v. 75, p. 420-439.

Pattison, S.A.J., 2005b, Isolated highstand shelf sandstone body of turbiditic origin, lower Kenilworth Member, Cretaceous Western Interior, Book Cliffs, Utah, USA: Sedimentary Geology, v. 177, p. 131-144.

Plink-Björklund, P., and Steel, R.J., 2004, Initiation of turbidity currents: Outcrop evidence for Eocene hyperpycnal flow turbidites. Sedimentary Geology 165:29-52.

Rindsberg, A.K., and Martin, A.J., 2007, Ichnodiversity does not equal biodiversity: Bivalve trace fossils from the upper Mississippian Pennington Formation of Georgia: Geological Society of America, Abstracts with Programs, v. 39, p. 36.

Røe, S.-L., 1995, Stacked fluviodeltaic cycles in the Upper Proterzoic Godkeila Member, Varanger Peninsula, northern Norway: Norsk Geologisk Tidsskrift, v. 75, p. 229-242.

Seilacher, A., 1962, Paleontological studies on turbidite sedimentation and erosion: Journal of Geology, v. 70, p.

227-234.

Sheehan, M.A., 1988, Ichnology, depositional environment, and paleoecology of the upper Pennington Formation (upper Mississippian), Dougherty Gap, Walker County, Georgia: Athens, University of Georgia, Unpublished Masters thesis.

Stanley, D.J., 1993, Model for turbidite-to-contourite continuum and multiple process transport in deep marine settings: examples in the rock record: Sedimentary Geology, v. 82, p. 241-255.

Stow, D.A.V., and Piper, D.J.W., 1984, Deep-water fine-grained sediments, in Stow, D.A.V., and Piper, D.J.W., eds., Fine-grained sediments: Deep-water processes and facies: London, United Kingdom, Special publication 15. Geological Society of London, p. 611-646.

Thomas, W.A., and Cramer, H.R., 1979, The Mississippian and Pennsylvanian (Carboniferous) systems in the United States – Georgia: Washington, D.C., U.S. Geological Survey Professional Paper 1110-H, p. H1-H37.

Tunis, G., and Uchman, A., 1992, Trace fossils in the "Flysch del Grivò" (Ypresian) in the Julian Pre-Alps, NE Italy: preliminary observations: Gortania, v. 14, p. 71-104.

Viana, A.R., Faugères, J.-C., and Stow, D.A.V., 1998, Bottom-current-controlled sand deposits—a review of modern shallow- to deep-water environments: Sedimentary Geology, v. 115, p. 53-80.

Walker, R.G., 1984, Turbidites and associated coarse clastic deposits, in Walker, R.G., ed., Facies Models, Second edition: Toronto, Ontario, Geoscience Canada, Reprint Series 1, p. 171-188.

Weir, J.C., Fenton, M.W., Tomlinson, K.M., and Wilson, C.J.L., 1988, Sedimentology of the Early Devonian Walhalla Group at Walhalla, Victoria: Australian Journal of Earth Sciences, v. 35, p. 405-419.